DARTMOUTH COLLEGE

Thayer School of Engineering

Hanover, New Hampshire

Report No. COO-2294-4

STEAM/WATER INTERACTION IN A SCALED PRESSURIZED WATER REACTOR DOWNCOMER ANNULUS

by

Christopher J. Crowley

Graham B. Wallis

and

David L. Ludwig

September 1974

AEC Contract AT(11-1) - 2294

DISCLAIMER

ABSTRACT

Steam/water countercurrent flow in a 1/30 scale, flat-plate, plastic model of a Pressurized Water Reactor downcomer annulus was investigated. Various inlet geometries, selected to simulate a number of different real reactor injection arrangements, were studied, as well as three water temperatures. Several types of baffling were used to determine their effect on the penetration of liquid through the annulus. Maps, showing the effects of the various parameters on the "end-of-bypass" in this experiment are presented and discussed.

The usefulness of this information in reactor safety studies is also discussed, including tentative scaling laws based on simplified theoretical models. Further work is recommended.

SUMMARY

This experiment was part of a program in which countercurrent flow in a scaled Pressurized Water Reactor (PWR) downcomer annulus was studied. Experiments had previously been conducted with air and water in a scale model (see the Supplement part of this report) and it was decided to run tests using steam and water as the countercurrent flow components in order to provide a better model of possible reactor conditions.

The countercurrent flow situation applies to the safety aspects of nuclear reactors. During a postulated major accident in which one of the large coolant pipes in the reactor breaks, it is possible that (after most of the liquid coolant has been expelled from the pressurized vessel) the escaping fluid will be steam. Emergency systems serve to inject water into the vessel where the water must fall through a narrow gap between the pressure vessel and the core barrel. If steam is produced in the core it could flow up this gap as the water comes down, and attempt to escape via the broken pipe - with the result that this steam flow might lift the incoming coolant and expel it out the break. This is the "accumulator bypass" situation of reactor accident terminology.

The model chosen as the next logical step in the experimental program to study accumulator bypass can be described briefly as a steam/water, 1/30 scale, flat plate annulus, with the capability of simulating a number of vessel designs by means of rearranging a set of adapters to the injection inlets.

Tests were conducted in which steam flow through the annulus was set at a constant value, the liquid flow increased from zero, and the liquid flow at which bypass of the water ended determined. Thus, a number of test points formed a locus of the "end of bypass" in the experimental geometries investigated.

Various injection geometries, such as alternating inlet legs, adjacent inlet legs, and separate injection inlets were tried. Several types of baffling were tried, in order to determine their effect on the end of bypass locus. The effect of water temperature was also investigated.

The locus determined was independent of injection geometry. Both baffling and increased sub-cooling of the inlet water were seen to end bypass at higher steam flows than tests without modifications. The bypass phenomenon was found to depend upon the location of steam condensation occurring. If that location was the lower plenum, no water would be bypassed. If steam entered the annulus, bypass would occur.

Three regions were found as part of the end of bypass locus in the experiment. The first region encompassed low liquid flows - at which there was more steam than was able to be condensed by the injected liquid - here the system behaved essentially like a system with a non-condensing gas and data agree with the Wallis correlation for flooding, plus a small factor to account for the amount of condensation which can take place. The second region lies along the borderline where steam is just able to be condensed by the liquid (the Thermodynamic Ratio equals unity). The third region shows a levelling off of the data at some critical steam flow where it suddenly requires large liquid flows to end the bypass of water. The magnitude of this critical gas flow depends upon the water temperature.

Water temperatures of 55, 100, and 140^{o}F were tested. The range of water flows in the experiment was up to 15 gallons per minute, and the steam flow range was 2-14 lb/min. With the 55^{o}F water, for example, the levelling off of the data occurs at a steam flow of about 7 lb/min when there are no modifications of the annulus. The

levelling off occurs at about 12 lb/min when certain baffles are installed. The level of the critical steam flow decreased with increasing water temperature.

As a result of varying parameters in the experiment and investigating several baffles, it was found that both the baffles and increased sub-cooling of the injected water could aid in ending the bypass of water. Altering existing reactors by adding baffles could create some problems in regard to the safety evaluation of a plant, the analysis of thermal stresses in pressure vessels, and controlling the distribution of coolant in the downcomer. The mechanics of the alteration itself in operating plants would be difficult, involving the removal of internals from the reactor and installing baffles under radioactive conditions. Designing the changes into new reactors, once the calculations had been done, would not involve the mechanical difficulties. Chilling accumulator water in the containment might accomplish an earlier end to bypass in the event of an accident, and the installation of refrigerators on the accumulator tanks would be accomplished relatively easily compared to the installation of baffles, though it would not be without its own problems to consider. The benefits to be gained by an earlier end to bypass were not evaluated as part of the study. No conclusions on the practicality and desirability of these changes from a system standpoint can be made.

Because baffles and chilled accumulator water were found to aid in ending bypass in this experiment, it is recommended that similar tests be performed on a larger scale. (Future tests could also model the hot reactor walls to determine the effect on the inlet water temperature.) Only after intermediate-scale tests have been performed, and the effects of scaling and system performance determined, could these changes be recommended for nuclear reactors. Based on analysis of

larger scale tests (Appendix F) there is some evidence to indicate that scaling effects may in fact be small. This small-scale experiment serves as a new guidepost and map for future research as well as suggesting two alternative solutions deserving further consideration.

ACKNOWLEDGMENTS

The Atomic Energy Commission supported this work under Contract AT(11-1)-2294.

Edith Henson provided invaluable secretarial work.

This report is substantially the same as the Master of Engineering Thesis submitted to the Thayer School of Engineering at Dartmouth College by Christopher J. Crowley in August 1974.

NOMENCLATURE

A	Area	ft^2
c_p	Specific Heat	$Btu/lb-^oF$
d,D	Diameter	ft
D*	Dimensionless diameter	
F_o	Froude number, dimensionless	
g	Gravitational constant	ft/sec^2
h	Height	ft
h_{fg}	Heat of Vaporization,	Btu/lb
h	Heat transfer coefficient, convective,	$Btu/hr-ft^2-^oF$
j	Volumetric fluid flux,	ft/sec
j*	Dimensionless momentum flux	
k	Conductivity,	$Btu/hr-ft-^oF$
Ku	Dimensionless Kutateladze number	
L	Length	ft
P	Dimensionless number relating viscosity of gas and surface tension of liquid in drop flow	
p	Pressure	lb/in^2
Δp^*	Dimensionless pressure drop	
Q	Volumetric flow rate,	ft^3/sec
q	Rate of heat transfer,	Btu/hr
r	Radius	ft
R	Thermal Resistance	$hr-^oF/Btu$
r*	Dimensionless radius	ft
R_t	Thermodynamic Ratio	
ΔT	Temperature difference	^oF
v,V	Velocity	ft/sec
v*	Dimensionless Velocity	
V_∞	Terminal velocity	ft/sec
W	Mass flow rate,	lb/sec
We	Dimensionless Weber number	

Subscripts

c	Continuous component
f	Liquid
g	Gas
H	Hydraulic (as in D_H, Hydraulic Diameter)
o	Stagnation reference
s	Steam
w	Water

Greek

α	Void Fraction
σ	Surface Tension
ν	Specific Volume
ρ	Density
$\Delta\rho$	Density difference, $(\rho_f - \rho_g)$
μ	Viscosity

Terms

The term "flooding" in this investigation refers to the expulsion of water in countercurrent flow and carries the same connotation as "bypass". It does not refer to the reflood stage of a LOCA.

THIS PAGE
WAS INTENTIONALLY
LEFT BLANK

TABLE OF CONTENTS

INTRODUCTION

This study investigates the interaction of steam and water in a countercurrent annular flow situation. In particular, a linearly-scaled, "unwrapped" plastic annulus - simulating the downcomer of a Pressurized Water Reactor (PWR) - is used as the model.

Reactor safety analysis programs called for by the AEC require the reactor vendors to postulate breakage of one of the pipes carrying coolant into (or out of) the pressure vessel and to predict the subsequent events. One portion of this Loss of Coolant Accident (LOCA) involves a period of time during which the fluid escaping the pressure vessel is mainly steam, under high pressure, exiting through the break in the piping. When the pressure drops to a certain value (either 600 or 200 psi., depending upon the design), large amounts of water from pressurized storage tanks are rapidly injected through pipes which branch into the cold legs - the inlet pipes. Hence, these unbroken cold legs direct the Emergency Core Coolant (ECC) water into the annulus, where it is intended to fall and fill the lower plenum, in spite of the presence of a strong steam momentum flux upward. It is believed, however, that the steam flow may carry some, perhaps all, of the cooling water out of the break for a time rather than allowing it to fall into the plenum and begin to resubmerge and cool the hot core of the reactor. This is called the "accumulator bypass" phenomenon.

The engineering aspects of accumulator bypass involve calculating the quantity of water which actually is bypassed for a given steam flow. The AEC ruling at the present time regarding the bypass calculations is to assume, in the absence of better information, that all of the ECC water injected into the system prior to the "end-of-bypass" is removed from the system.

This is most likely too conservative since, for instance, a good deal of water may be stored or held up in the annulus, only to reach the lower plenum when the steam flow falls below a critical value. In their calculations, the vendors would like to be able to credit some of the ECC water to the amount of fluid refilling the vessel during the blowdown phase, but the phenomena involving steam/water countercurrent interactions must first be understood before any model can be approved.

None of the previously proposed models takes into account two-dimensional flow patterns available to the steam and the water, or possible asymmetries of pressure vessel design. More importantly, the effects of condensation are also slighted. (The two-dimensionality may actually be advantageous, if the asymmetry allows steam to escape and yet allows the coolant to penetrate.) The applicability of one-dimensional models to the scaled reactor geometry is discussed in this study. Effects of variations in the arrangement of the injection legs, and design modifications such as baffles, are also included.

Briefly, the apparatus consists of a transparent polycarbonate parallel plate "annulus" with a 0.375 inch gap between the plates (1/30 scale). This is mounted on a barrel 22 inches in diameter and 2 feet high (not to scale). Steam enters the barrel, and proceeds upward through the annulus. Water is injected into the annulus via tubes perpendicular to it, as in a reactor. The downward water flow in the gap creates a countercurrent flow condition which is intended to model the accumulator bypass situation.

The types of tests which may be carried out with such an apparatus are as follows: The location or size of the injection pipes may be altered depending upon whether different designs of the pressure vessel are modelled. Baffling by means of straight channels or curved

collars may be added, with the intent of helping to direct the water flow downward. The effects of the presence of a simulated thermal shield will be discovered. In the experimental procedure, tests may be conducted in which the water flow is held constant and the steam flow varied, or it may be done vice versa (corresponding more closely to the bypass situation). Finally, the effects of inlet water temperature upon the results may be discovered. The tests were basically steady state and the effects of transients minimal.

The experiment seeks to determine the locus of "flooding" points - that is, under what conditions a bypass of water out the break occurs and the amount of the bypass - in the presence of condensation effects, and demonstrate the effect of the above-mentioned design modifications upon this locus. As the experiments show, when bypass was occurring at the water flow rates tested, the amount of water entering the lower plenum was negligible. It is important, however, to determine whether the modifications will aid or hinder water from reaching the lower plenum.

BACKGROUND

A brief background introduction to the Pressurized Water Reactor, the Loss of Coolant Accident, and the Emergency Core Cooling System is prerequisite to understanding the accumulator bypass phenomenon and also to understanding any suggestions for improvements to the system.

Figure 1 illustrates the path of primary coolant through the PWR. Water enters the pressure vessel through several pipes thirty inches in diameter (there are typically four of these). There it flows downward in the annulus formed by the core barrel and the pressure vessel. At the bottom of the annulus, in the lower plenum, the water turns and flows upward through the core and is heated by the fissioning uranium. The heated water leaves the pressure vessel through a second set of large pipes (hot legs) which penetrate the pressure vessel and the core barrel. From there, the water enters a steam generator, cools, and recirculates into the vessel again.

The worst case postulated under which the Emergency Core Coolant System (ECCS) would function involves an instantaneous and complete severance (guillotine rupture) of one of the cold leg pipes. The subsequent events in the LOCA have been divided into three stages:

1) BLOWDOWN. The rupture, either a partial split or a complete guillotine rupture, takes place. In a matter of about 18 seconds, because of the large pressure drop to the atmosphere, almost all of the primary coolant is lost out of this break. During the latter stages, the escaping fluid has been calculated to be mostly steam. (Figure 2).

2) REFILL. Toward the end of blowdown, the refill period begins. Injected coolant enters the lower plenum, until such time as the level reaches the bottom of the core. (Figure 3).

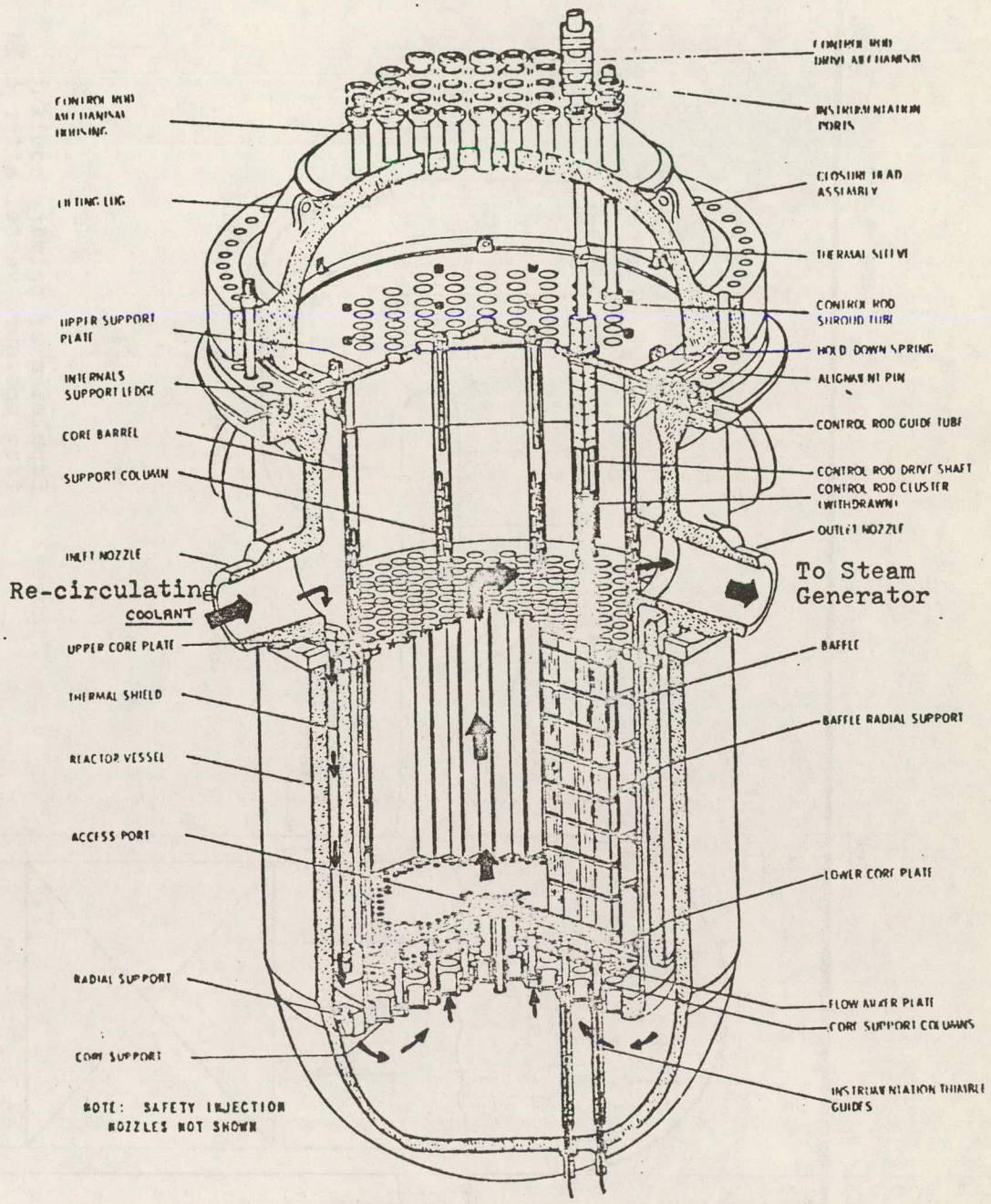

Figure 1. Primary Coolant Flow Path in Reactor Core. (From Ref. 2).

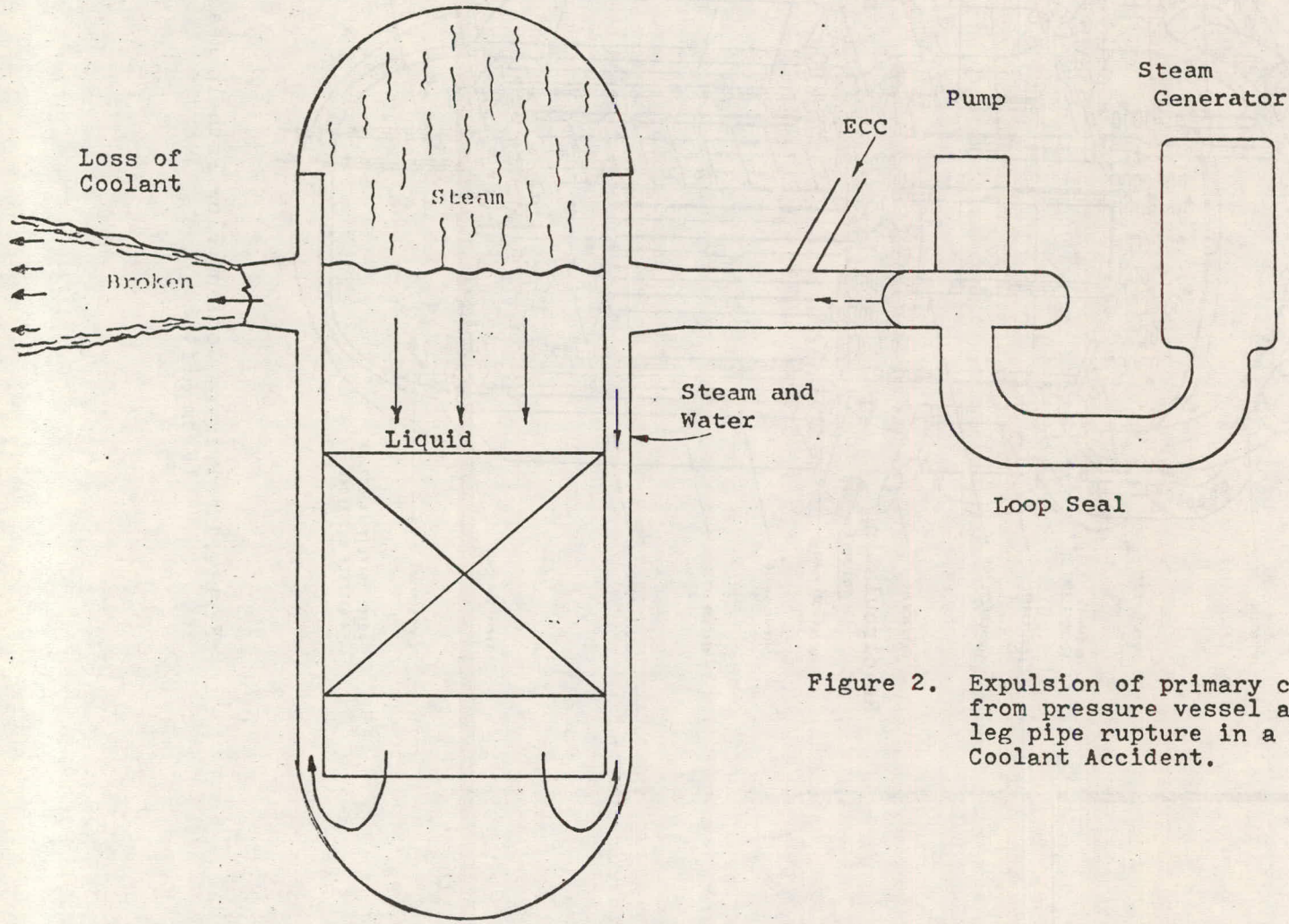

Figure 2. Expulsion of primary coolant from pressure vessel after cold leg pipe rupture in a Loss of Coolant Accident.

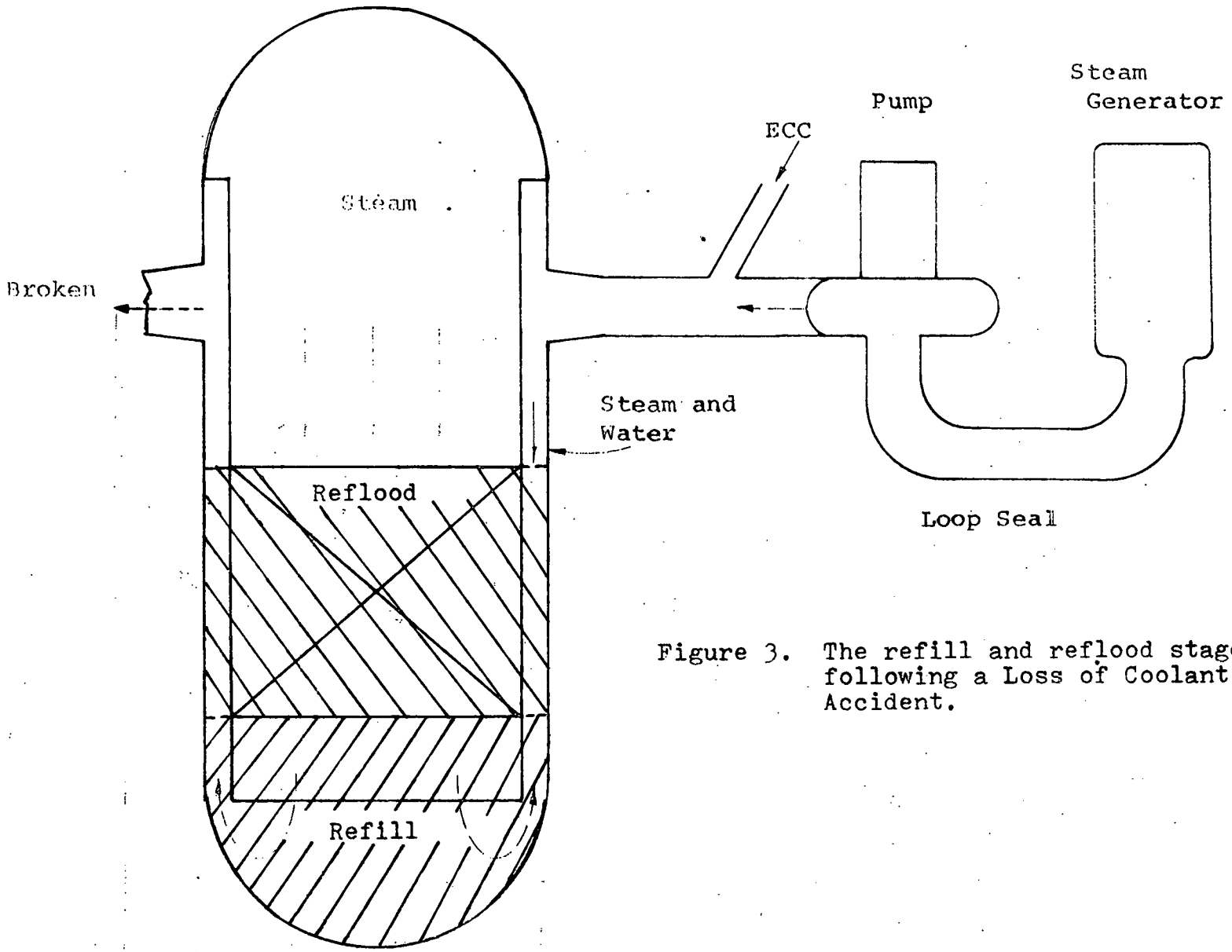

Figure 3. The refill and reflood stages following a Loss of Coolant Accident.

3) REFLOOD. The reflood period involves the time during which the level of coolant contained in the pressure vessel rises from the bottom to the top of the core, completing the resubmergence of the core.

Table I is a typical timetable of the sequence of events under consideration, in this case for complete severance of a cold leg pipe. The table is typical of all designs for a complete break. For lesser breaks, injection and blowdown events occur slightly later, but maximum fuel temperatures are less.

The period of time between 10 and 30 seconds after rupture is the most crucial as far as continued cooling of the core is concerned. Provision must be made for removal of stored and decay heat from the core after the loss of the original coolant. (Fission product decay continues to supply heat for many days after the reaction itself stops. The decay heat is initially on the order of 1% of the full reactor power, later declining to lower levels.)

It is the function of the ECC system to rapidly replace that coolant lost during blowdown, such that this heat is removed and the peak temperature in the cladding of the fuel rods does not exceed $2200^{\circ}F$, which is considered a conservative limit to fuel cladding failure[1]. The sooner the refill and reflood stages begin, the lower will be the peak temperature actually reached. Quenching the fuel rods from higher temperatures not only requires more available coolant, but creates higher thermal stresses in the fuel rods. This argues that the ECC system must function to inject cooling water all the way into the lower plenum in the greatest amounts possible, as soon as possible.

The operation of the ECC system can be described in five stages. The descriptions also give an indication of some of the areas open to study:

DOUBLE-ENDED COLD LEG
GUILLOTINE RUPTURE
TIMETABLE

time (sec.)	event
0	Rupture occurs and a simultaneous loss of electrical power is assumed.
1.0	Trip signal for control rods.
1.5	Core rods trip and neutron poisons smother the fission reaction.
6	Safety injection signal activates.
11	Accumulator injection begins.
18	End of blowdown.
25	Pump injection takes over.
31	Recovery of coolant to bottom of core (refill).
47	Accumulators empty.
78	Reflood complete.

TABLE I.

1) Injection and pumping of emergency coolant.

2) The configuration of the vessel injection system.

3) The location of the injection points.

4) Behavior of the ECC water in the downcomer.

5) Behavior of the ECC water in the lower plenum.

Concerning the method by which ECCS injection is initiated: A number of large tanks of borated water (usually one for each cold leg) are present within the reactor containment. (Figure 4 and Table II.) The tanks are pressurized to 650 psi. with nitrogen gas. When the pressure in the reactor vessel drops to 600 psi. (or 200 psi. in one design) injection becomes automatic through the action of check valves, which do not require electrical power, automatic switching, or operator action. Water enters the annulus of each of the cold legs. (It is assumed to spill into the containment instead of the pressure vessel in the broken loop.) Figure 5 shows a typical injection curve versus time for the accumulators following a guillotine rupture. According to one source: "The use of the gas-activated accumulator tanks solves the water addition problem provided the (nitrogen) gas from the accumulator does not enter the reactor vessel and expel the coolant" [2]. If there should be a critical steam flow limit below which all the coolant penetrates, perhaps the timing of the moment of injection would become important in assuring that most of the injected water enters the reactor rather than being splashed into the containment instead.

As the accumulators exhaust themselves, several pumps (with backups) commence action to continue to supply coolant at a rate which is also indicated in Figure 5.

The configuration of the injection piping itself may be important in terms of ECC operation. Figure 6 shows how ECC enters the cold leg pipe and then the pressure vessel in most designs (one has separate

SEQUOYAH Reactor--Westinghouse

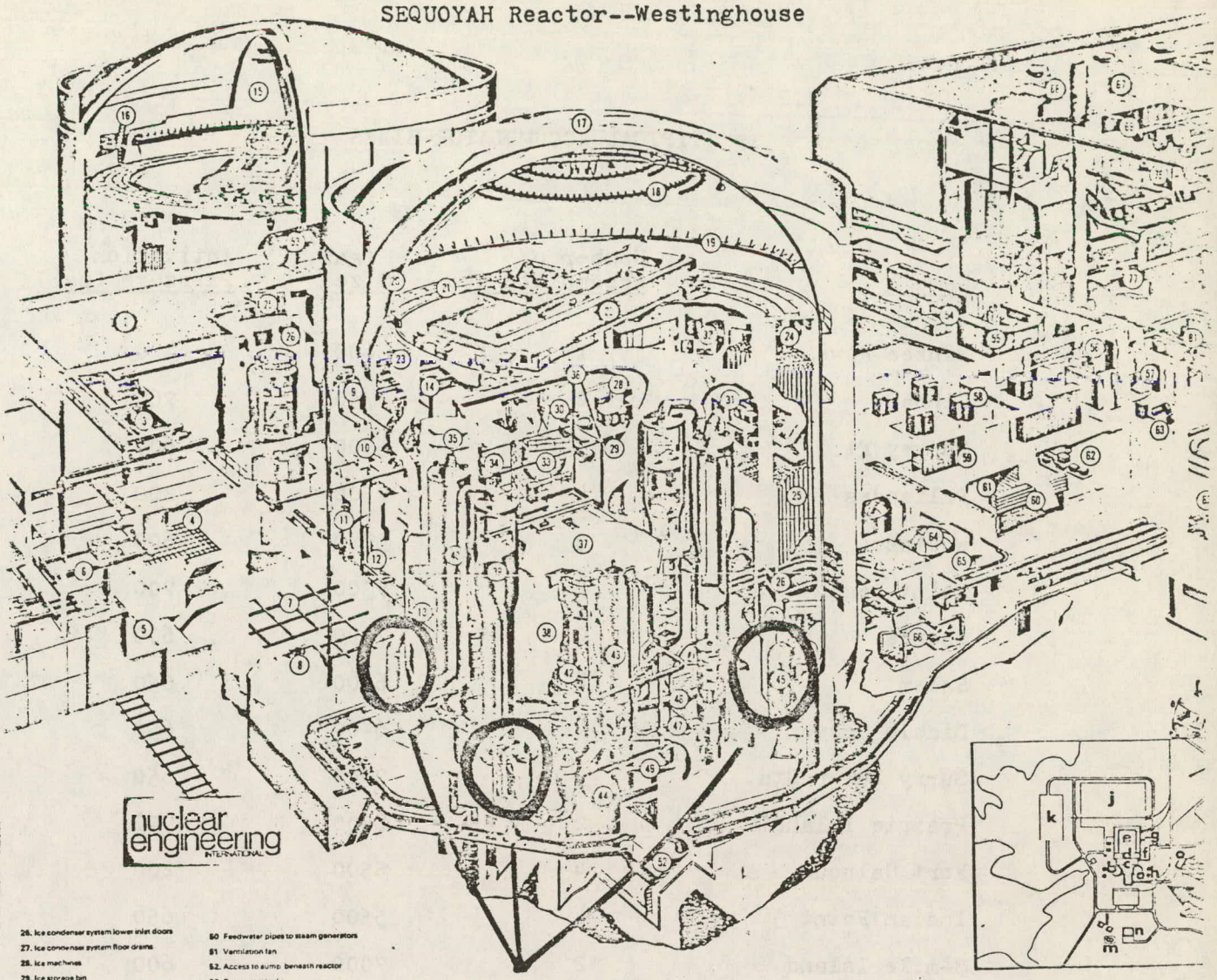

26. Ice condenser system lower inlet doors
27. Ice condenser system floor drains
28. Ice machines
29. Ice storage bin
30. Boron solution mixing tanks
31. Package chillers
32. Control rod drive equipment room
33. Equipment hatch – reactor building
34. Personnel hatch – reactor building
35. Steam generator containment
36. Manipulator crane
37. Control rod drive missile shield
38. Gate to refueling cavity
39. Steam generators (4)
40. Main steam pipes
41. Reactor coolant pumps (4)
42. Pressure Vessel – unit 1
43. Pressurizer
44. Pressurizer relief tank
45. Accumulators (4)
46. Reactor - steam generator main coolant piping
47. Pump – reactor main coolant piping
48. Steam generator pump main coolant piping
49. Pressurizer surge pipe
50. Feedwater pipes to steam generators
51. Ventilation fan
52. Access to sump beneath reactor
53. Raw water tanks
54. Main control room
55. Unit 1 control boards
56. Shift engineer's office
57. Kitchen and lunch room
58. 480 V shut-down board transformers
59. 480 V shut-down boards
60. Air intake housing
61. Filter units
62. Auxiliary building lighting board
63. Mechanical equipment room
64. Hold-up tanks (2)
65. Gas decay tanks
66. Component cooling pumps
67. Turbine building
68. Fresh air intakes
69. Gland seal water tank
70. Fire/raw water tanks
71. Turbine building crane – turbine 1
72. Turbine building crane – turbine 2
73. H.P. turbine – unit 1
74. L.P. turbines – unit 1
75. Generator – unit 1
76. Turbine – unit 2
77. Auxiliary boilers
78. Reheaters – turbine 1
79. Reheaters – turbine 2
80. Heating and ventilating equipment
81. Turbine oil tank
82. Feedwater control station – reactor 1
83. Heaters – low pressure
84. Turbine by-pass pipes
85. Feedwater pump turbines
86. Feedwater pump turbine condenser
87. Condenser
88. Service building
89. Service building loading dock
90. Switch yard
91. Heaters – high pressure
92. Exhaust fan housing

Accumulator Tanks (4)

Figure 4. Showing the location of the Accumulator Tanks in the Reactor Containment.

TYPICAL ACCUMULATOR SIZES

Name	Number of Accumulators	(gal.) Size	Activation Pressure (psi)
Yankee Rowe	1	3600	420
Ginna	2	3750	760
Turkey Pt.	3	5800	600
Palisades	4	7500	200
Robinson	3	5800	600
Point Beach	2	7500	700
Oconee	2	7000	600
Salem	4	6500	650
Diablo Canyon	4	6400	650
Surry Power Sta.	3	7000	650
Prairie Island	2	8600	700
Fort Calhoun	4	5500	200
Indian Point 3	4	5500	650
3-mile Island	2	7000	600
Zion	4	6400	650

TABLE II.

From:

Design Data and Safety Features of Commercial Nuclear Power Plants, Heddleson, F. A., ORNL, 1973.

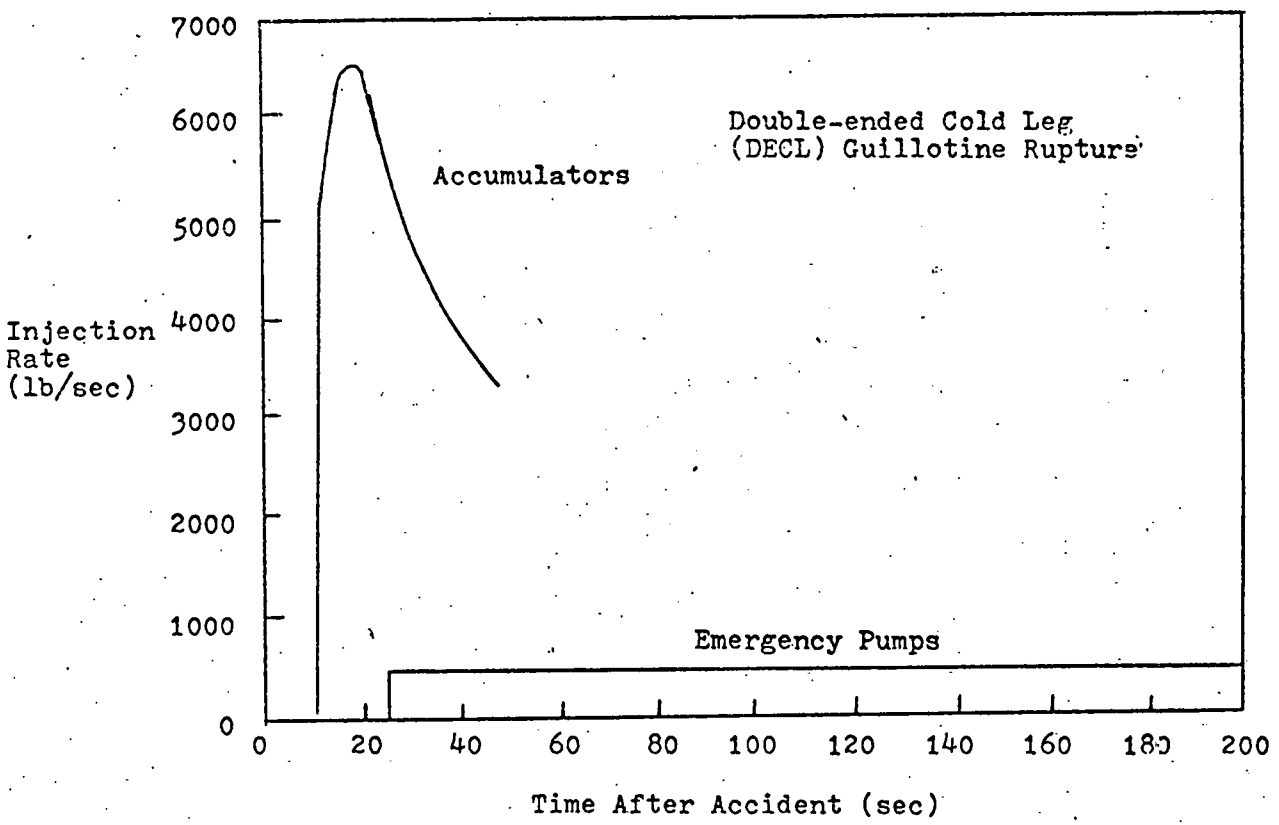

Figure 5. Accumulator Rate-of-injection curve for a complete guillotine rupture.

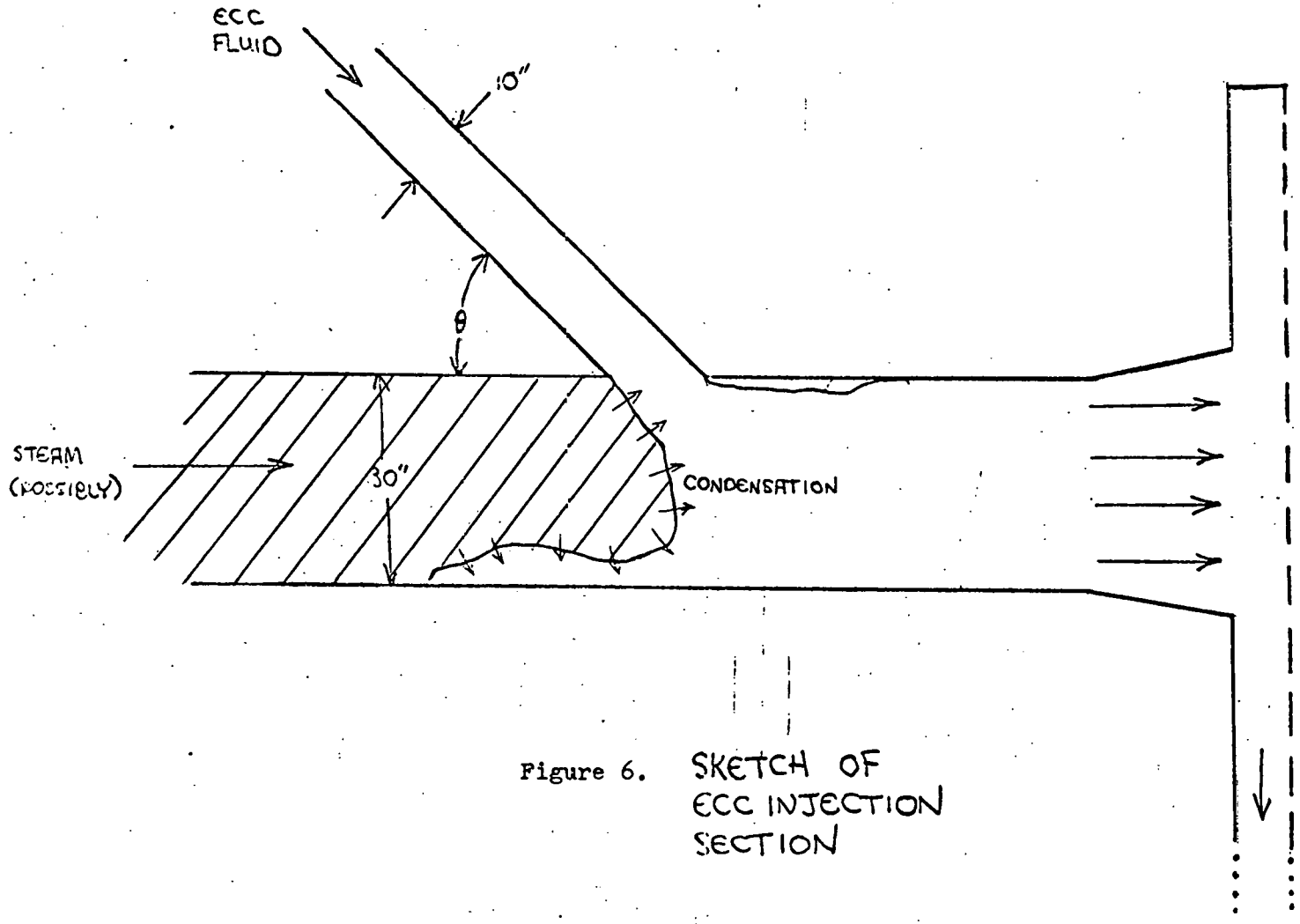

Figure 6. SKETCH OF ECC INJECTION SECTION

injection inlets). If the primary coolant loop of the reactor is full of steam toward the end of blowdown, a situation could arise with this section of the injection system in which this node operates like a jet condenser or a jet pump and - under certain conditions of instability - result in oscillations of the liquid flow in the cold legs (and hence oscillations in the injection rate into the pressure vessel). The mechanisms accounting for such instabilities in scale models are being investigated elsewhere.

Next, considering the injection location: in most cases the ECC water enters, as mentioned, via the cold legs. The location of the incoming ECC is then relegated to fixed positions around the vessel, again depending upon the design. (Figures 7 and 8.) The shape of the inlet itself might be important, but perhaps more important from the two-dimensional standpoint is the location. The location will influence the amount of interaction of water with steam in the downcomer (discussed in more detail later).

One scheme has separate ECC inlets, one on either side of the vessel, and does not utilize the cold legs in the emergency system. One scheme has two cold legs adjacent to each other; another system has a hot leg in between. Thus, a certain amount of asymmetry may be postulated.

The behavior of the fluid in the downcomer is an important consideration. The main considerations here are the hot walls of the reactor and the "accumulator bypass" phenomenon which has already been mentioned.

In the first moments after injection begins, "the water intended for the reactor core may bypass the core if a large break occurs in a pipeline coming from the plenum that accepts the emergency coolant. The back pressure required to accelerate the coolant as it turns to steam might prevent rapid admission of the emergency coolant to the

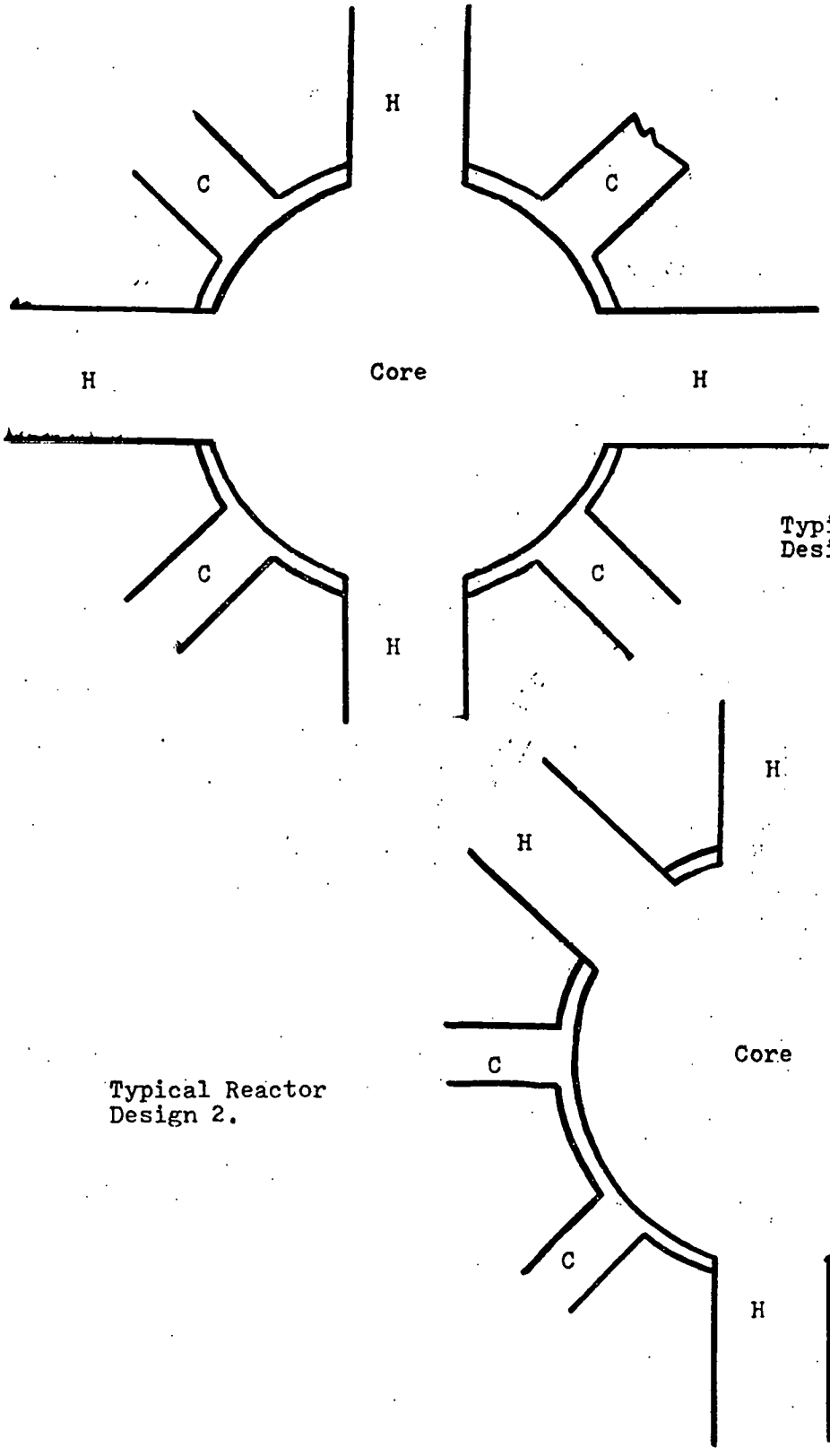

Figure 7. Typical Reactor inlet (C) and outlet (H) arrangements. Top view.

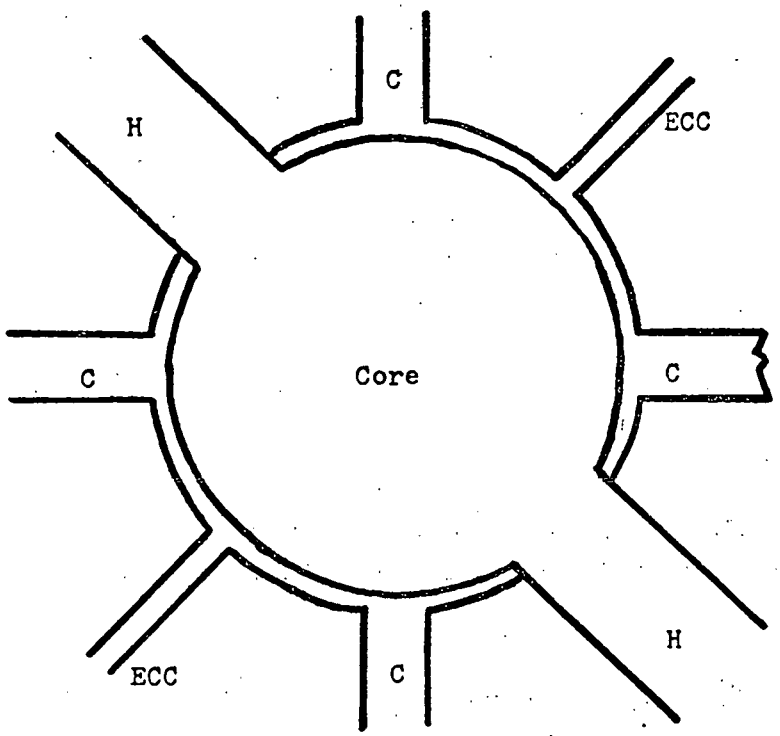

Typical Reactor
Design 3.
(Separate Injection)

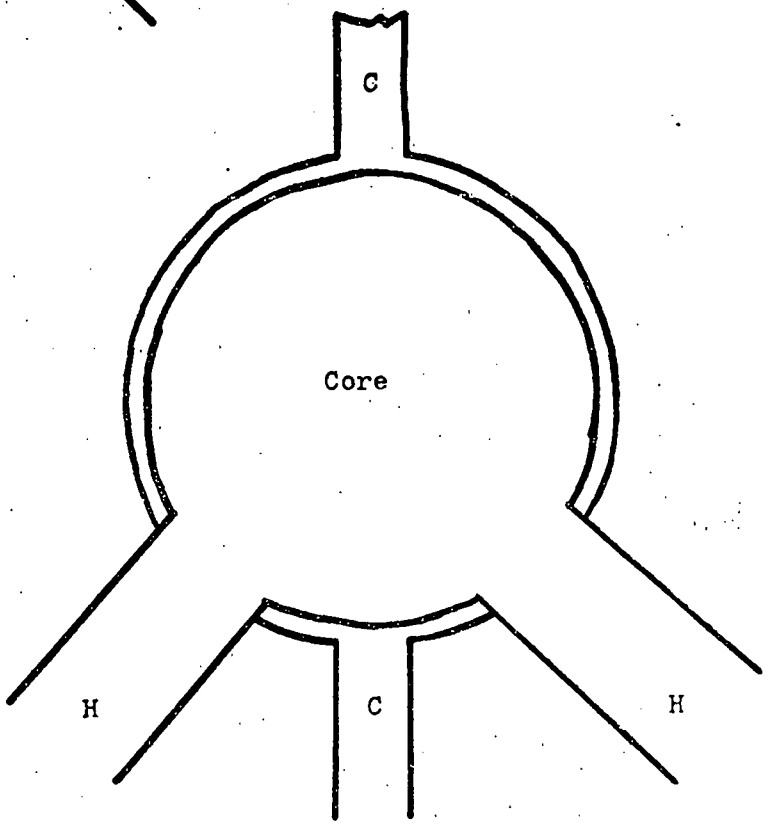

Hypothetical Reactor
Design 4.

Figure 8. Other reactor inlet (C) and outlet (H) designs.
Top view.

core region and force the fluid out the break in the pipe" [3]. (See Figure 9.) Backflow from the steam generators as blowdown proceeds is postulated to be the major source of steam causing bypass. ECC will be blown upward in the annulus formed by the core barrel and the pressure vessel and out of the orifice created by the rupture. It is possible that the escape of the steam may be limited by some type of choking condition at the break.

As it now stands, it has been mentioned, no accumulator water may be credited to the coolant inventory after blowdown until the "end of bypass" - a very small countercurrent steam flow. No credit is taken either for water which may be stored in the annulus, or an amount of water which may penetrate despite bypass. The AEC states: 'As more data become available the staff believes other methods (of modeling bypass) should be proposed and, if acceptable, should be adopted for use" [4]. This investigation is intended to provide some of that data in the form of experimental results, and hopefully some understanding of the mechanics as well. Finally, some suggestions for design improvements are made.

As far as events in the lower plenum are concerned, it is possible that even should some water penetrate to the plenum, interaction with steam may be important there, i.e., plenum voiding, in which the steam entrains water from below the core and lifts it out the break. Some reactor designs have flow skirts or mixing baffles in the lower plenum which might prevent this.

It is hoped that baffling of some kind, for example, like that sketched in Figure 10, may, by helping to direct the emergency coolant downward, increase the amount which reaches the lower plenum in the face of the countercurrent steam flow.

(One might note that in devising schemes involving additions or alterations to the pressure vessel, the changes may alter the "steady

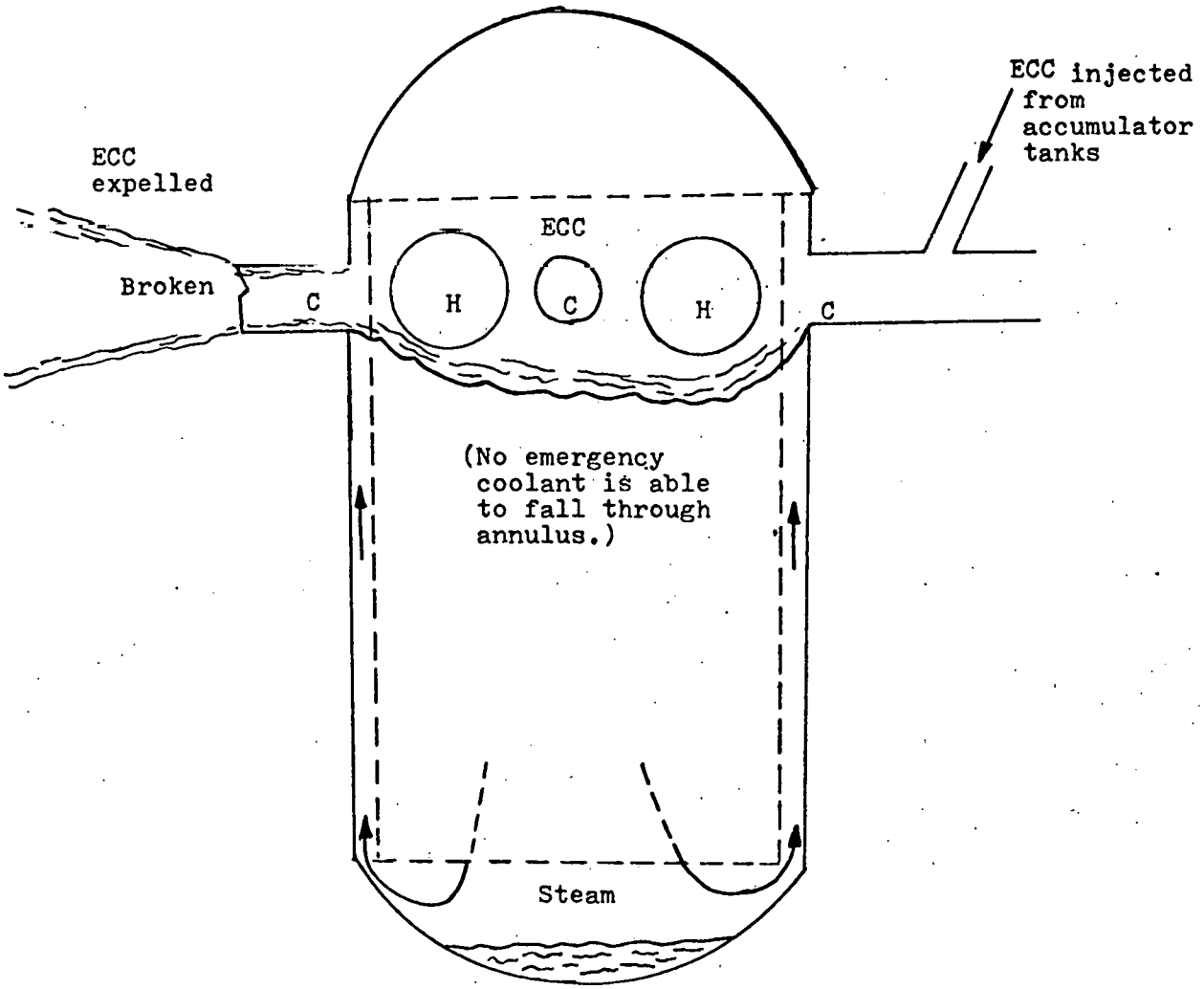

Figure 9. Momentum of steam flow may levitate emergency coolant and expel it out the broken cold leg.

ACCUMULATOR BYPASS

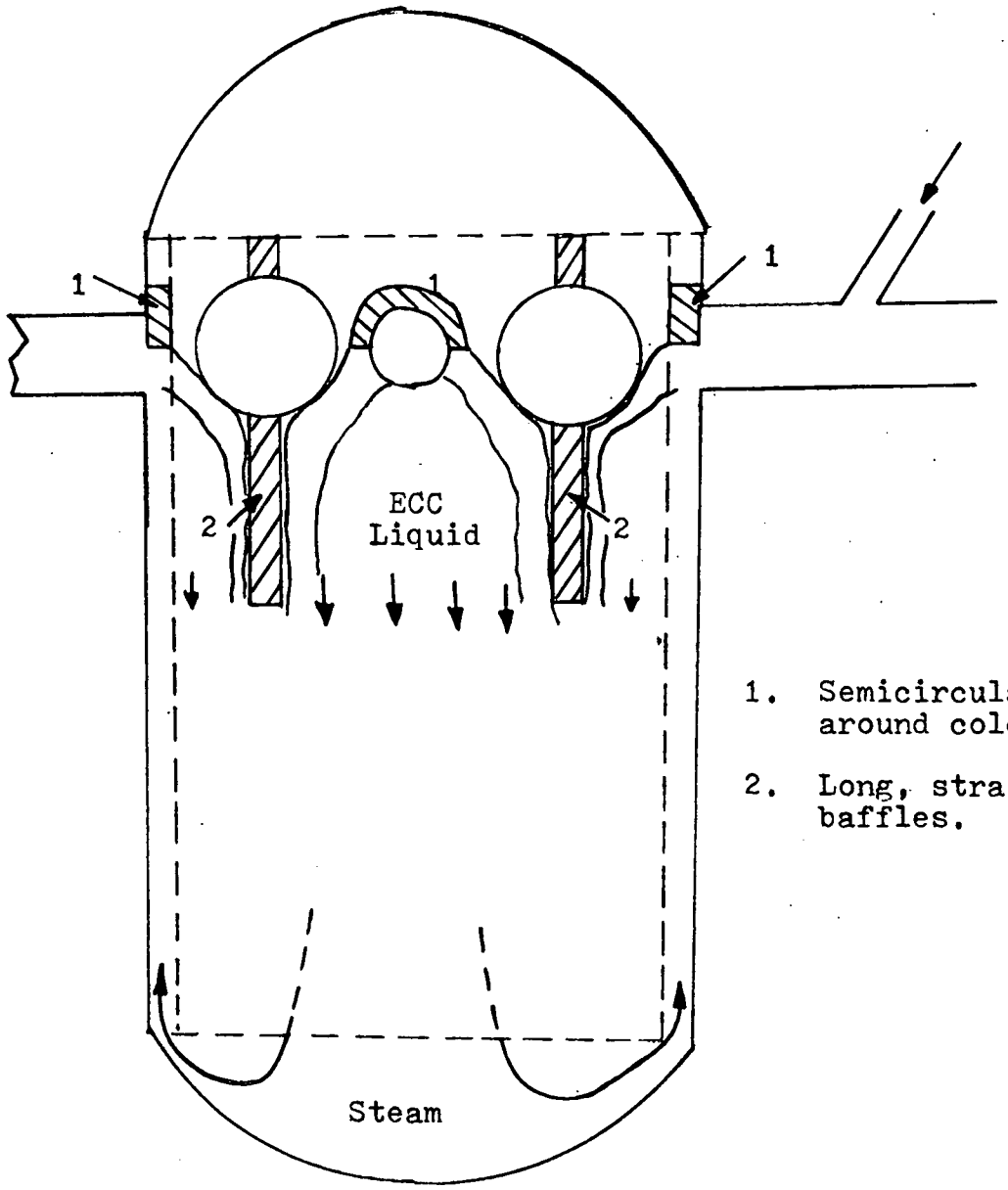

Figure 10. Two types of baffling which might be proposed to help direct ECC downward against steam flow.

state operation" of the reactor as well as the course of various postulated accidents, including the loss-of-coolant accident. The ECC system - which may never be called into actual use - should not intrude on the day-to-day operation of the reactor. The limits of what is an acceptable change will have to be defined in the light of the benefits gained and in the light of potential disadvantages which the modifications could introduce.

PRIOR KNOWLEDGE AND SPECULATION

Scope

The effectiveness of the ECC system in limiting fuel rod cladding temperatures hinges upon the events taking place in the downcomer. Whether the coolant reaches the lower plenum in some amount or is expelled by the countercurrent flow determines whether refill occurs or the cladding temperature approaches its limits instead. Because of the pivotal significance of bypass, and because so little is now known about what actually would happen, this area is open to contributions.

At the long sessions of hearings which led to the Acceptance Criteria for the ECC systems in 1973 (particularly that no ECC water is credited to the plenum until the "end of bypass") several models were proposed for acceptance.

One of the reactor vendors, Babcock and Wilcox, presented three separate formulas for quantifying the ECC bypass flow. The Regulatory staff concluded that the most conservative of these, based upon entrainment of drops and their ejection, could be used to replace the phrase "the end of blowdown" in the previous standard with a new term - "the end of bypass" - in describing the point at which ECC water could begin to be credited. This permitted a small amount of countercurrent steam flow (compared to none previously) in the calculations, without also assuming loss of all the water.

The Rule reads:

P. Cooling Water Injected During Blowdown (Applies only to Pressurized Water Reactors). For postulated cold leg breaks, all emergency cooling water injected into the inlet lines or the reactor vessel during the bypass period shall in the calculations be subtracted from the reactor vessel calculated inventory. This may be executed in the calculation during the bypass period, or as an alternative the amount of emergency core cooling water calculated to be injected during the bypass period may be subtracted later in the calculation from the water

remaining in the inlet lines, downcomer, and the reactor vessel lower plenum after the bypass period. This bypassing shall end in the calculation at a time designated as the "end of bypass", after which the expulsion or entrainment mechanisms responsible for the bypassing are calculated not to be effective. The end-of-bypass definition used in the calculation shall be justified by a suitable combination of analysis and experimental data. Acceptable methods for defining "end of bypass" include, but are not limited to, the following: 1. Prediction of the blowdown calculation of downward flow in the downcomer for the remainder of the blowdown period; 2. Prediction of a threshold for droplet entrainment in the upward velocity, using local fluid conditions and a conservative critical Weber number.[5]

Westinghouse suggested using the "Wallis correlation" (equation 6) in the calculations to define the "end of bypass" (it was also one of the three B & W proposals) but "Westinghouse has not presented anywhere on the hearing record any comparisons of the Wallis correlation with steam-water data or with decompression data. As a result, the staff can not now recommend adoption of the Wallis correlation for ECC bypass, but we do not rule out such acceptance in the future, based on appropriate supporting information" [6].

Adopting the very conservative drop flow model is the best that could have been done at the time, since two-dimensional effects are ignored and "these mechanisms are based on two-component flow theory and ignore the condensation effect that would accompany the interaction process" [7].

The omissions of the proposed models may be categorized more clearly:

1) Non-uniform steam flow

2) Water channeling

3) Condensation and non-equilibrium effects.

In a reactor, the cold legs inject water at various locations (and at changing rates) around the pressure vessel. When one considers that there is no water flow through the broken cold leg, it seems possible that a path, unblocked by water, could be provided for the

escaping steam. Steam could "prefer" this path of least resistance, reducing the steam flow in areas away from the break, where water injection is more concentrated, allowing more water to penetrate.

Conversely, "water channeling" refers to the flow pattern of the water in the annulus. Recent work at Dartmouth identifies a number of different regimes which occur in injection of water into an annulus (without countercurrent flow) [8]. These were observed to be either narrow rivers or film flow with enveloping bands of liquid.

In experiments which used a plastic downcomer model the same size as the one in this experiment, but included countercurrent air flow [9], the flow patterns when no water "bypass" was occurring looked like those observed with no countercurrent flow. When "bypass" was occurring, however, the flow patterns tended to be wavy films which generally spread across the annulus. (Figure 11). If asymmetrical effects were present then in most cases they were not as readily visible as when bypass was not taking place. (In the case where two cold legs were adjacent some asymmetry was observed, as illustrated in Figure 12. Therefore, some effect of asymmetry cannot be ruled out in the other cases.)

Droplet type flow was not observed to any great extent at any time. The critical steam velocity to support a "river" in countercurrent flow is greater than that for wavy films (which is in turn greater than that for droplets - the present end-of-bypass criterion), and leads to the hypothesis that the flow patterns achieved may influence the amount of accumulator bypass significantly. If the results of experiments show that the Wallis correlation (film flow) is the more appropriate model, the "end of bypass" could be re-redefined, allowing a slightly higher steam flow.

The hot legs, which pass through the annulus to the outside, may also have some effect. Since they are at the same level as the injection pipes in all designs, they can aid in preventing water from

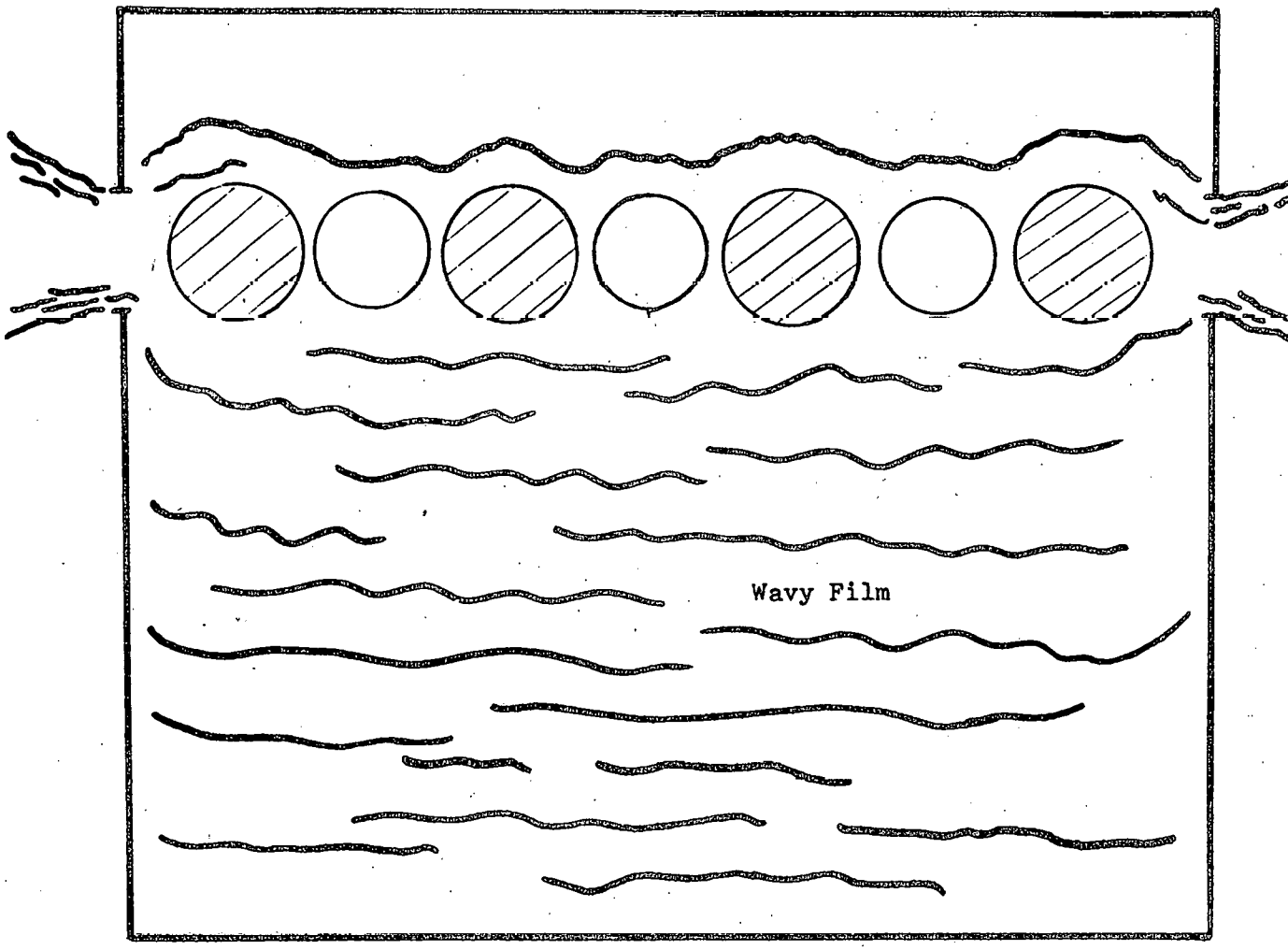

Figure 11. Illustrating flow patterns during bypass in air/water experiment. The pattern is a wavy film spread across the annulus, with water being expelled at the break.

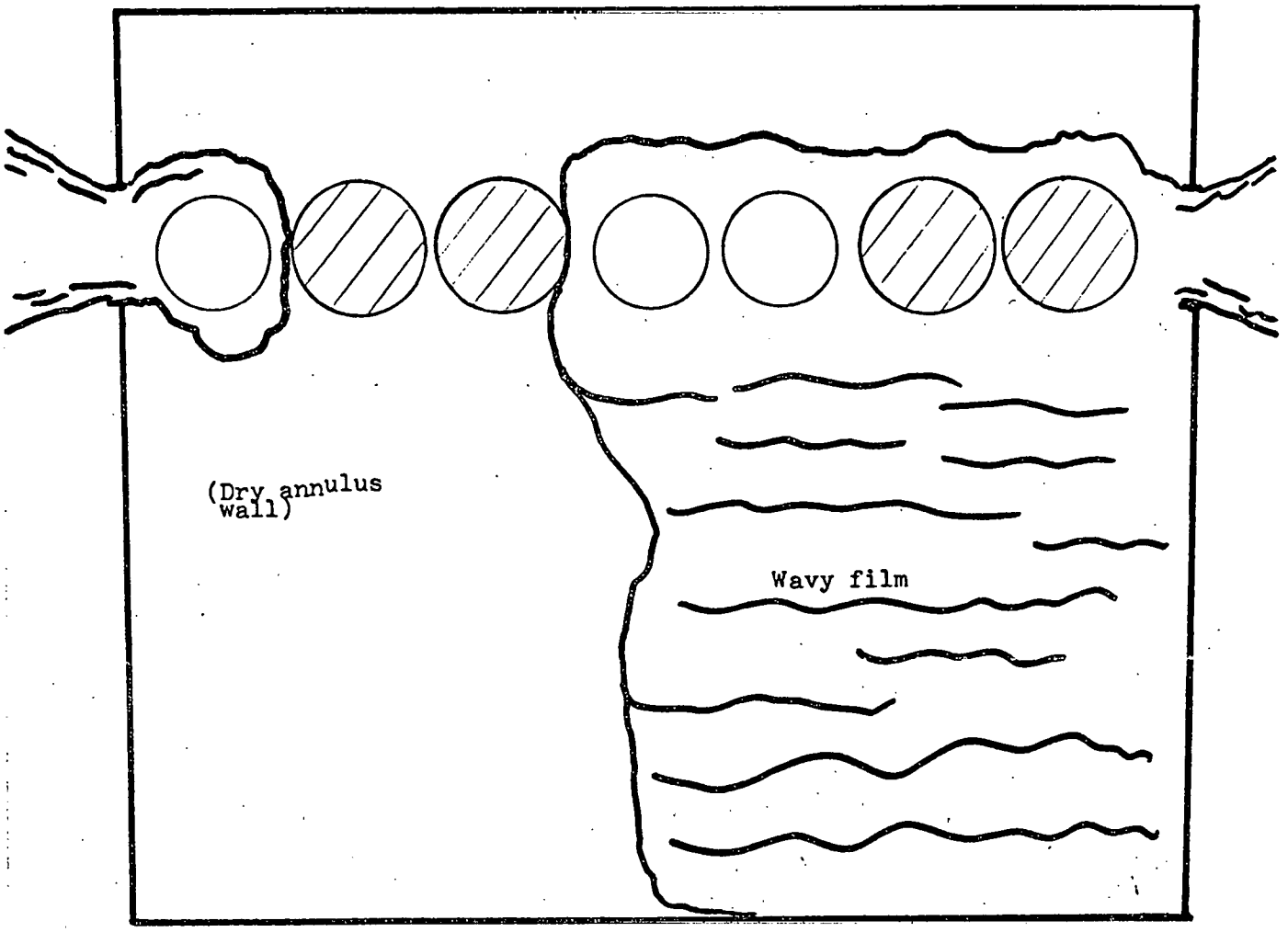

Figure 12. Observed asymmetrical flow pattern during bypass in air/water experiment. When two cold legs were adjacent, the film filled only one half of the annulus.

being carried transversely out the break. The countercurrent air flow tests found a slight effect on the flow patterns when simulated hot legs were placed in the annulus.

The third aspect refers to the condensing of steam by the emergency coolant. The interactions here are not yet fully understood. The hot walls of the reactor may heat the coolant to saturation in the downcomer, precluding any condensation in the annulus or the lower plenum.

On the other hand, if the water is sub-cooled, condensation can occur and then an important question is where the condensation takes place - in the annulus or the lower plenum. Condensing some steam in the annulus would reduce the rate of steam flow there, i.e., allow more water down. Or if condensation occurs in the lower plenum, it could substantially reduce steam flow to the annulus. Pessimistically, if all the water is being bypassed, then condensation effects would be minimal.

Thus, condensation cannot be overlooked in developing a successful model for accumulator bypass, though the hot walls may limit this. Two-dimensional effects also cannot be overlooked, although the flow pattern seems to be a wavy film that does spread across the annulus during a bypass of water.

Order of Magnitude of Flows

Figure 13 provides an idea of the magnitude of the countercurrent flows being discussed for bypass. It is a compilation of the ECCS safety calculations made by the vendors. The chart shows the cold leg momentum flux (which is the coolant flux) versus the annulus momentum flux (which is the countercurrent steam flux). Both are seen to be large.

Arrows indicate the direction in which time proceeds. Also shown for reference are various pressure points.

EMERGENCY CORE COOLANT MASS FLUX IN COLD LEG VS
ANNULUS MOMENTUM FLUX

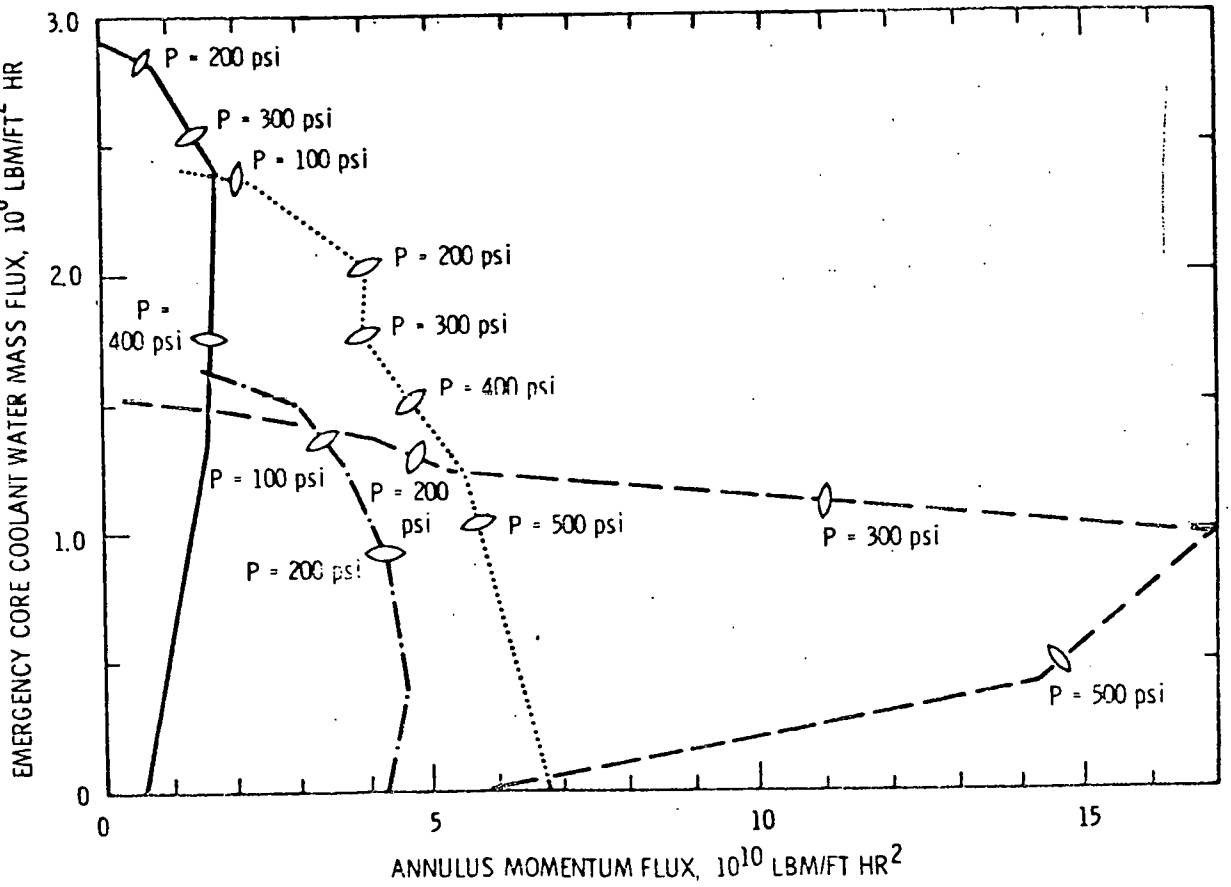

Figure 13. ECC Versus Annulus Momentum Flux
(Four typical designs)
From: STEAM-WATER MIXING, Letter Report,
Battelle-Columbus, May 17, 1974

A plot such as this will be useful in determining, on the basis of the experiment, whether the interacting flows are at levels which promote bypass or not.

THEORY

This section contains a discussion of the parameters which may be important in countercurrent flow and the accumulator bypass problem. The various one-dimensional theories (involving non-condensible gases) which might be proposed to describe the "end of bypass" are reviewed along with their nomenclature.

Wallis suggests presenting the gas and liquid momentum fluxes in terms of dimensionless variables [10]:

$$j_g^* = j_g \rho_g^{1/2} [g D \Delta \rho]^{-1/2} \tag{1}$$

$$j_f^* = j_f \rho_f^{1/2} [g D \Delta \rho]^{-1/2} \tag{2}$$

which represent a balance between the inertial and hydrostatic forces of each component.

Pushkina and Sorokin indicate that the Kutateladze number, which expresses a balance between inertial forces, buoyancy forces, and surface tension forces is appropriate for the gas flow over a wider range of tube diameters (or annulus sizes) [11]:

$$Ku = j_g \rho_g^{1/2} [g \sigma \Delta \rho]^{-1/4} \tag{3}$$

where σ is the liquid surface tension.

The two dimensionless forms may be related by defining,

$$D^* = D[g \Delta \rho / \sigma]^{1/2} \tag{4}$$

from which,

$$j_g^* = Ku / D^{*\,1/2} \qquad (5)$$

Films

Experimental work conducted at Dartmouth produced the results in Figure 14 for the minimum Kutateladze number to support a hanging film [12]. If D* is bigger than 30, the critical gas flux is independent of diameter (and contact angle) and $Ku_{min} = 3.2$ Surface tension effects become increasingly more important as tube diameters become smaller. The effect is small down to about D* = 20 and grows rapidly after that.

Using the definition in Equation 5, the minimum j_g^* to support a hanging film in a reactor annulus of 10" (D* = 180) is $j_g^* = 3.2/180^{1/2} = 0.24$.

Another way of looking at the bypass problem is the Wallis flooding model [13]. It was observed with vertical tubes of diameters from .5 to 2 inches that up to a certain value of the gas flow, there is no effect on a given liquid flow. Then, as that critical level (termed the flooding point) is reached, waves suddenly appear on the film of fluid in the tube. The waves increase the shear stresses on the surface of the fluid and increase the pressure drop in the tube by an order of magnitude. The result is that some liquid is entrained by the gas flow and prevented from reaching the bottom of the tube. The amount of entrainment (bypass) increases as the gas flow is increased above the critical value, eventually reaching a point where no liquid reaches the bottom of the tube. (This type of mechanism suggests that some water might reach the lower plenum during accumulator bypass at certain steam flows.) The observed results were correlated by an equation of the form:

$$j_g^{*\,1/2} + j_f^{*\,1/2} = C \qquad (6)$$

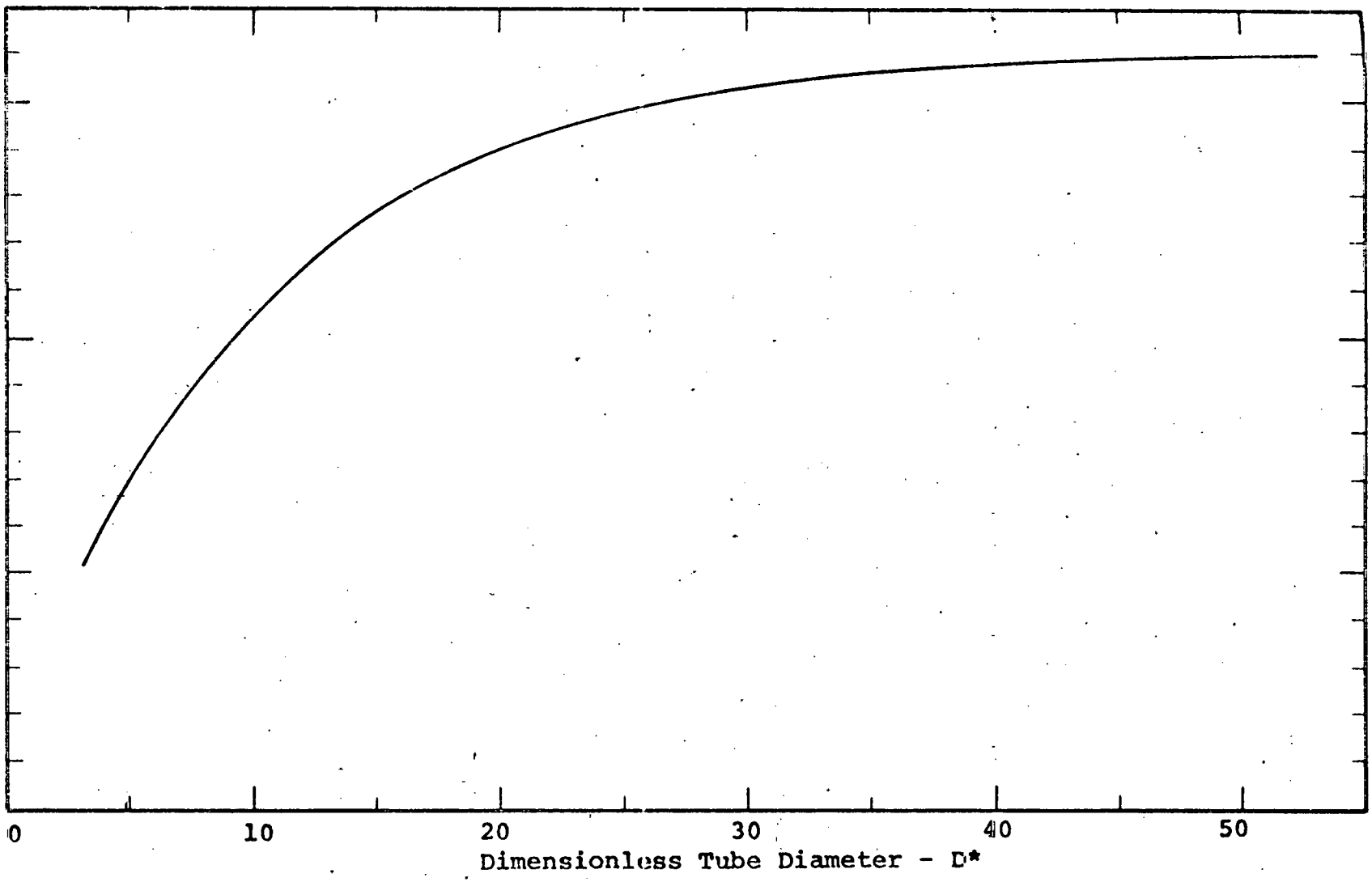

Figure 4

MINIMUM KUTATELADZE NUMBER TO SUPPORT A HANGING FILM AS A FUNCTION OF NONDIMENSIONAL TUBE DIAMETER

where C is a constant and depends upon the manner in which liquid is injected into the tube.

In the author's countercurrent air flow experiments (with an annulus the same size as this experiment), the data taken followed a correlation of this type with C = 0.94 when a single inlet was used. When other inlets or simulated hot legs were added, data lay asymptotically between the limits of being unaffected by the gas flow (straight vertical line at a given liquid flow) and the line of Equation 6 with $C \approx 1.0$ as gas flow was increased.

Rivers

We observed that at some combinations of gas and liquid flow rates water ran down the annulus in streams rather than as a film. For a rather small width stream compared to the annulus dimensions, we can neglect the effect of shear forces on the surface of the fluid in order to get an order of magnitude estimate to the minimum gas flow to support a "river". The pressure drop required to support the liquid is that required to balance the weight of the liquid, $-dp/dz = \rho_f g$, and the two-phase dimensionless pressure drop,

$$\Delta p^* = \frac{-dp/dz - \rho_g g}{(\Delta \rho) g} \tag{7}$$

becomes equal to unity.

Using Equation 11-124 from Wallis' One-dimensional Two-phase Flow [14]

$$\Delta p^* = 10^{-2} j_g^{*2} \left(\frac{1+75(1-\alpha)}{\alpha^{5/2}}\right) \tag{8}$$

with the void fraction $\alpha \approx 1$ gives the result that

$$j_g^* = 10 \tag{9}$$

to support a river of liquid in an annulus. This means that water could penetrate the annulus despite a countercurrent steam flow forty times that at which the film flow can penetrate. It indicates the kind of improvements that might be made by controlling flow patterns in the annulus.

Drops

For droplet type flow - which does not seem likely to be the prevalent type flow, but which nevertheless forms the basis for the conservative limit now in effect concerning bypass - other parameters can be identified.

The first of these balances the momentum of the gas flux against the surface tension forces in the droplet of fluid and is called the Weber number,

$$We = \frac{2 \rho_c V_\infty^2 r}{\sigma} \tag{10}$$

For falling droplets in an infinite medium, Wallis identifies [15] dimensionless parameters v* and r* to predict terminal velocity where,

$$v^* = V_\infty \left(\frac{\rho_c^3}{\mu_c g \Delta\rho}\right)^{1/3} \tag{11}$$

and

$$r^* = r \left(\frac{\rho_c g \Delta\rho}{\mu_c^2}\right)^{1/3} \tag{12}$$

which, along with a parameter,

$$P = \frac{\sigma^3 \rho_c^2}{\mu_c^4 g \Delta\rho} \tag{13}$$

are useful in determining an expression for the Kutateladze number in drop flow,

$$Ku = v^* P^{-1/12} \tag{14}$$

For large droplets (larger than about 1 mm in radius) the terminal velocity is independent of size. Very large droplets always break up into smaller drops so the minimum Kutateladze number to lift drops that are not microscopic is between 1.4 and 1.56. The j_g^* for this range is approximately 0.12 for a 10" annulus.

We see then how the "end of bypass" might be defined on the basis of different types of flow regimes (or combinations of them) in the annulus, and also how some water might penetrate despite bypass. Therefore the hope is held out that alterations like the contemplated baffles will push the flow toward the "river" regime, and take advantage of the higher critical steam flow required to cause bypass - the difference being twice as much from droplet to film flow and on the order of at least thirty times between film and river flow under the one-dimensional assumption.

THE CHOICE OF A MODEL

Selection

A study of accumulator bypass could have been conducted in a number of possible experimental rigs, using a variety of geometries, scale factors, or fluids.

The first major decision in the modeling was whether or not to include the effect of having hot annulus walls. In the reactor, the wall temperature may be on the order of several hundred degrees Fahrenheit. In this experiment, it was decided not to model this effect for two reasons. First, another student was engaged in experimentation to determine some of the effects of "hot walls". Second, it was decided to try to isolate the condensation effect in the steam/water interaction and to try to understand this piece of the problem first, before proceeding to put the whole puzzle together. The separate effects must be understood first before attempting to understand the problem as a whole.

The remaining modeling alternatives may be charted as below:

TABLE III

Alternative Models

countercurrent component	geometry	configuration	scaling
1) none	1) cylinder	1) 1 inlet	1) full
2) air	2) flat plate	2) 1 loop	2) scaled
3) steam	3) other	3) 2-4 loops	
4) other		4) variable	

Thus, flow to a lower plenum could be simulated by a scale model of one cold leg inlet to a downcomer annulus in the flat parallel plates mode, with air countercurrent flow, for example - or any combination of the possibilities in Table III.

Some of the options from the preceding table may be discarded on the grounds that they would contribute nothing new to the understanding of accumulator bypass, e.g., having no countercurrent flow at all. Similarly, countercurrent air/water studies in the flat plate geometry were already investigated. A second option that seemed out of bounds for this level of research was a full scale mock-up of a reactor.

After careful consideration of the alternatives, two major choices remained open. Either air/water interaction could be studied further, using a cylindrical geometry rather than a flat plate annulus to determine if centrifugal forces due to the pattern of the fluid flow have an effect, or a steam/water interaction could be investigated using the flat plate, or better, the cylindrical geometry.

The condensation effect was assigned priority over the geometry effect on the basis of interest stimulated by some steam/water tests at Combustion Engineering (see Appendix F). The flat plate geometry was also selected over the cylindrical geometry because transparent materials, permitting flow visualization, were much less expensive in sheets than in large tubes. Further, conducting these experiments in the same scaling (1/30) and geometry as the air/water tests permitted comparisons between the two investigations.

Ideally, it would be useful to be able to model all possible reactor geometries and test each one. To do that with exact scaling would be expensive. An "average" reactor might be hypothesized, and that one design alone tested, but the number of loops, and hence the ECC inlets and their locations, varies. (Refer to Figures 7 and 8.) However, by fitting a number of adapters to uniformly sized holes in a single model annulus, and rearranging scaled cold legs and hot legs to simulate typical designs merely by changing adapters, the typical reactor designs could all be closely reconstructed with one model.

It has already been mentioned that the choice of the flat plate geometry eliminates some centrifugal effects that may be present in a cylindrical geometry. The injected water, because of centrifugal forces, might tend to "hug" the walls of the pressure vessel more than in the flat plate geometry, and therefore aid water in reaching the lower plenum.

Cylindrical geometry could also eliminate the necessity of sealing a lot of joints in the experimental apparatus, but hopefully any leakage from the joints could be minimized with a little judicious glueing and clamping.

In the flat plate geometry the "break" is modelled by two holes - each one half the area of a cold leg - in the spacers on the side of the apparatus, centered at the level of the rest of the cold legs. Again, there may be some geometry effect in "break" modelling because emergency coolant in the reactor would have to make a turn outward in the process of being bypassed, whereas it does not have to in the apparatus. However, if the arguments are correct, then both of these shortcomings err on the conservative side - they make it easier to bypass water in the model.

The model chosen as the next logical step in the experimental program to study accumulator bypass can be described briefly as a steam/water, 1/30 scale, flat plate annulus, with the capability of simulating a number of vessel designs by means of rearranging a set of adapters to the injection inlets.

Size

It has already been noted that the 1/30 scaling was used because it was the same as that used in the air/water tests, and because it fit the available steam supply (Appendix A).

The scaling of each dimension was linear, that is, no dimensions were significantly distorted, particularly: the cold leg centerline height

TABLE IV.

TYPICAL REACTOR DIMENSIONS

Height of Annulus--28 feet

Height above Pipe Centerlines--6.5 feet

Cold Leg Inside Diameter--30 inches

Hot Leg Outside Diameter--51 inches

Inner Diameter of Pressure Vessel--172 inches (14.3 feet)

Spacing of Hot and Cold Legs--45°

Lower Plenum Radius--90 inches (approximately)

Gap between Pressure Vessel and Core Barrel--10 inches

Annulus Area--35.5 square feet

TABLE V.
EXPERIMENTAL DIMENSIONS

Height of Annulus--1 foot

Height above pipe centerlines--3 inches

Cold Leg Inside Diameter--1 inch

Hot Leg Outside Diameter--1.7 inches

Width of Annulus--17.5 inches

Spacing of Hot and Cold Legs--45° (2.3 inches)

Gap between Plates of Annulus--0.375 inches

Annulus Area--6.56 square inches (0.046 feet square)

compared to the annulus length, or the annulus gap size over the annulus length. Such distortion has been carried out in other tests, but it was decided to keep as close as possible to linear scaling in the absence of a good rationale for doing it any other way. (In a few instances for the convenience of using standard sizes, some dimensions were rounded off slightly.)

Just as it is helpful to have some idea of the actual bypass steam and water flows, it is also helpful to have some idea of the actual size of the reactor. Information compiled from several drawings lists typical sizes for a reactor (Table IV). By rearranging hot and cold legs in the model, typical design variations may all be closely simulated by the single annulus.

The scaled apparatus dimensions are listed in Table V, and are the ones used in construction of the model.

EXPERIMENTAL APPARATUS

Figure 15 illustrates the annulus and the lower plenum portions of the experimental apparatus in detail.

The annulus consisted of two 12 x 18 inch polycarbonate plates (3/8 inch thick) separated by 1/4-inch spacers (also 3/8 inch thick) which were placed around the perimeter of the plates except for the bottom, thus forming a sandwich of a 3/8 inch plate, a 3/8 inch gap, and another 3/8 inch plate. Polycarbonate was chosen as the material because, unlike acrylic, it is able to take the steam temperatures without softening. The two blowholes which simulated the cold leg break were located on either edge of the annulus and were 3/8 x 1 1/16 inch segments removed from the side spacers at the cold leg height. The spacers on the side were glued and clamped. The top spacer was clamped only so that access to the annulus was possible.

The hot legs were plugs 1.7 inches in diameter that bridged the annulus as they would in a reactor. All of the inlet holes in the annulus were the size of the hot legs. Cold legs could be fitted to the holes by means of adapters. In this way, the arrangement of the hot and cold legs could be varied.

The annulus was mounted on a 14 x 14 x 1/2 inch polycarbonate baseplate so that it could easily be bolted onto the top of the barrel. (It was mounted diagonally on the baseplate to take full advantage of the opening on the top of the barrel.)

The barrel itself was not a scaled lower plenum, being too large in volume. It was used because it was already equipped with a number of features desired (drains and taps) and therefore construction of a plenum from scratch was circumvented. The apparatus then models the downcomer, but not the lower plenum of the reactor. When the steam is present in the annulus (followed by water injection) the size of the

lower plenum is not expected to matter much since the steam fills the annulus and the barrel and heat losses are small. (In Appendix B these heat losses from the barrel and the piping are estimated and found to be negligible at all steam flows. The annulus itself was assumed to be adiabatic.) The actual barrel dimensions are 22 inches diameter and 24 inches high.

Steam entered the barrel through a 2-inch pipe located on the side of the barrel near the top. A pressure tap was located on the top of the barrel, and a quick-opening drain valve (a lever-activated gate valve) was located on the side, near the bottom. Viewing windows of thick Plexiglas were already on it, as shown in Figure 15. A sightglass was also added.

The steam supply was Thayer School's heating and hot water main steam line. Flow was controlled with a gate valve, and measured with an orifice plate. The orifice plate design was based on information from the handbook "Steam Flow Meter Engineering" by Brown [15] (Appendix C). The complete piping layout, following ASME code for the pressure taps, is shown in Figure 16. The condition of the steam entering the barrel was saturation or slight superheat at 215-217°F.

The water supply was the school ground water supply at about 55°F. For some test runs, 100°F and 140°F water was obtained from the hot water faucets. Flow rates were measured either by a single 12.4 gpm maximum rotameter, or by that one plus a 6.3 gpm maximum rotameter. The lowest readings on each were 8% rated flow.

The 12.4 gpm rotameter was used in tests where one or two inlets were required. With two inlets, the flow was divided into two branches. With three inlets, flow was divided in the 12.4 gpm device, and the 6.3 gpm device was added in parallel. Maximum possible flow with one or two inlets (or hot water) was about 11 gpm, and 15 gpm with three inlets.

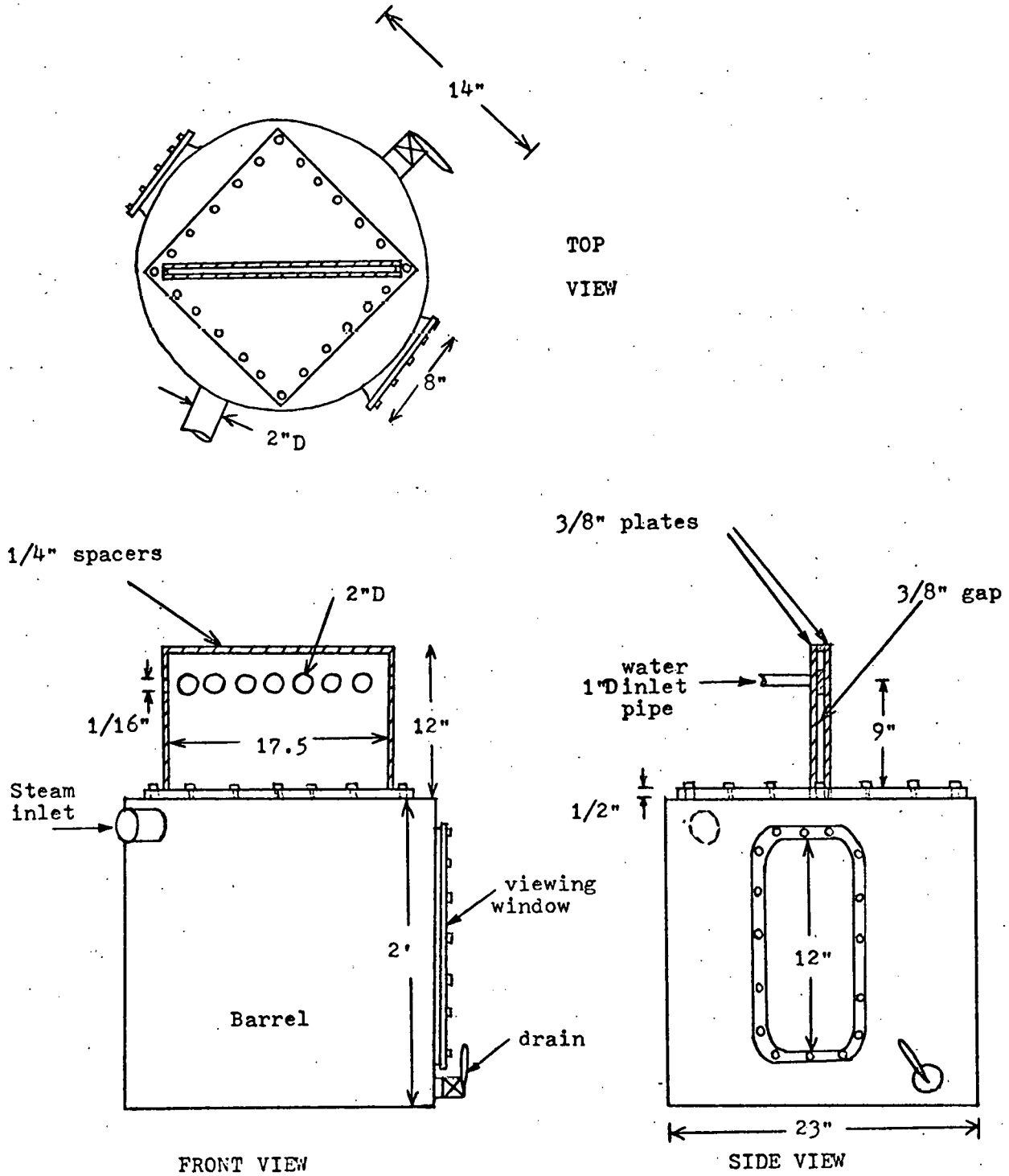

Figure 15. Apparatus

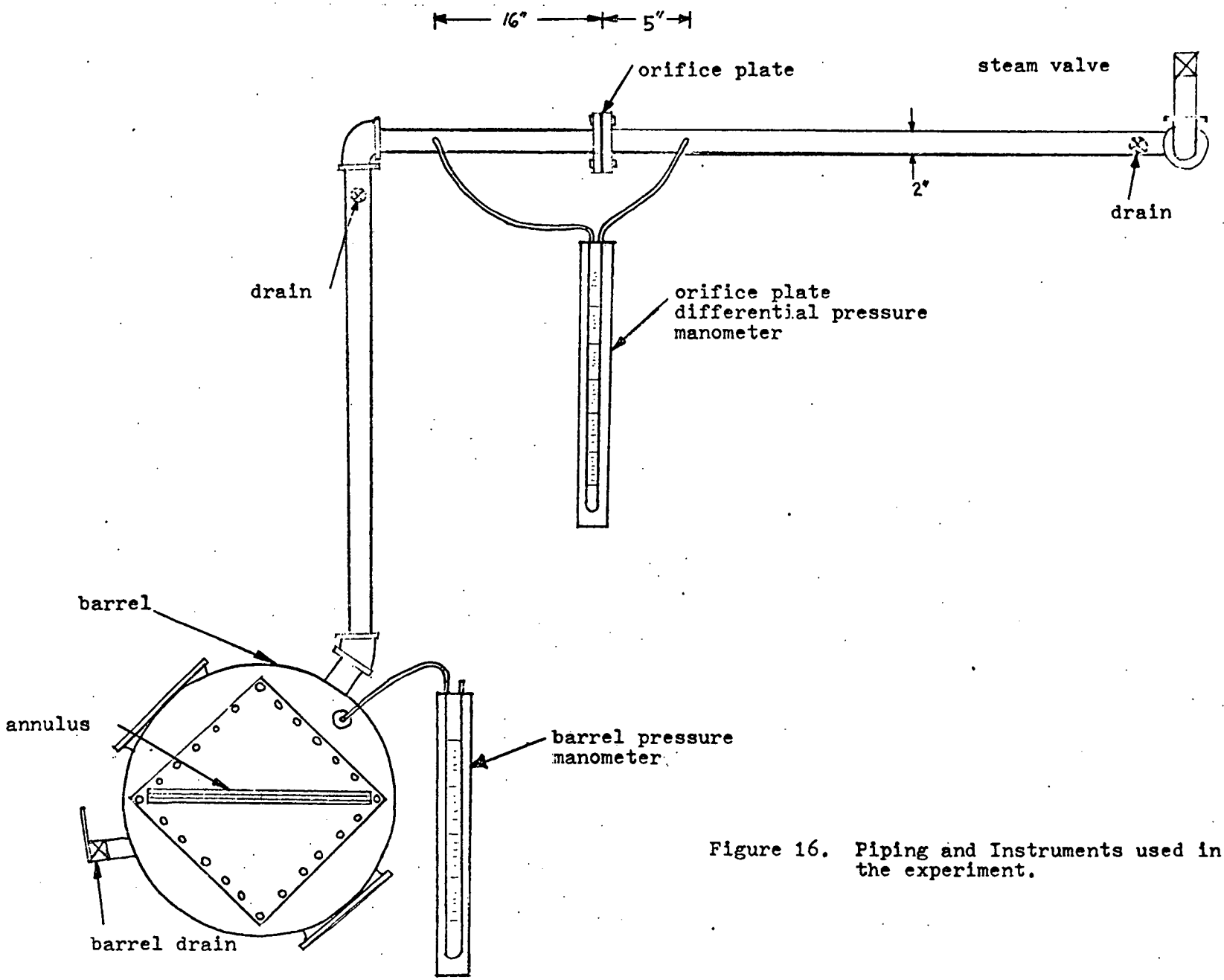

Figure 16. Piping and Instruments used in the experiment.

THE EXPERIMENTAL PROCEDURE

Tests were conducted both by setting the water flow and increasing the steam flow to the flooding point (water-first), and by setting the steam flow and increasing the water flow to the point where flooding ceased (steam-first). This latter technique more realistically models the actual ECC injection and bypass process.

Water-first

In a test like this, the water flow would be established at a certain value (after prior warming of the barrel by steam flow). The steam flow, having been shut off after readying the apparatus, would then be increased in increments from zero until flooding occurred.

At each steam flow level, the differential pressure across the orifice plate would be observed and the corresponding mass flow rate recorded. In early tests, the static pressure of the steam was recorded to establish the condition of the steam, but this measurement was later discontinued. Steam temperature and inlet water temperature were also recorded. For each steam flow increment, the temperature of the water issuing from the lower plenum was read, and pressure measurements from the barrel were made - with the drain closed. The standard procedure was to leave the drain open for awhile at the new steam flow rate, close it, take the pressure measurement, then open the drain again and measure the water temperature with a thermometer.

When bypass occurred, the drain was left closed long enough for flow to establish itself and institute a new pressure in the barrel, although it usually oscillated.

The original intention of the experiment had been to measure the flow rate of the water into the lower plenum during bypass, but in all cases, when the system was expelling water, the amount of fluid

reaching the lower plenum was not large enough to measure (see EXPERIMENTAL RESULTS). The system was found to either allow all of the water to penetrate, or virtually none.

Steam-first

In tests where steam flow was established first, the drain valve would remain closed throughout the test. Since little water got into the lower plenum during flooding (bypass), the water temperature there could not be measured. Vessel pressure, however, could be recorded if the limits of the 52-inch manometer were not exceeded (which they sometimes were during oscillations).

The water flow would be increased to the point where flooding ceased. This was identified by 1) a drop in plenum pressure, and 2) the water penetrating the annulus.

In tests where two rotameters were necessary, increasing the liquid flow uniformly was sometimes difficult, but the data seem to show that even large discrepancies between the two rotameter flow rates did not produce large discrepancies in the results.

In both cases, visual observations supplemented the experimental determinations, and are discussed in the appropriate areas of the Experimental Results.

EXPERIMENTAL RESULTS

Test Series I - Vessel Design

The first series of experiments simulated the reactor designs with no obstructions other than scaled hot legs in the annulus. Figure 17 illustrates the placement of the cold (C) and hot (H) legs in each of the three typical reactor designs, plus a fourth arrangement with a single inlet.

Sketch 17a represents the typical design, in which hot and cold legs alternate.

Figure 17b shows a design which has separate emergency coolant inlets that are 1/3 the diameter of the cold legs (C/3) and located at the same level as the cold legs. The cold leg inlets, which in this design are not then used for ECC injection, were merely blocked off by plugs (P) in the appropriate inlet holes of the model.

Another simulated design is shown in Figure 17c. Here, pairs of hot and cold legs are placed adjacent to each other.

The fourth arrangement (17d) is intended to model the CE Annulus Penetration Test rig in a flat plate geometry. In the CE experiment, there was a single cold leg inlet and a single outlet located 180^{o} around the vessel from the inlet.[17] In my experiment, two hot legs were also left in, a factor which was not expected to alter the results significantly.

From now on, when the designs are referred to by number, the understanding will be that this is as they were modelled in the experiment and sketched in Figure 17.

Steam-first and water-first tests were conducted with each of the designs and the flooding locus plotted.

Preliminary Results

The first result that became immediately apparent from the experiment was that the transition from complete water penetration in the an-

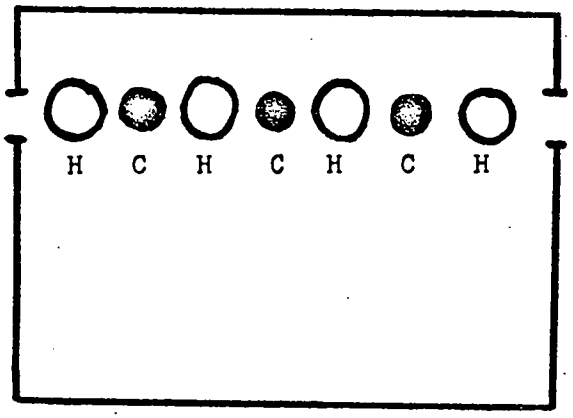

17a. Design 1.

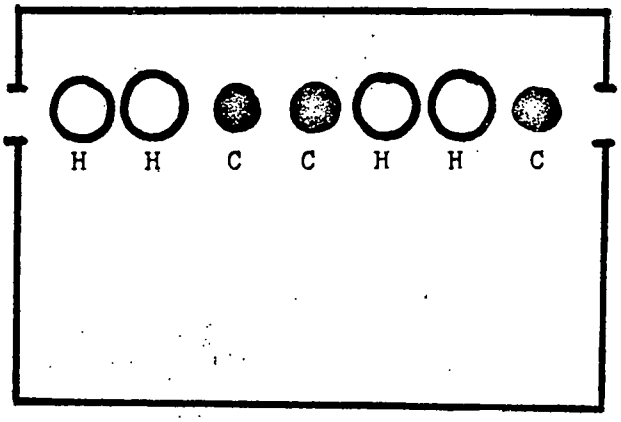

17c. Design 2.

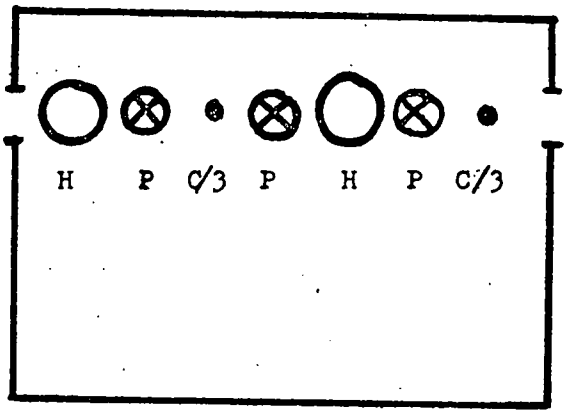

17b. Design 3.

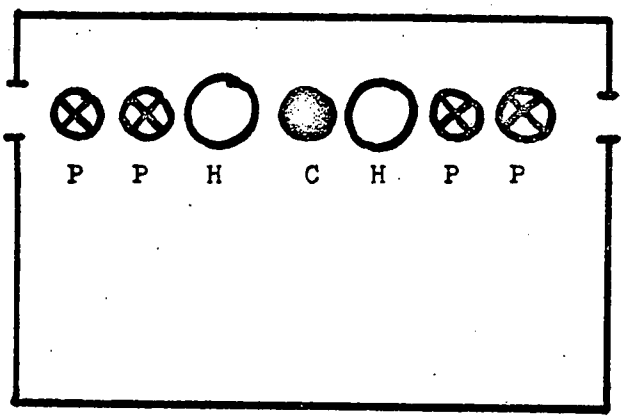

17d. Design 4.

H -- Hot Leg disk

C -- Cold Leg water inlet

P -- Plug

Figure 17. Arrangement of water inlets to simulate typical reactor designs in experiment. (See Figures 7 and 8)

nulus to zero water penetration in the annulus was fairly sharp. Thus, flooding - the appearance of the water surface waves and the increase in pressure - coincided with complete bypass of the injected water. The water penetration was essentially an all or none proposition.

Although it is maintained that almost no water penetrated, there are irregularities to consider. Some spurts of water could be seen (through the viewing windows in the barrel) to penetrate the annulus and drop into the lower plenum while bypass was occurring - especially when tests were being run with hot water - but the amount of this was so small in all cases that measurement was not possible with this apparatus (less than 1 gpm). Further, this small amount of penetration was irregular rather than a steady flow. It appeared that the penetration was due more to chance interactions of the water in the annulus, or was a result of the pressure oscillations allowing a little water to penetrate, rather than a steady phenomenon.

The experimental results did not follow anything like the Wallis correlation (Equation 6) over the majority of the flow rates tested. In the water-first tests, a critical steam flow would be reached at which flooding suddenly occurred and all of the water would be expelled from the annulus (prior to that all the water would enter the lower plenum). In the steam-first tests, a critical liquid flow would be reached at which flooding suddenly ceased, and all the water would penetrate.

The locus of points plotted in all the graphs of experimental data represents the transition from 100% water penetration to (essentially) zero penetration for the given values of steam and water flow. Above the plotted locus (either steam- or water-first) flooding and complete bypass would occur. Below the plotted locus, the system would not be flooded, and all water injected would enter the lower plenum.

Because of this "all or none" nature of the result, it was decided to plot the data using the (annulus) inlet momentum flux of the

liquid component rather than the outlet momentum flux, since after bypass occurred, the momentum flux of the liquid into the lower plenum would be zero.

In addition, data are plotted as a function of the dimensionless momentum flux j* rather than $\sqrt{j^*}$, since j* is proportional to the mass flow rate and thus it is easier to visualize for example that two times a given j_g^* corresponds to twice the steam mass flow rate.

Graphical Procedure

Figures 18-21 show the results of simulating the different reactor designs. The manner of presentation in the graphs is outlined in this section so that the graphs may be understood.

The coordinates on the graphs, j_f^* and j_g^*, are the dimensionless momentum fluxes of each countercurrent component (as defined in Equations 1 and 2). Steam flow generally ranged from $j_g^* = 0.4$ to 2.0. Water flow ranged from $j_f^* = 0$ to 0.5 with three inlets, and to 0.4 with one or two inlets. Appendix C shows how j_g^* and j_f^* are calculated from the experimental flow measurements.

It was useful to include one reference line in the figures. The solid line labelled $R_t = 1.0$ in each graph represents the locus where the enthalpy of the steam is just enough to raise the water to saturation temperature (the steam can just be condensed by the water). Mathematically,

$$R_T = \frac{W_w C_p \Delta T}{W_s h_{fg}} = 1.0 \qquad (15)$$

A more extensive discussion of this subject can be found in Appendix D, along with the calculations of the slope of the line from the fluid properties. In the Figure 18 test, only one water temperature (55°F) was used in the experiment, and therefore there is only one line $R_{t\,55} = 1$ -

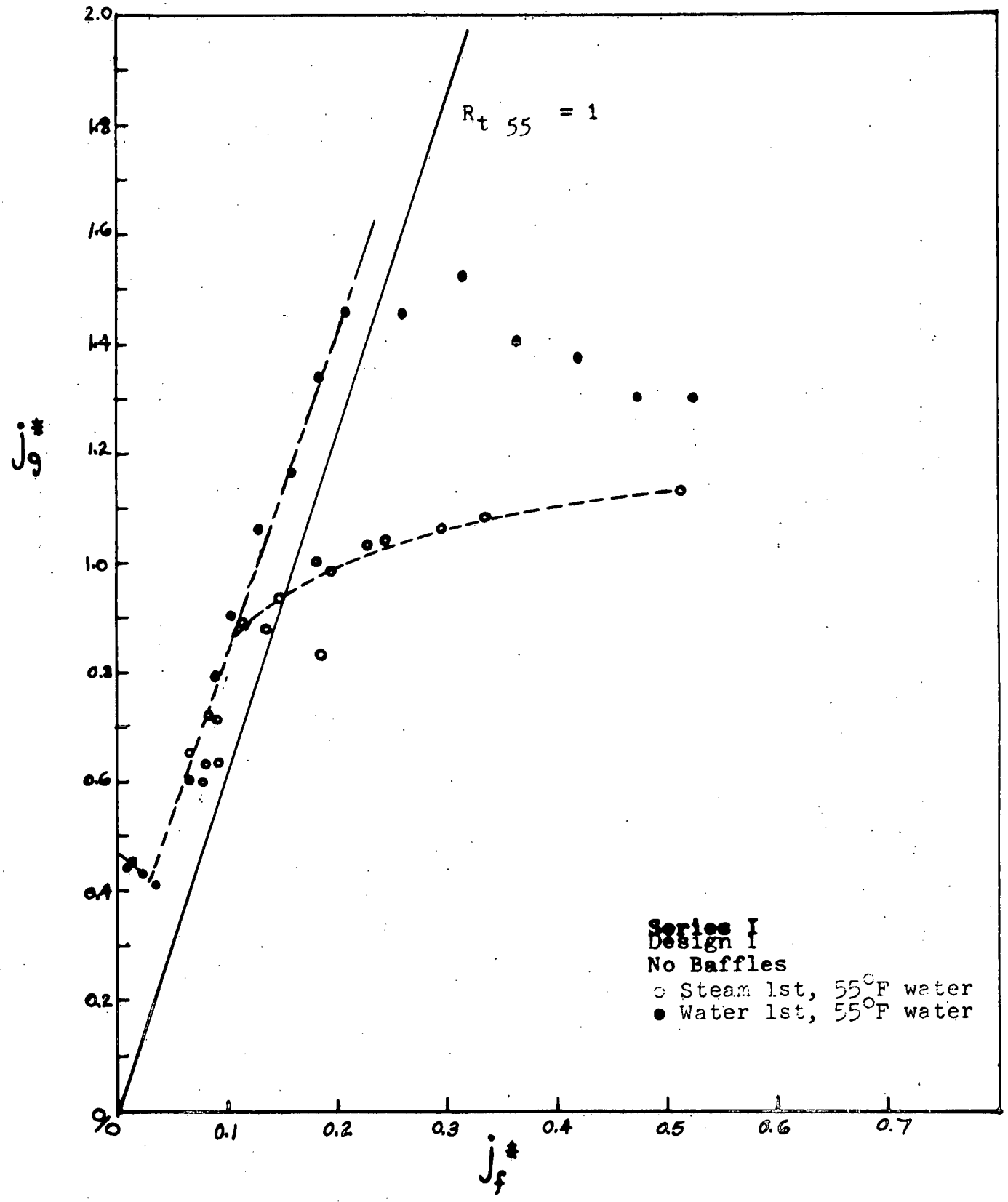

Figure 18. Series I.
Experimental Results, Design 1 with no baffles.

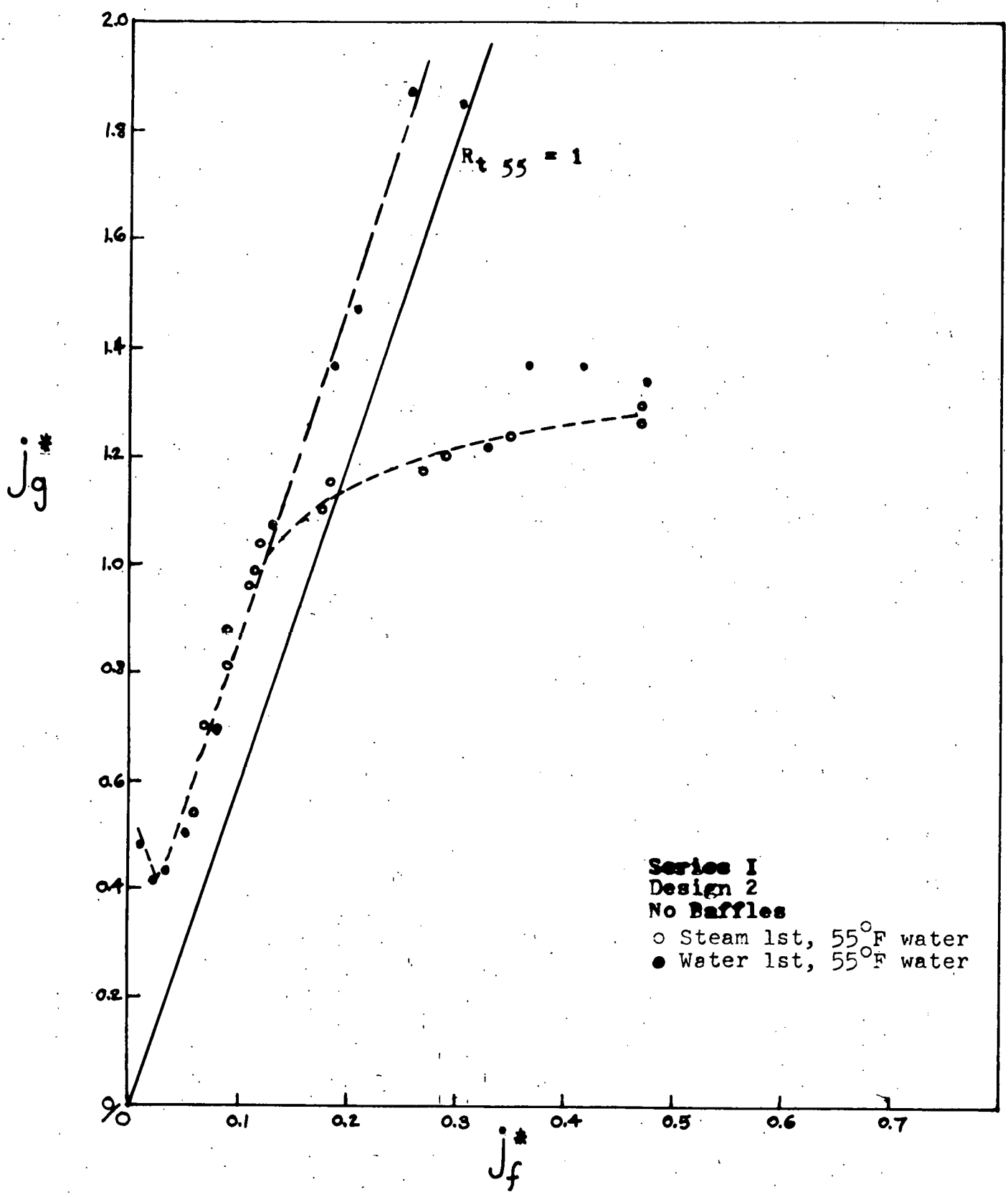

Figure 19. Series I.
Experimental Results, Design 2 with no baffles.

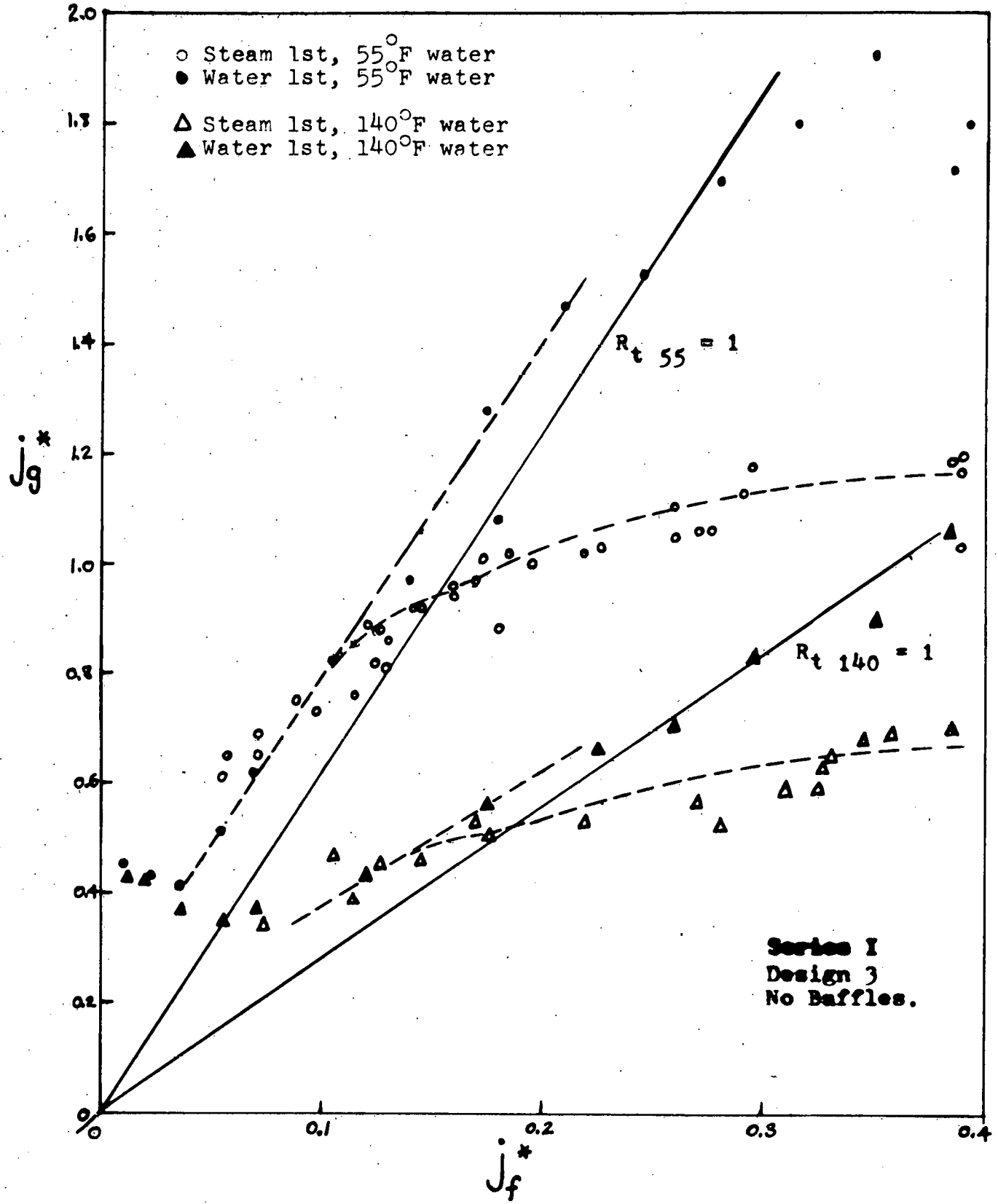

Figure 20. Series I.
Experimental Results, Design 3 with no Baffles

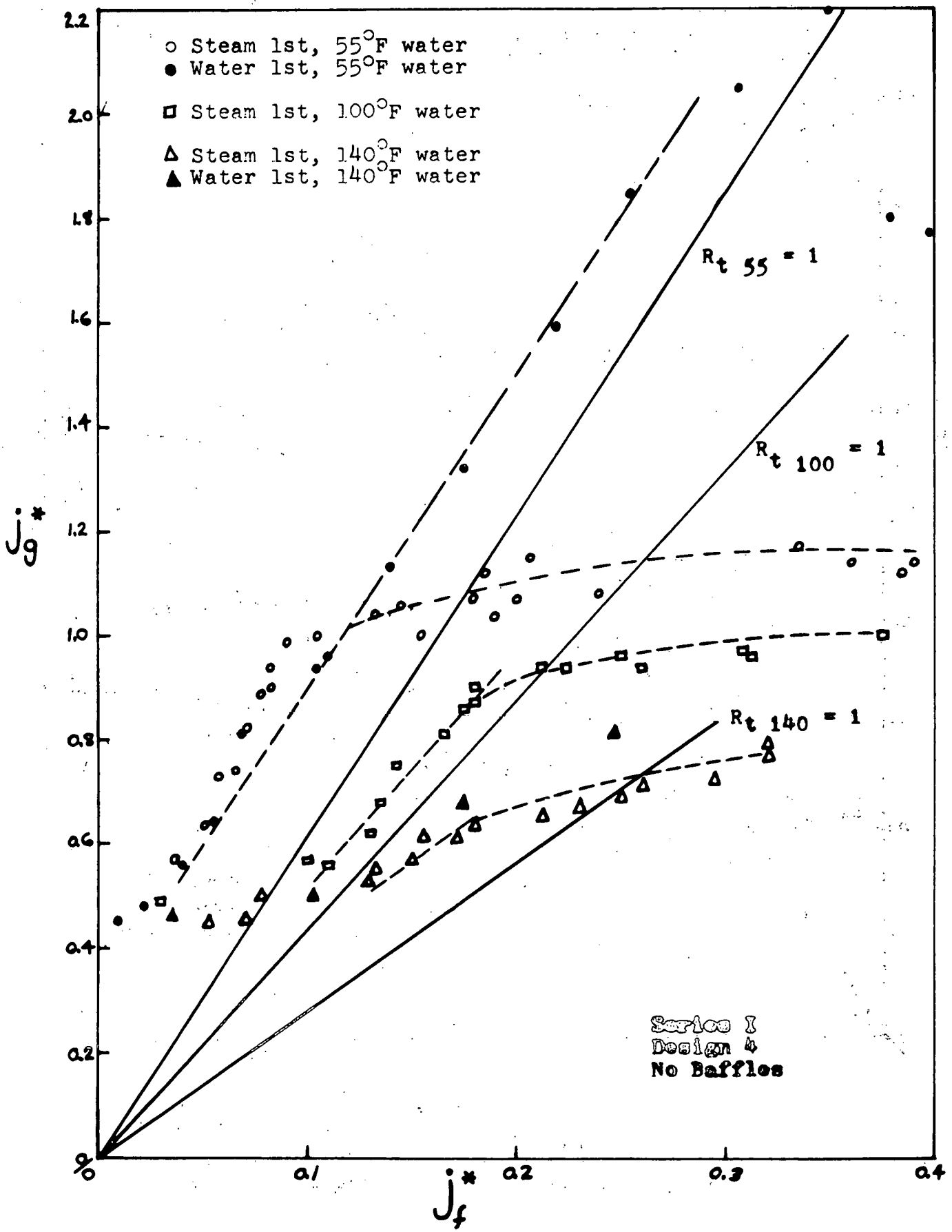

Figure 21. Series I.
Experimental Results, Design 4 with no Baffles.

the subscript indicating the water temperature. In the Figure 21 test, three water temperatures were used (55^{o}, 100^{o}, and 140^{o}F) and each water temperature signifies a new locus for $R_t = 1$, since the amount of sub-cooling of the inlet water is different. Again, the subscript indicates the water temperature.

Solid symbols always indicate water-first tests; open symbols, steam-first tests. A dashed line is drawn through the steam-first data points to indicate that locus because this type of test more closely simulates accumulator bypass. Water-first data points are shown, but the complete locus is not drawn, to avoid overly cluttering the graphs (from the point of view of studying bypass, these tests are mainly of academic interest anyway). Table VI is a key to the experimental plots.

Description of Results

Figures 18-21 represent the results of modeling the four designs in Figure 17, in the same order. The same pattern emerges in each test for the steam-first and for the water-first results.

Water-first.

The data for the extreme left hand portion ($j_f^* = 0\text{-}0.05$) in the graphs indicates that the steam flow required to cause flooding decreases with increasing water flow. Water flows were determined by direct measurement at the very low flow rates.

The decreasing trend continues down to a point near the intersection with the line representing $R_t = 1$, and then the data parallel this line upward, at higher j_g^* values than predicted by the locus $R_t = 1$.

Increasing steam flow rates are required to cause the flooding transition until $j_f^* \tilde{\sim} 0.3$ when the trend again becomes decreasing, eventually leveling off at a constant steam flow rate to cause bypass.

TABLE VI.

KEY TO FIGURES.

Lines.

————————	Thermodynamic Ratio equals unity ($R_{t\ x} = 1$). The locus representing an energy balance in which the the inlet water can just condense the steam flow. The subscript (x) indicates the water temperature.
- - - - - - - - - - - -	Locus of end-of-bypass data points for steam-first experiments
——— – ———	A portion of the locus of bypass for water-first tests, parallel to $R_{t\ x} = 1$ line.

Symbols.

●	Water-first test, 55°F water data
▲	" " ", 140°F water
o	Steam-first test, 55°F water
□	" " ", 100°F water
△	" " ", 140°F water

Steam-first (dashed lines).

Because of the rotameter limitations, data were not available at very low liquid flows in the steam-first tests.

The data exhibit the same upward trend as the water-first tests (parallel to the $R_t = 1$ line) on the left portion of these curves. However, rather than continuing upward along that line to high steam flows, as the water-first data did, the steam-first results level off immediately to some constant steam flow level. The leveling off begins at about $j_f^* = 0.2$ and $j_g^* = 1.0$ (for 55°F water). In terms of the experiment this means that in a small range of steam flows it suddenly begins to require much greater liquid flows to cause the apparatus to end the bypass of water.

Geometry Effect

It is clear from the graphs that the results for the different designs modelled are similar. In particular the steam-first data for 55°F inlet water levels off at approximately $j_g^* = 1.1\text{-}1.2$ for all four configurations, and the locus has the same shape in each case. Therefore, geometry seems to have only a small effect on the results.

Inlet Water Temperature

Figures 20 and 21 include data from tests conducted with higher inlet water temperatures (100° and 140°F). It can be seen that the curves of the data follow the same pattern as the 55°F inlet water results, but that the curves level off (require much more water to end bypass) at lower values of steam flow with increasing water temperature. This result is important in interpreting the data from the tests performed by Combustion Engineering (Appendix F). The steam-first tests thus show a family of curves for the "end of bypass" locus which depend upon the temperature of the water.

Pressures

Plenum pressures prior to and after flooding were recorded for different liquid flow rates. At times, condensation of steam in the line to the manometer interfered with the manometer readings, but the results plotted for two tests (Figures 22 and 23) are typical of all tests. Generally, the onset of flooding and bypass in the water-first tests resulted in an increase in pressure drop of roughly ten times. (In the steam-first tests, the opposite would be observed - pressures would be high while bypass occurred, but as soon as it ended, the pressure drop would decrease by about a factor of ten.)

The pressures recorded increased with increasing flow rate of water up to about 8 gpm, after which the plenum pressure seemed to be around 45 inches of water during bypass, independent of the liquid flow (for cold water). Pressures would be less for hot water. The pressures indicated on the graph are actually average readings, since the pressure tended to oscillate plus or minus several inches from the recorded value.

Visual Observations

When the system was not expelling water, the flow patterns of the water in the annulus corresponded to those charted by Wallis et al (Reference 8). When the system was on the verge of bypass, waves began to appear in the bottom of the annulus and the plenum pressure increased. The waves spread across the annulus and up into the annulus very quickly, and water started to be expelled from the blowholes.

During flooding and bypass, the pattern of the water in the annulus was like that sketched in Figure 24. The water was held in the upper portion of the annulus (several inches from the bottom) as it was almost completely expelled out the "break". Warm water extended

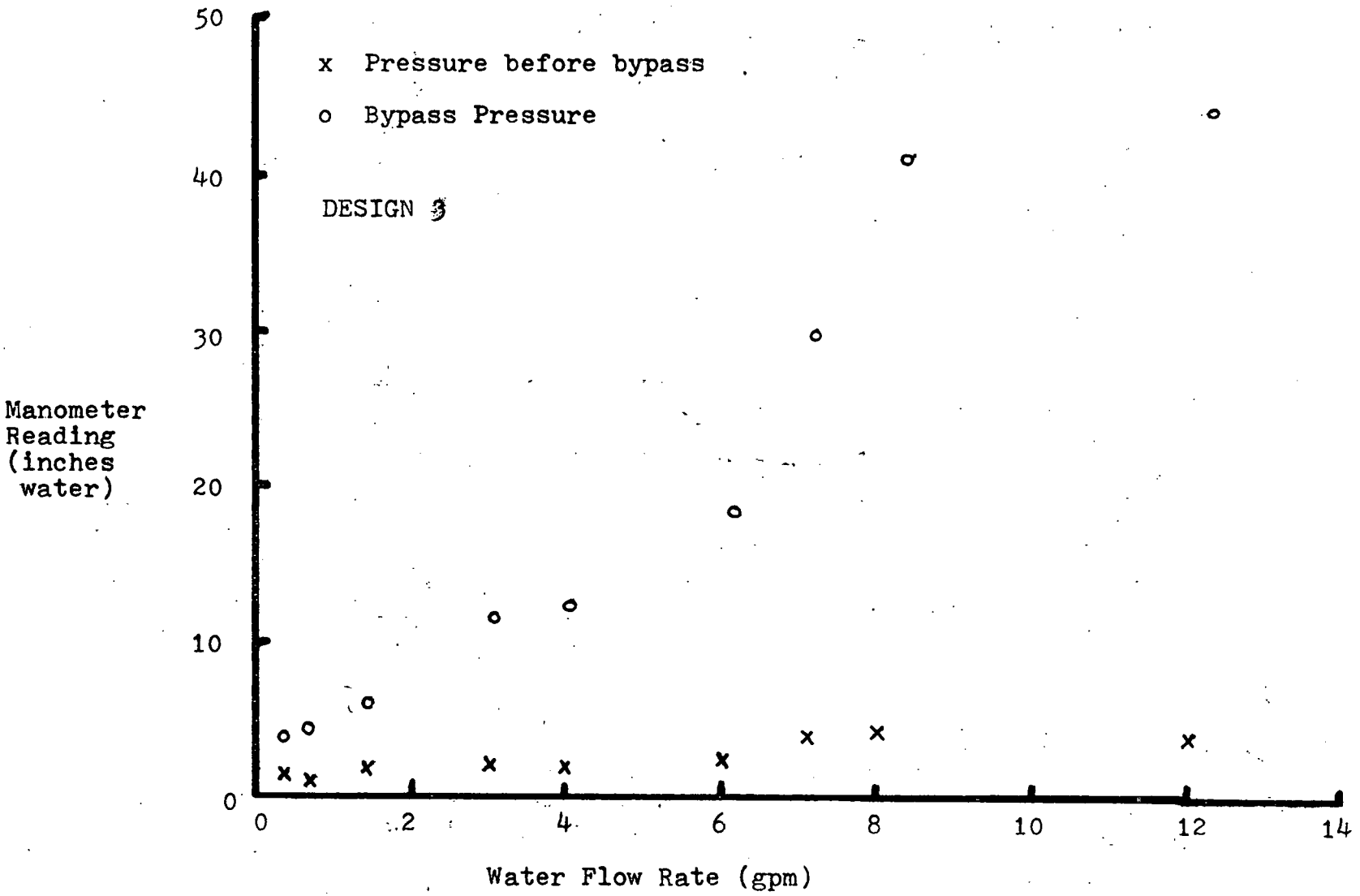

Figure 22. Lower Plenum Pressures prior to and after bypass occurred.

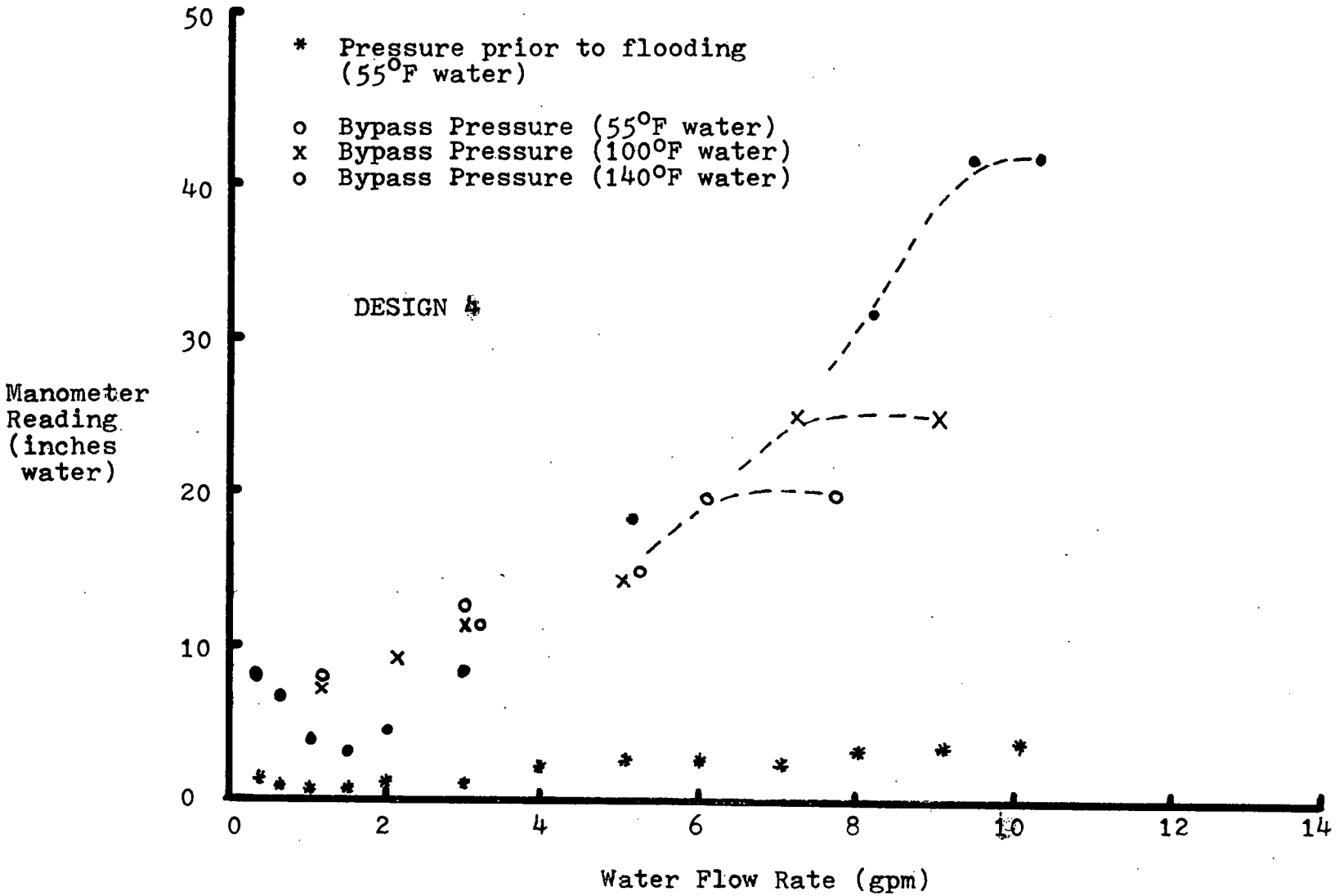

Figure 23. Lower Plenum Pressures prior to and during liquid bypass.

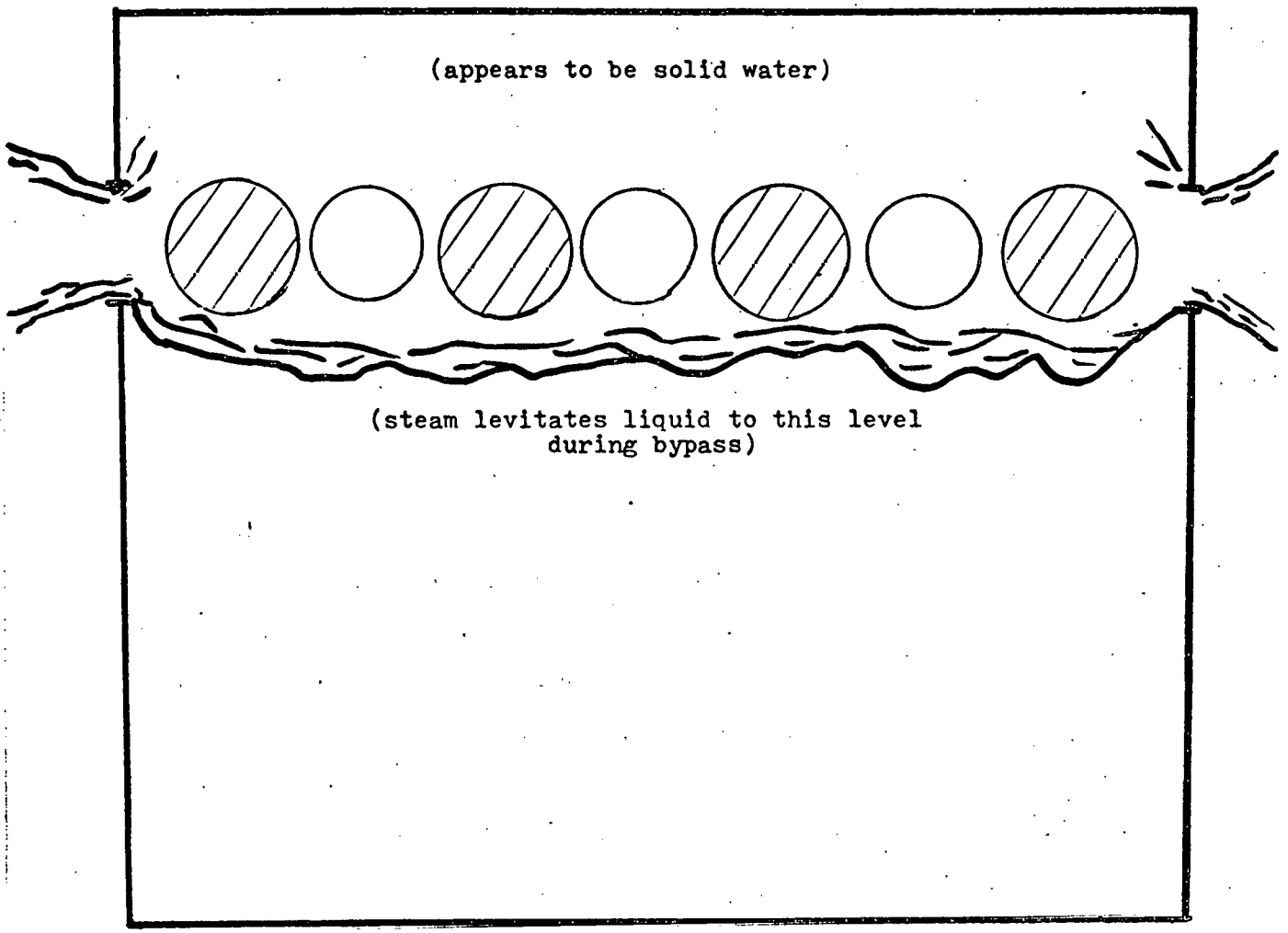

Figure 24. Flow pattern in annulus during bypass in Steam/Water tests. This pattern is typical of cold inlet water (55°F); with warmer water the flow pattern extends further down into the annulus.

further down into the annulus. This lower boundary was very turbulent and unstable. Eventually, an amount of water would fall through the annulus, and flooding would cease. It was not possible to determine the quantity of water being held in the upper region of the annulus because it was not known if the water filled, or only partially filled, the annulus there. Water was ejected from the blowholes for several yards on either side.

In the water-first tests, steam plumes were continuously visible at each blowhole prior to flooding at all liquid flows. This indicated that some steam was passing through the annulus and escaping without being condensed.

Also in the water-first tests, just prior to flooding (at values of j_f^* greater than 0.3), oscillations were observed in the flow patterns of the water. As shown in Figure 25a, the water would begin to be disturbed and spread across the annulus, the plumes of escaping steam would cease to be visible, and the plenum pressure would increase a little. Then, the pressure would decrease again and the water would go back to its original pattern (25b). The phenomenon would repeat

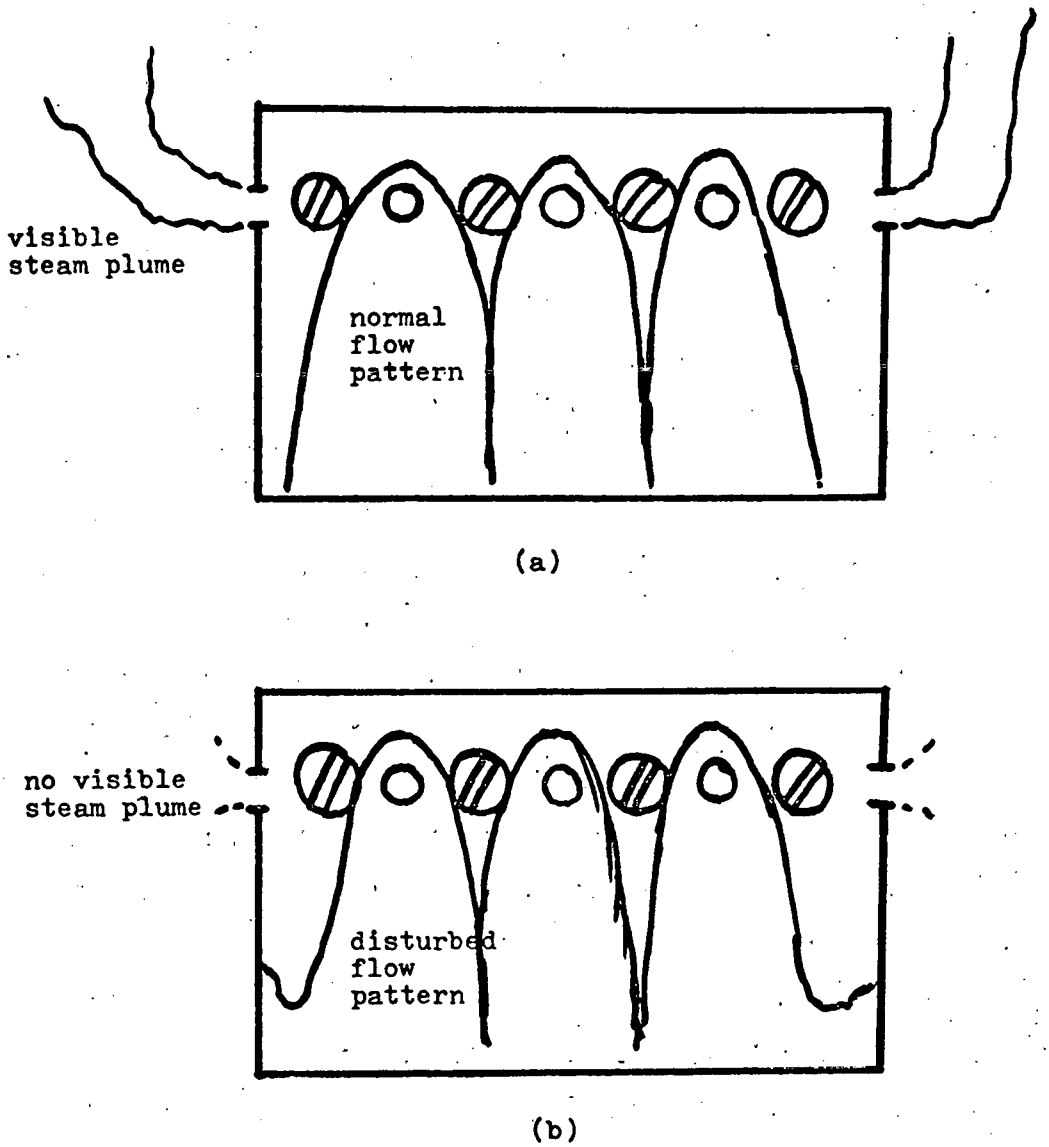

Figure 25. Illustrating the oscillatory behavior of the system in water-first tests at steam flow rates just below those which result in bypass.

itself at each increasing steam flow rate, until a critical flow rate was reached where the pressure would continue to increase during the oscillations, steam would enter the annulus, and the system would flood.

Test Series II - Thermal Shield

In this test run, a galvanized metal sheet was inserted into the annulus to simulate the thermal shield that is present in some reactors. The thermal shield is a steel cylinder concentric with the reactor vessel and the core barrel, located in between the two. The purpose of the thermal shield is to decrease the amount of radiation energy absorbed by the pressure vessel walls and reduce the thermal stresses in the vessel. The shield extends from just below the hot legs down to the core support level. This feature was deemed important to test in the experiment because it was believed that by dividing the downcomer into two concentric annuli, the thermal shield provided a means for separating the steam and water flows from each other in bypass. For example, liquid could pass through one annulus, while steam passed through the other.

The galvanized metal sheet modelling the thermal shield was located in the annulus, extending from one side spacer to the other, and from just below the hot legs to the bottom of the annulus (Figure 26). It was centered in the gap by small nubs glued to the "thermal shield".

The results of this modelling are shown in Figures 27 and 28. Since there appeared to be little difference between the results obtained in the Series I, only two configurations were tested with the simulated thermal shield - the design 1 (17a) and the design 4 (single inlet) arrangement (17d) which represented the two extremes of a spreadout (3-inlet) flow and a single inlet.

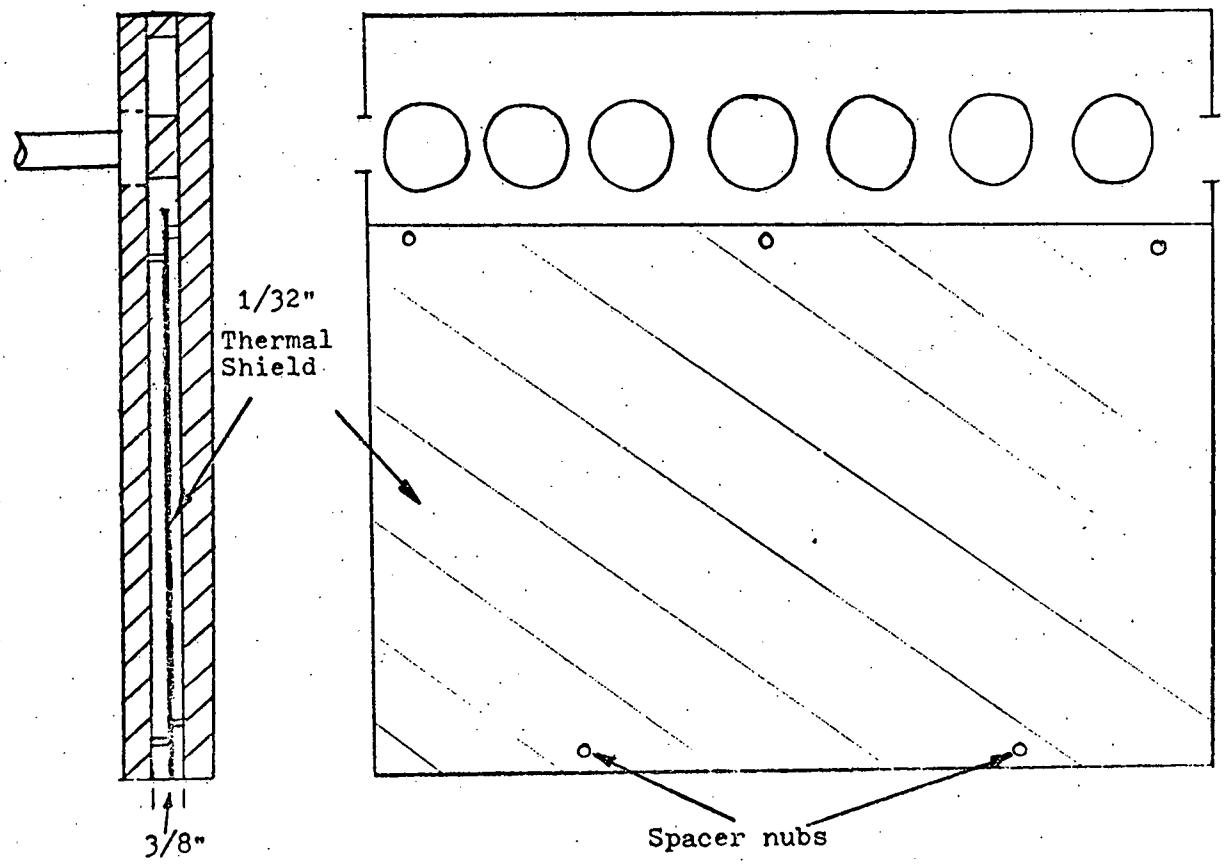

Figure 26. Placement of "thermal shield" in experimental apparatus.

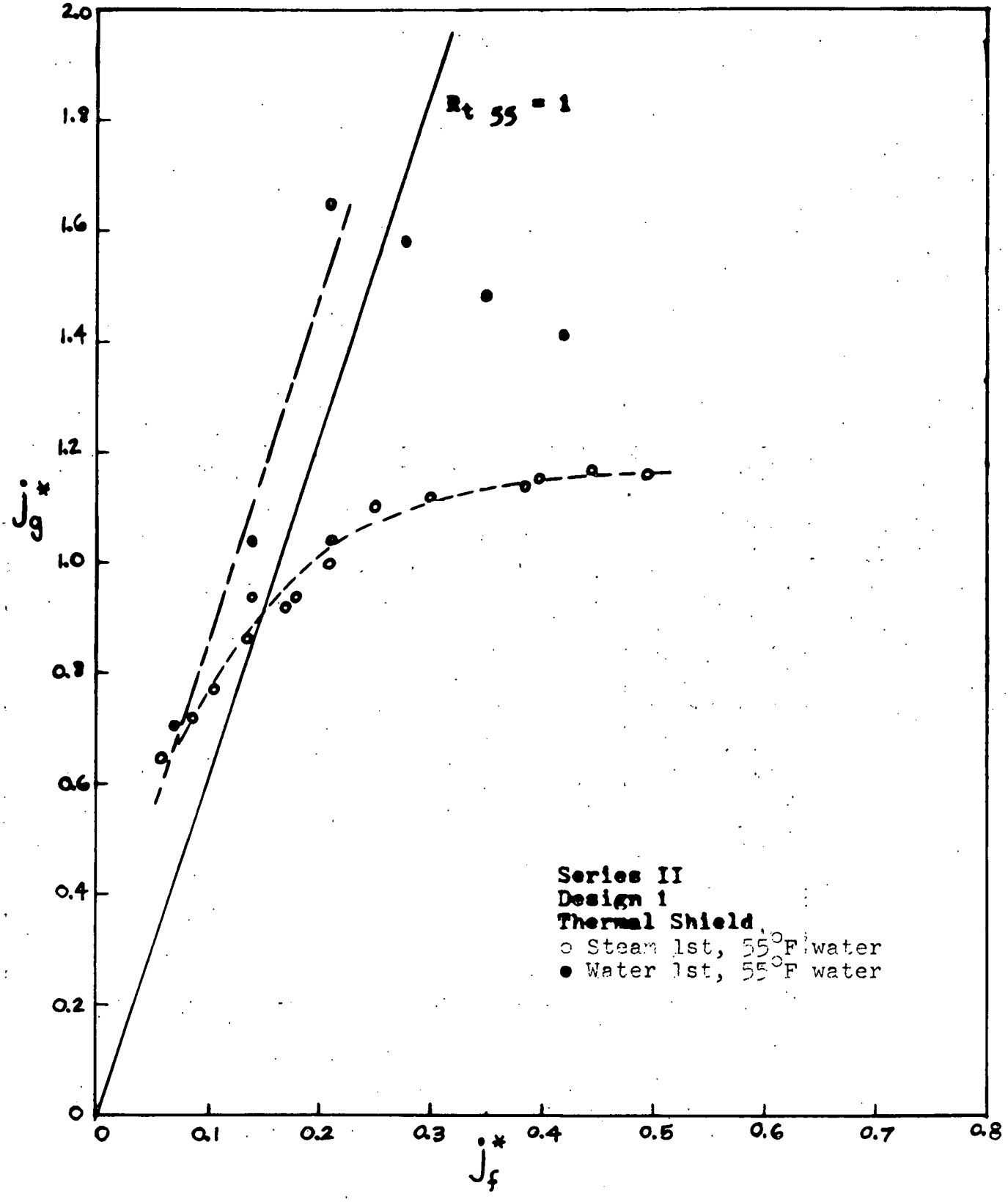

Figure 27. Series II.
Results of Design 1 with Thermal Shield.

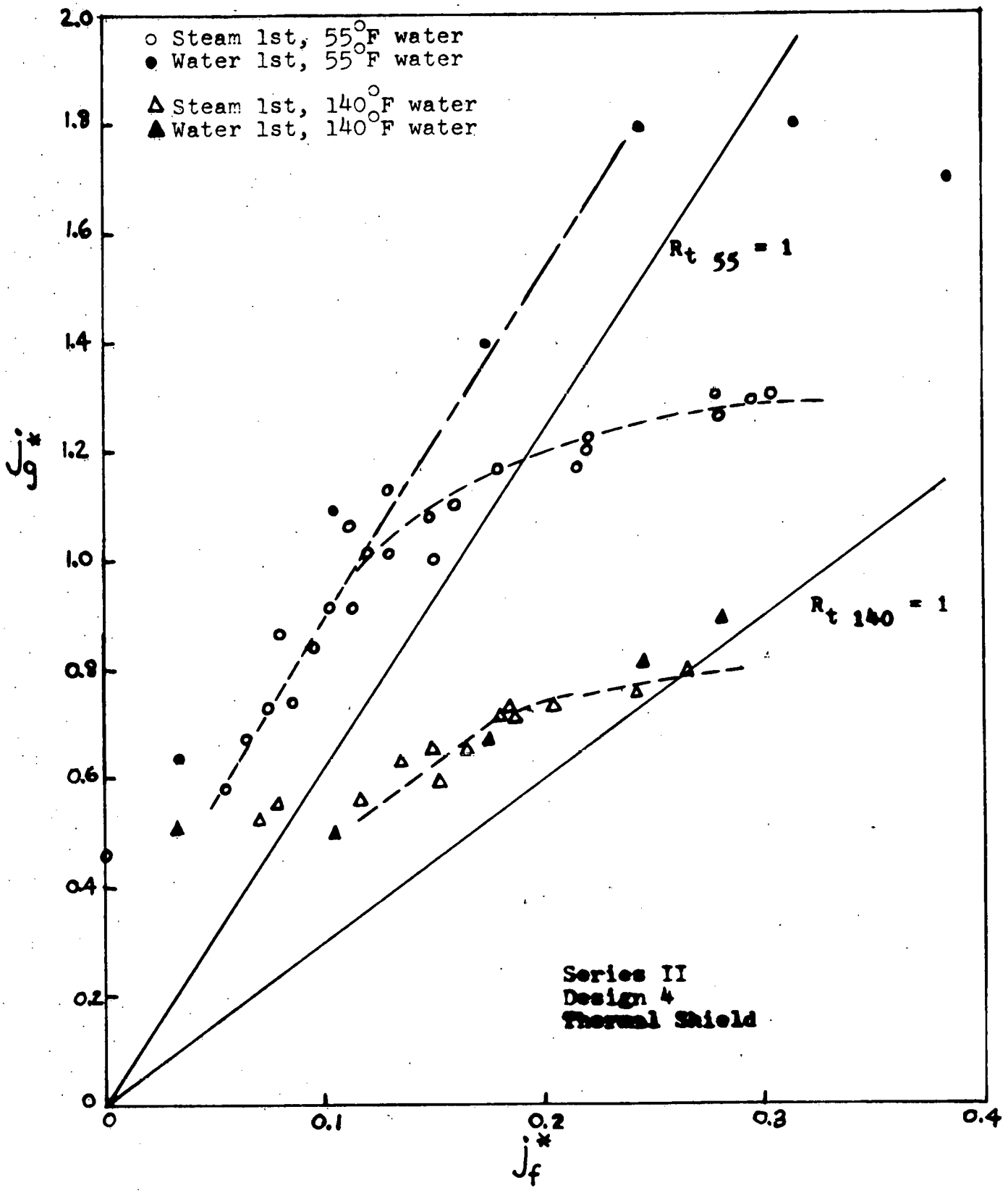

Figure 28. Series II.
Results of Design 4 with Thermal Shield.

The results exhibit exactly the same pattern as seen in the Series I tests. The effect of the simulated thermal shield is minor, if any at all. The design 1 arrangement results are identical to Series I. The single inlet data reach a limit at a slightly higher steam flow than in Series I (for both water temperatures), but the difference is not very great.

In short, the effect of the thermal shield in reducing bypass or changing the locus is negligible. This is probably because the thermal shield is below the inlet leg level. When bypass is occurring the water is held up in the upper portion of the annulus, where the thermal shield does not really come into contact with it and cannot have an influence. The pressure measurements also show about the same characteristics as the Series I results.

Test Series III - Long, Straight Baffles

One of the purposes of this experiment was to investigate the effect that baffling had on the bypass-no bypass locus. The first type of baffling to be tested consisted of straight bars of polycarbonate about 1/4 inch wide and 3/8 inch thick, which snugly bridged the annulus.

Series III test runs with baffling used segments 1.9" long above the hot legs in the model, and 3.8" lengths directly below (and abutting) the hot legs as illustrated in Figure 29. Locating the segments above and below the hot legs takes advantage of the ability of the hot legs to block the flow. The segments were held in place with C-clamps.

Test results are given in Figures 30 and 31. Again, the Design I and the Design 4 arrangements were tested. It is immediately seen that this baffling made a favorable difference in comparison to the results from the Series I and II. The steam-first results break away from

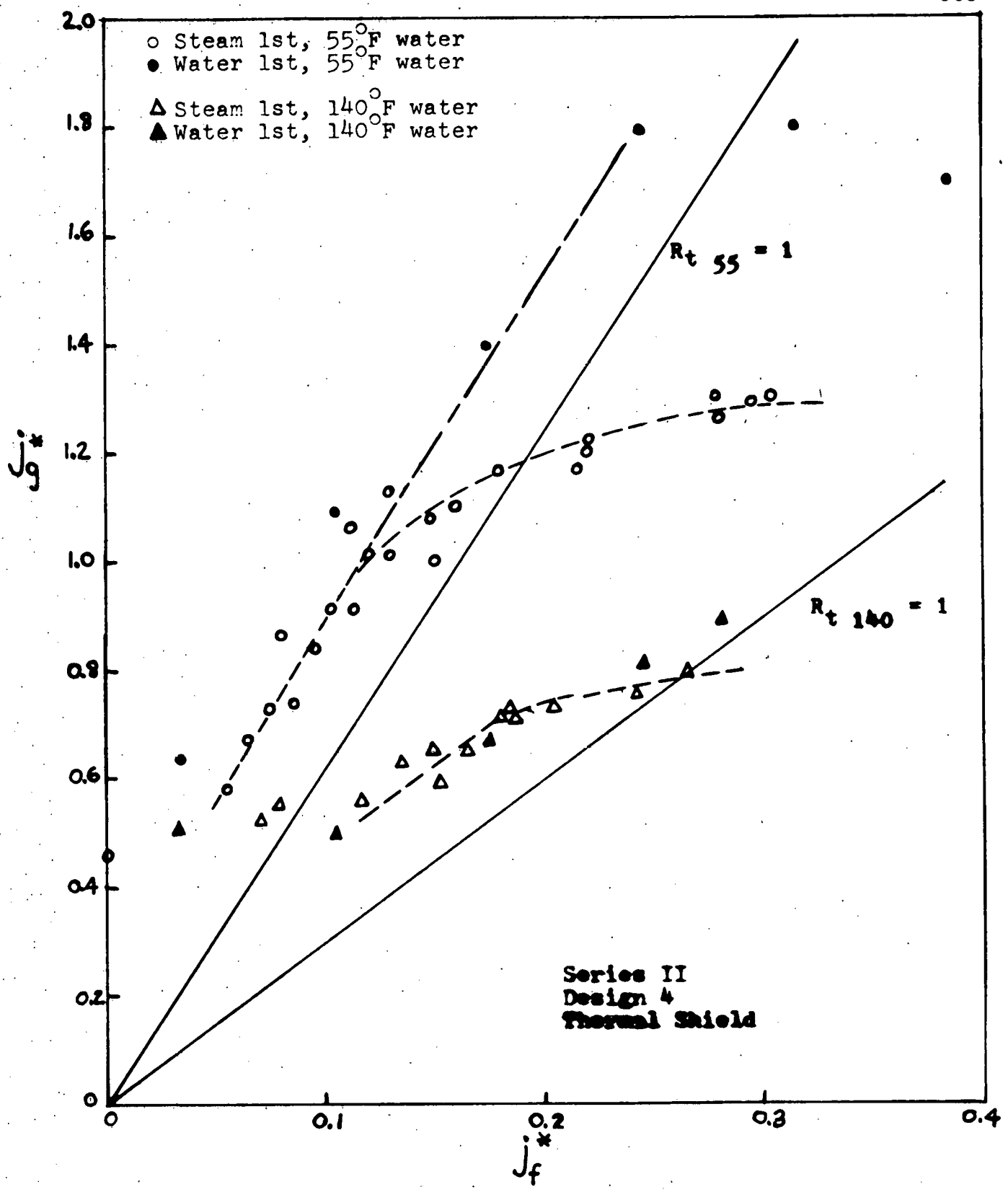

Figure 28. Series II.
Results of Design 4 with Thermal Shield.

The results exhibit exactly the same pattern as seen in the Series I tests. The effect of the simulated thermal shield is minor, if any at all. The design 1 arrangement results are identical to Series I. The single inlet data reach a limit at a slightly higher steam flow than in Series I (for both water temperatures), but the difference is not very great.

In short, the effect of the thermal shield in reducing bypass or changing the locus is negligible. This is probably because the thermal shield is below the inlet leg level. When bypass is occurring the water is held up in the upper portion of the annulus, where the thermal shield does not really come into contact with it and cannot have an influence. The pressure measurements also show about the same characteristics as the Series I results.

Test Series III - Long, Straight Baffles

One of the purposes of this experiment was to investigate the effect that baffling had on the bypass-no bypass locus. The first type of baffling to be tested consisted of straight bars of polycarbonate about 1/4 inch wide and 3/8 inch thick, which snugly bridged the annulus.

Series III test runs with baffling used segments 1.9" long above the hot legs in the model, and 3.8" lengths directly below (and abutting) the hot legs as illustrated in Figure 29. Locating the segments above and below the hot legs takes advantage of the ability of the hot legs to block the flow. The segments were held in place with C-clamps.

Test results are given in Figures 30 and 31. Again, the Design I and the Design 4 arrangements were tested. It is immediately seen that this baffling made a favorable difference in comparison to the results from the Series I and II. The steam-first results break away from

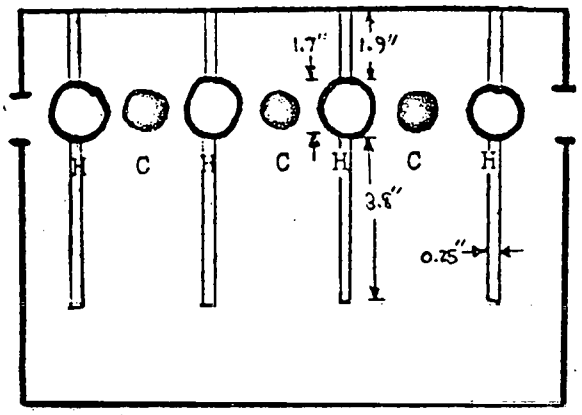

29a. Design 1.

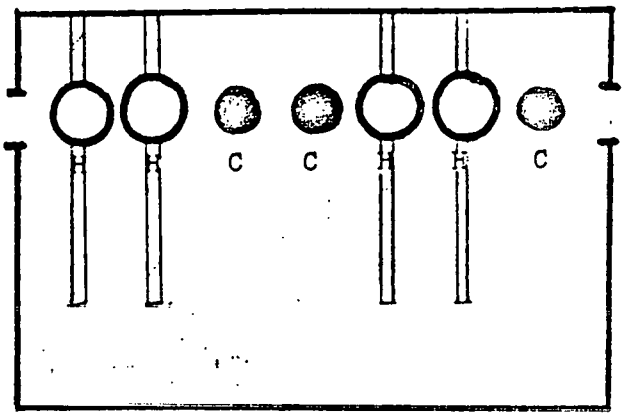

29c. Design 2.

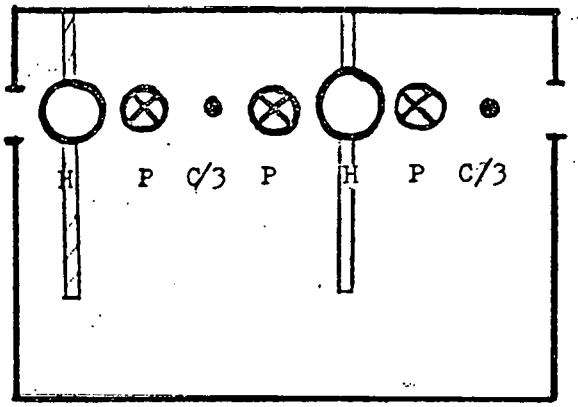

29b. Design 3.

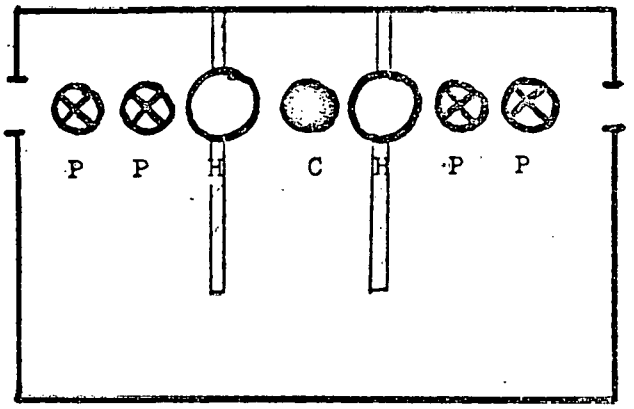

29d. Design 4.

H -- Hot Leg disk

C -- Cold Leg water inlet

P -- Plug

Figure 29. Typical Reactor designs with baffles used in experiment. The baffles filled the gap. Refer to Figure 17.

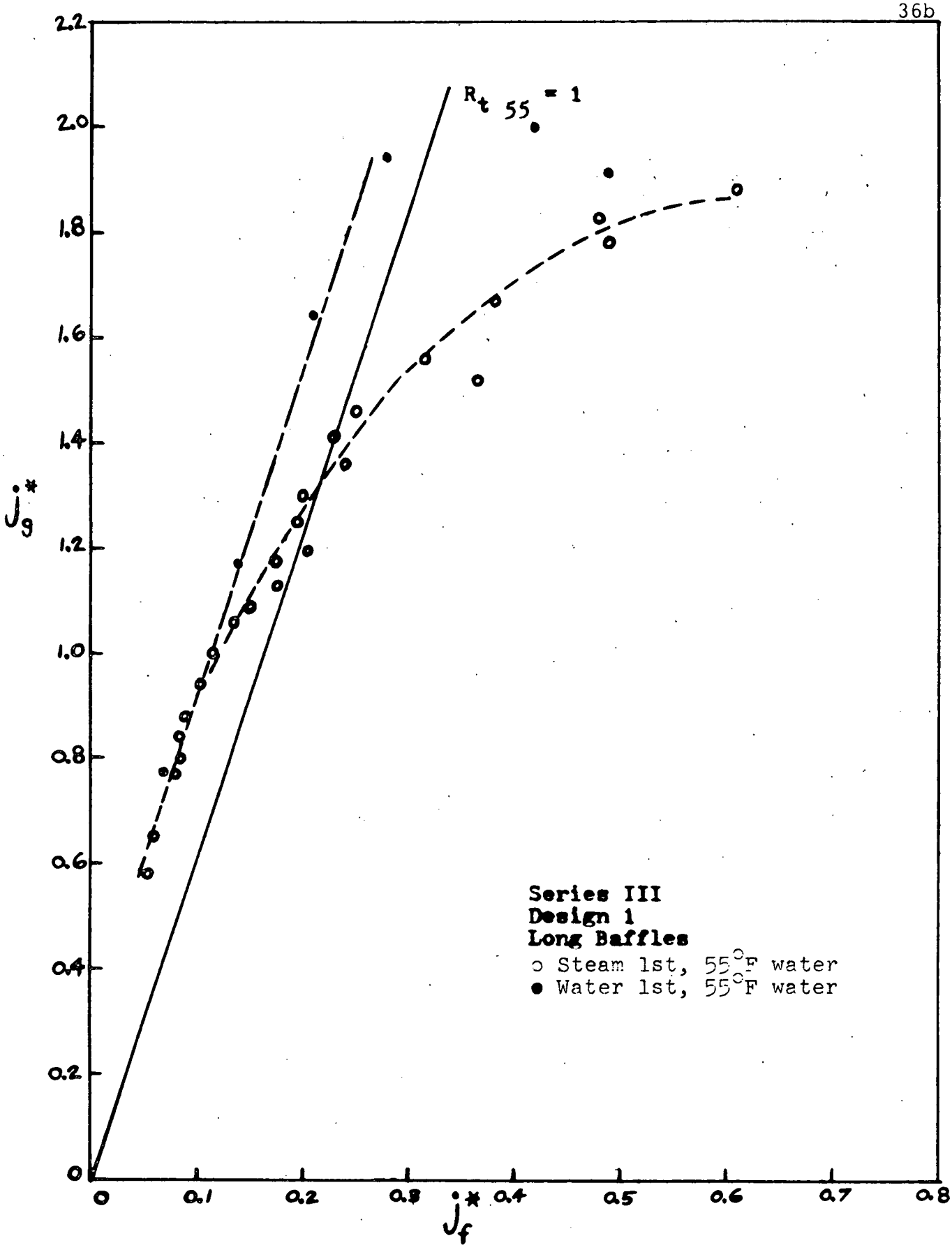

Figure 30. Series III.

Results of Design 1 with baffle segments above and below hot legs.

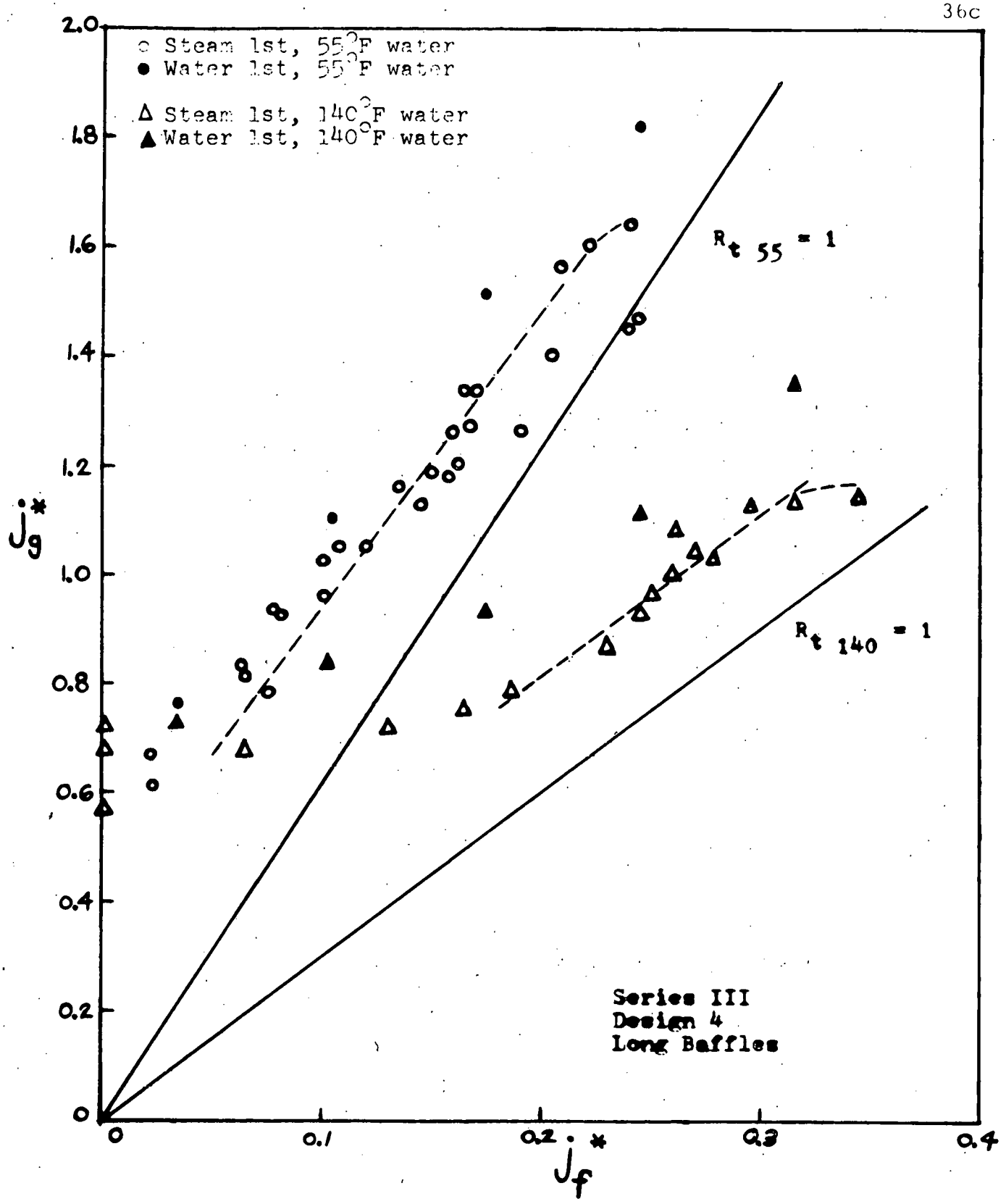

Figure 31. Series III.
Results of Design 4 with baffle segments above and below hot legs.

paralleling the line $R_t = 1$ at about the same point as before ($j_g^* = 1.0$ for $55^{\circ}F$ water), but instead of reaching a limit rapidly, the results show a more gradual approach to a limit about 50% higher than in the previous tests.

This means then that the baffled system was able to deflood with less liquid injection and at higher steam flows than was possible in previous tests. By the shape of the curves, it can be seen that the improvement due to baffling is greater at higher steam flows.

The water-first data show the same behavior as before, except that they level off at a higher steam flow - the same as the steam-first tests. With a higher inlet water temperature, the same magnitude of improvement is also seen.

The pressure readings just prior to and after flooding do not show much difference when compared with the previous results - there was still an increase of about 10 times in the pressure drop when flooding occurred.

Observations

In the steam-first tests with these baffles, changes in the patterns of the water flow in the annulus could be observed. The baffling, as it was installed here, essentially creates a "pocket" (Figure 32) around a cold leg where the steam, if it flows up into the pocket, finds itself with nowhere to go except back out again (unless it pushes the water back into the cold leg - which did not happen). This contrasts with the situation not using baffles, where the steam flow appears to be fairly uniform across the annulus. With baffles, the liquid builds up in the area around the cold leg blocked off by the baffles. (For one thing, this means that a larger volume of water is being stored in the annulus). The liquid stored in a pocket swirls around violently,

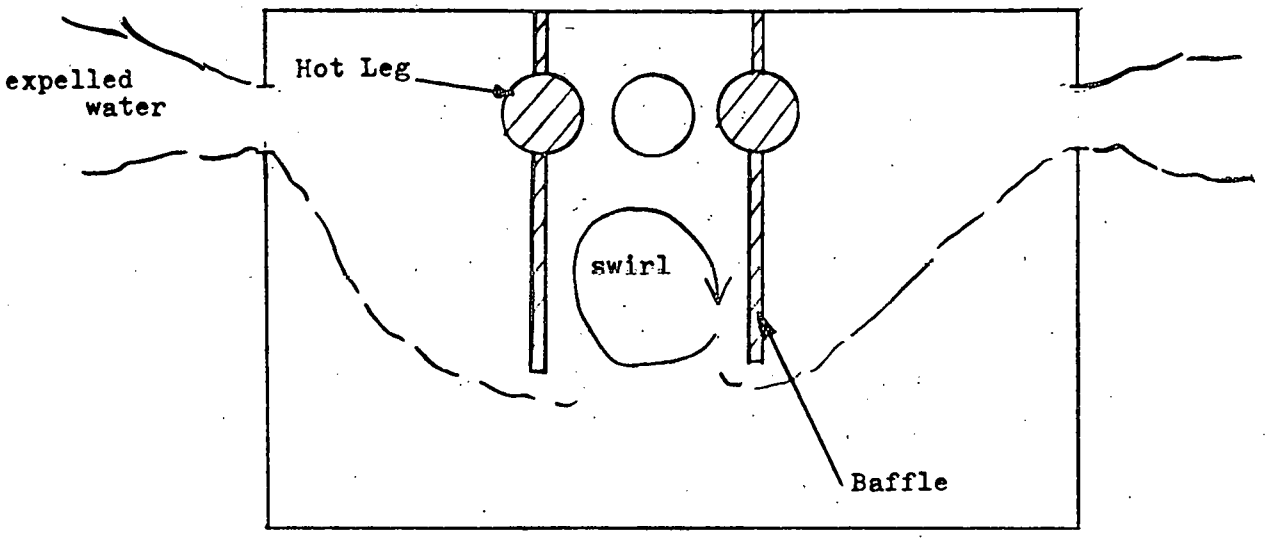

Figure 32. Flow pattern of water in annulus during bypass with baffles installed.

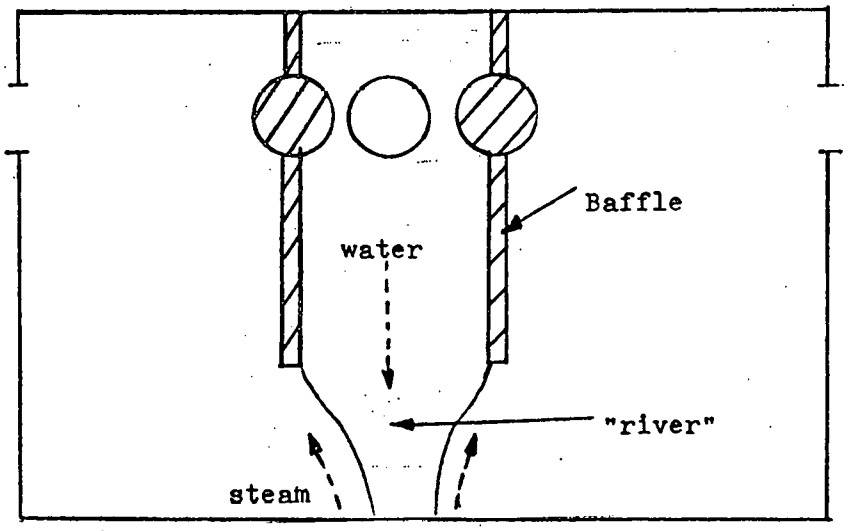

Figure 33. "River" flow pattern observed in water-first tests prior to bypass.

and the swirling appears to aid in sending water into the lower plenum and causing the bypass to end. The height of the liquid stored in the pocket is also greater than the height of the liquid stored in the annulus when there are no baffles. There is then a larger hydrostatic head of the water above the steam flow with the baffles, which may also aid in ending bypass.

Further, it will be seen that the entering water must all be carried upward in order to be blown out the break. It must travel around the baffle, up, and out. Without baffles, the water need not be lifted so much as carried transversely across the annulus and out. Since the baffles prevent water from being carried transversely, it is harder to eject the water. These then are qualitative explanations, based on the observations of the flow patterns, postulating how the asymmetry induced by the baffles aids in liquid penetration of the annulus.

In the water-first tests, an interesting observation was made. The baffles did help to direct the water in a more downward direction, confining the width of the flow pattern to the width between the baffles. At high liquid and steam flows, the incoming water was observed to form what can only be described as a "river" type of flow. Below the level of the baffles, the water collected together, as sketched in Figure 33, and fell into the lower plenum as a river. At a critical gas flow however, this stream which was much thinner than its width, became unstable, broke up, and bypass took place.

Series IV - Medium, Straight Baffles

In Series IV the length of straight baffling below each hot leg was reduced to 1/2 of the Series III length to see if a shorter baffle could accomplish the same thing as the long baffle.

Figures 34, 35, and 36 give the results of this alteration. Figure 34 is the Design 1 design results, and Figure 36 is the single inlet results, as before. Figure 35 represents Design 2 - adjacent cold legs. The latter was included because, although it had been demonstrated that the effects of geometry were small without any baffling, it was not known that geometrical effects would be unimportant with baffling. Putting two cold legs together in a "pocket" of baffles concentrates a larger amount of water in that one area, perhaps making it easier for the water to penetrate the annulus.

The results indicated that the shortened baffling worked as well as the longer baffles of Series III. Further, there was no evidence here that having two cold legs adjacent to one another effected any difference. The same improvements as Series III baffling were found for all designs and for other water temperatures.

Series V - Straight Baffles, Upper Segments Only

For Series V, the length of straight baffling below each hot leg was eliminated altogether to find out if the improvement with baffling was due mostly to the upper or lower segment of baffle adjoining the hot legs. The resulting curves are shown in Figures 37, 38 and 39. As in Series IV, the Designs 1, 2, and 4 were used.

The Design 1 results show that perhaps a small improvement is made when compared to no baffling (Figure 18), but the major effect of the baffling (compare with Figure 34) appears to have been removed along with the segment of baffling below the hot leg. The single inlet results show slight improvement over having no baffles, but again, the effectiveness of the baffling is severely reduced when compared with Series III and IV results (Figures 31 and 36).

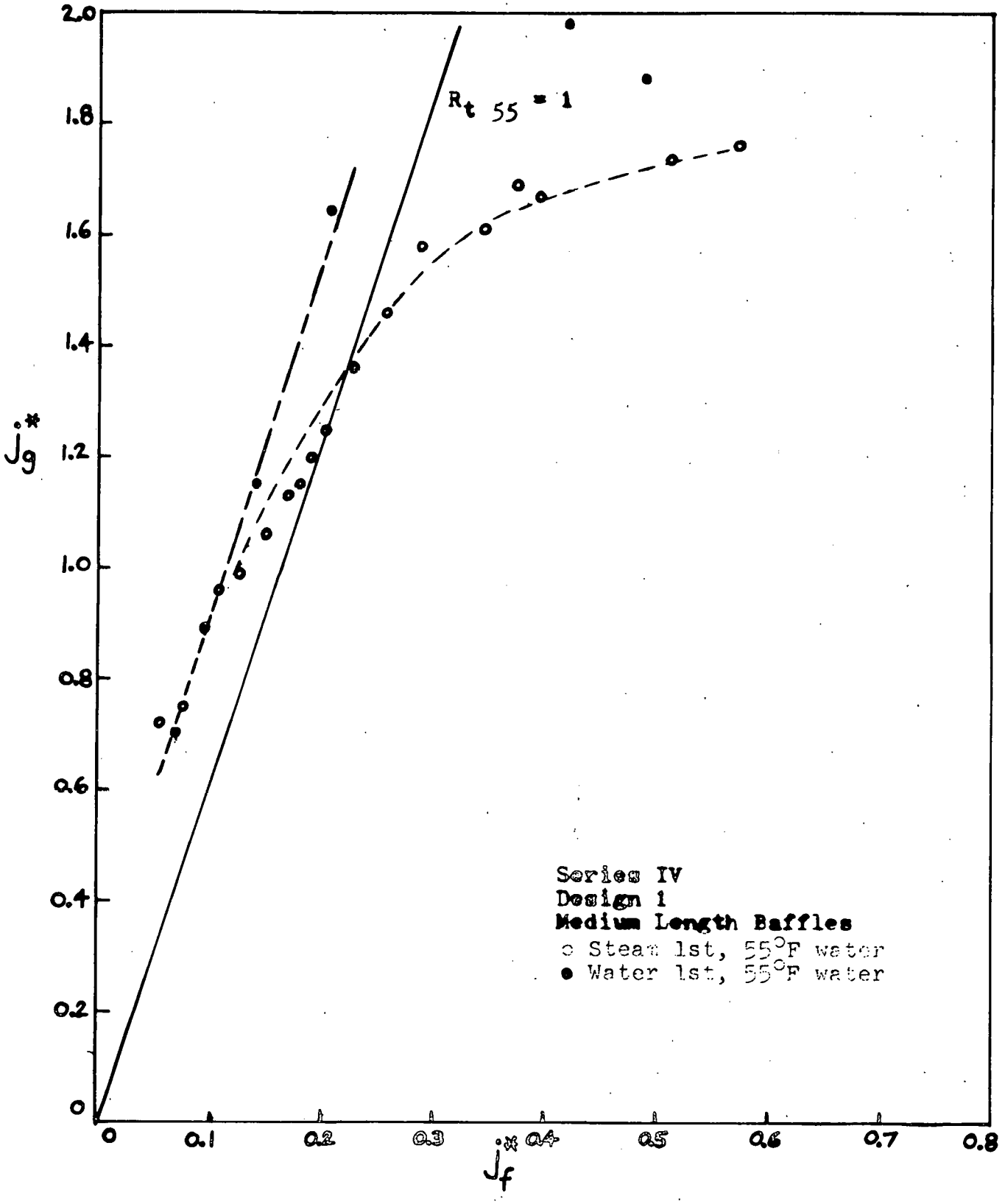

Figure 34. Series IV.

Results of Design 1 with baffles above and below hot legs and segment below hot legs shorter than Series III.

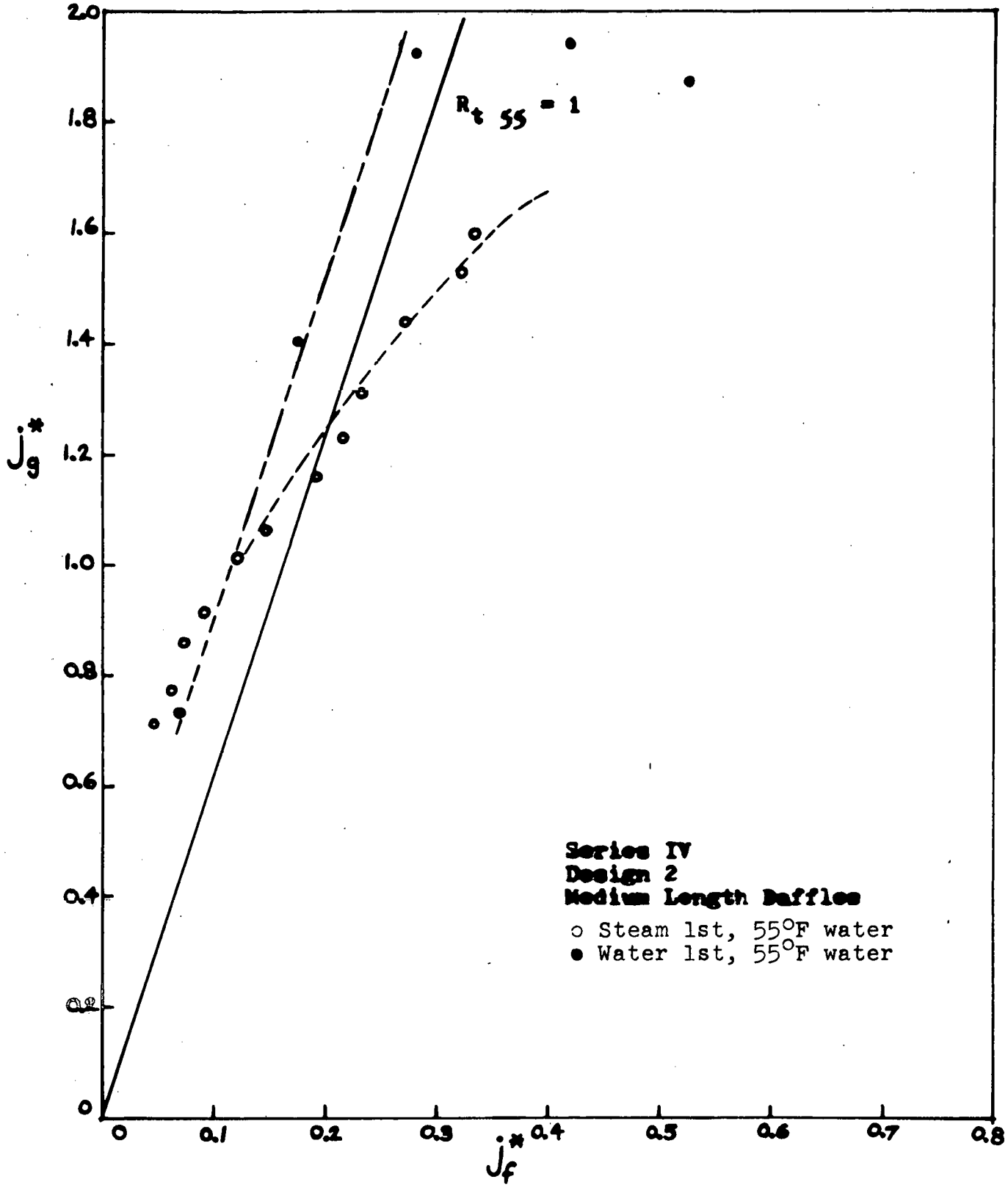

Figure 35. Series IV.
Results of Design 2 with baffle segments above and below hot legs and segment below half the length of Series III.

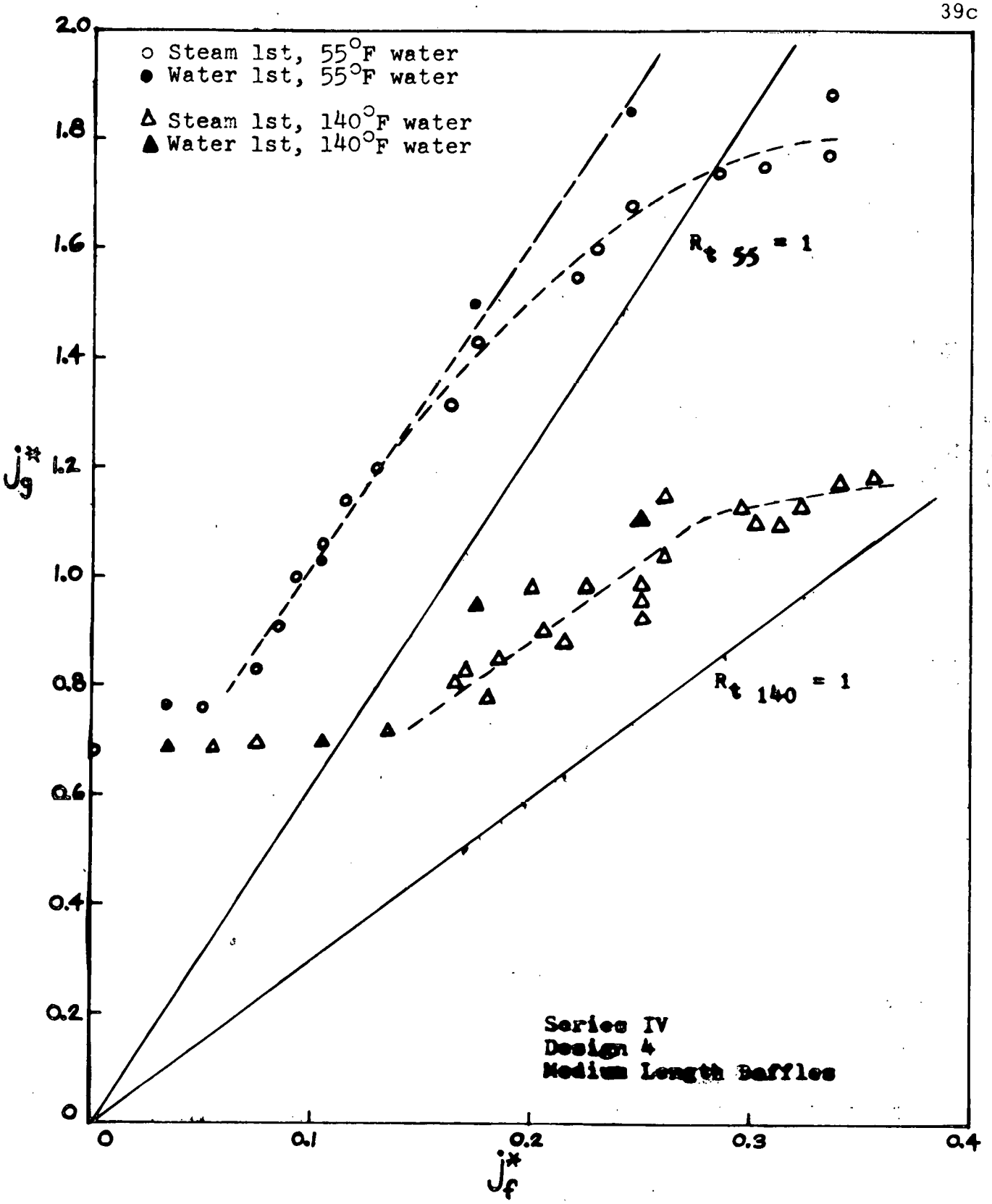

Figure 36. Series IV.
Results of Design 4 with baffle segments above and below hot legs and lower segment half the length of Series III.

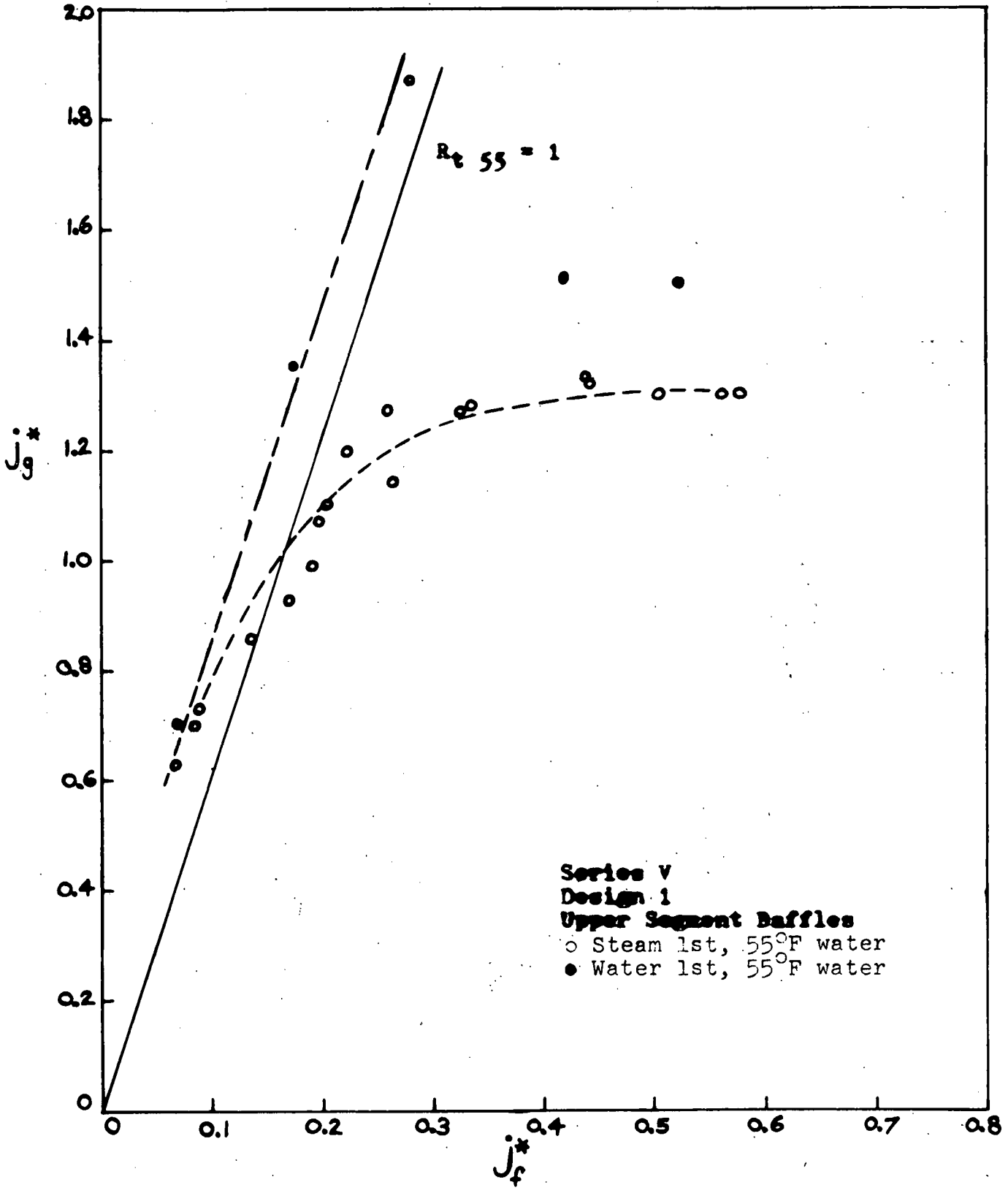

Figure 37. Series V.
Results of Design 1 with baffle segment above the hot legs only.

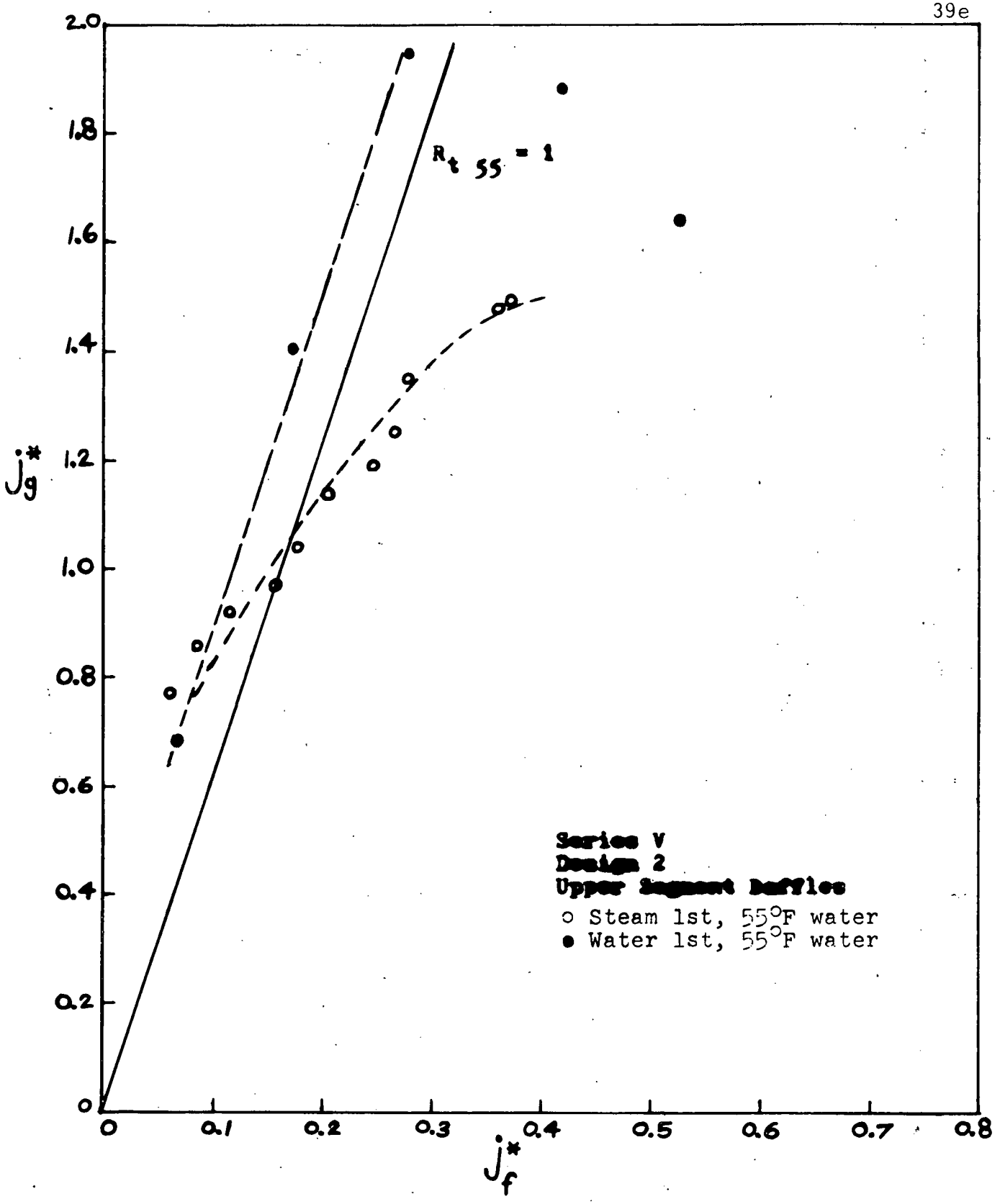

Figure 38. Series V.
Results of Design 2 with baffle segment above the hot legs only.

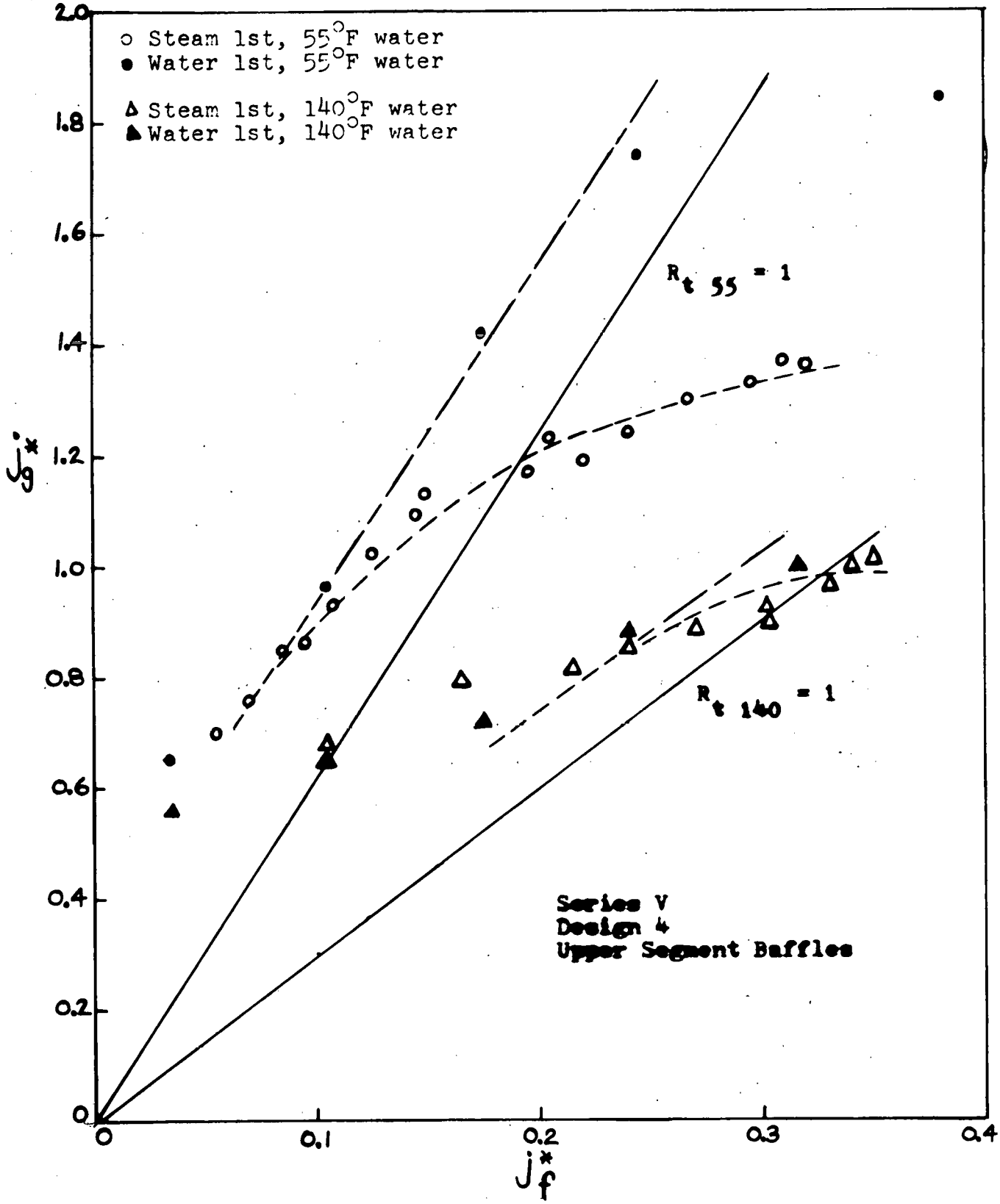

Figure 39. Series V.
Results of Design 4 with baffle segments above the hot legs only.

The results of testing the adjacent cold leg design do however show some improvement when compared to having no baffling (Figure 19). The effect is somewhere between the Series I and the Series IV (Figure 35) results. It is unclear why there should be a difference in this test alone for adjacent cold leg design while the other tests did not show any significant differences.

Series VI - Semicircular Collar

To investigate alternative baffling designs, the baffles in this Series VI run were semicircular arcs of polycarbonate which were placed directly above the cold legs in the annulus, and fit snugly in the annulus. (Figure 40). The purpose of these collars was to give the incoming water a greater downward velocity component.

Figures 41-43 demonstrate that there was about the same effect in using this type of baffling as in Series V. The observation that the baffles did not prevent water from being blown out the break by blocking its path to the hole perhaps indicates why this type of baffling had such a small effect on the end of bypass.

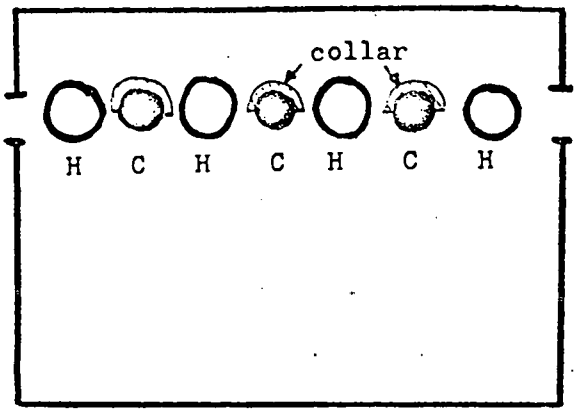

40a . Design 1.

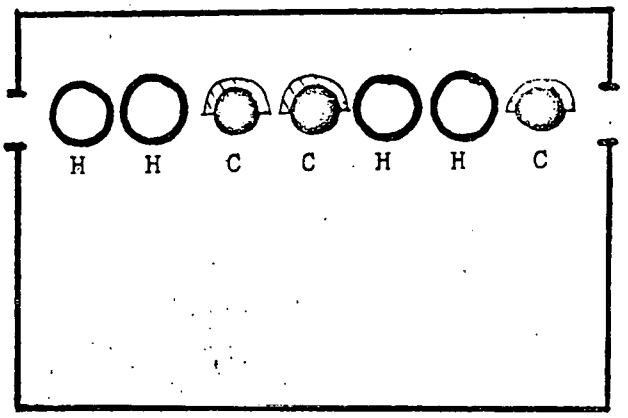

40c . Design 2.

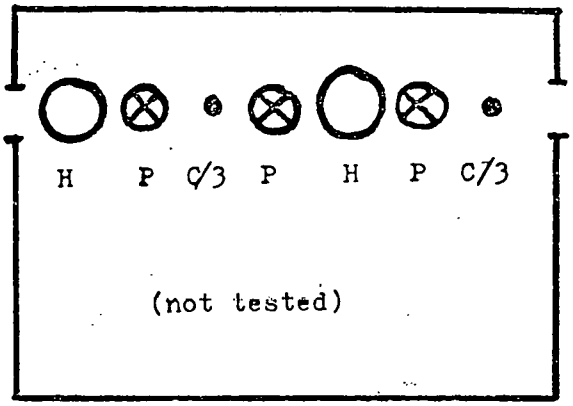

40b . Design 3.

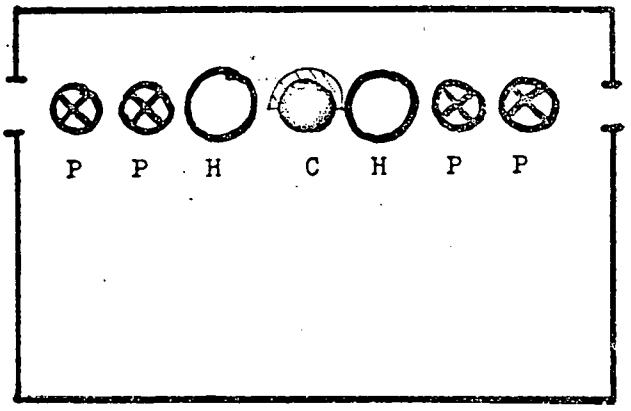

40d . Design 4.

H -- Hot Leg disk

C -- Cold Leg water inlet

P -- Plug

Figure 40. Typical reactor designs with semicircular collar baffles. Baffles fit snugly in gap space.

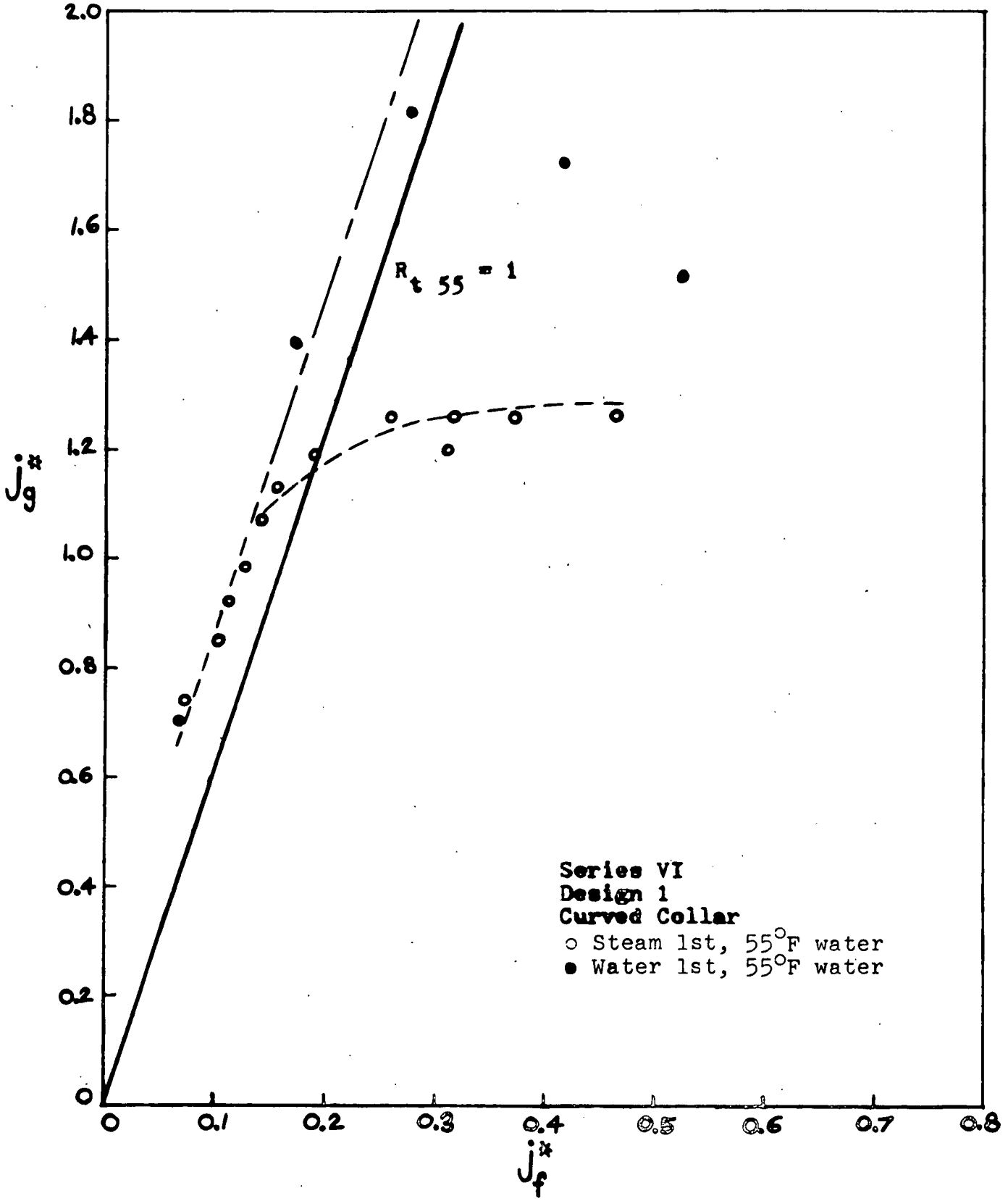

Figure 41. Series VI.
Results of Design 1 with semicircular collar baffle.

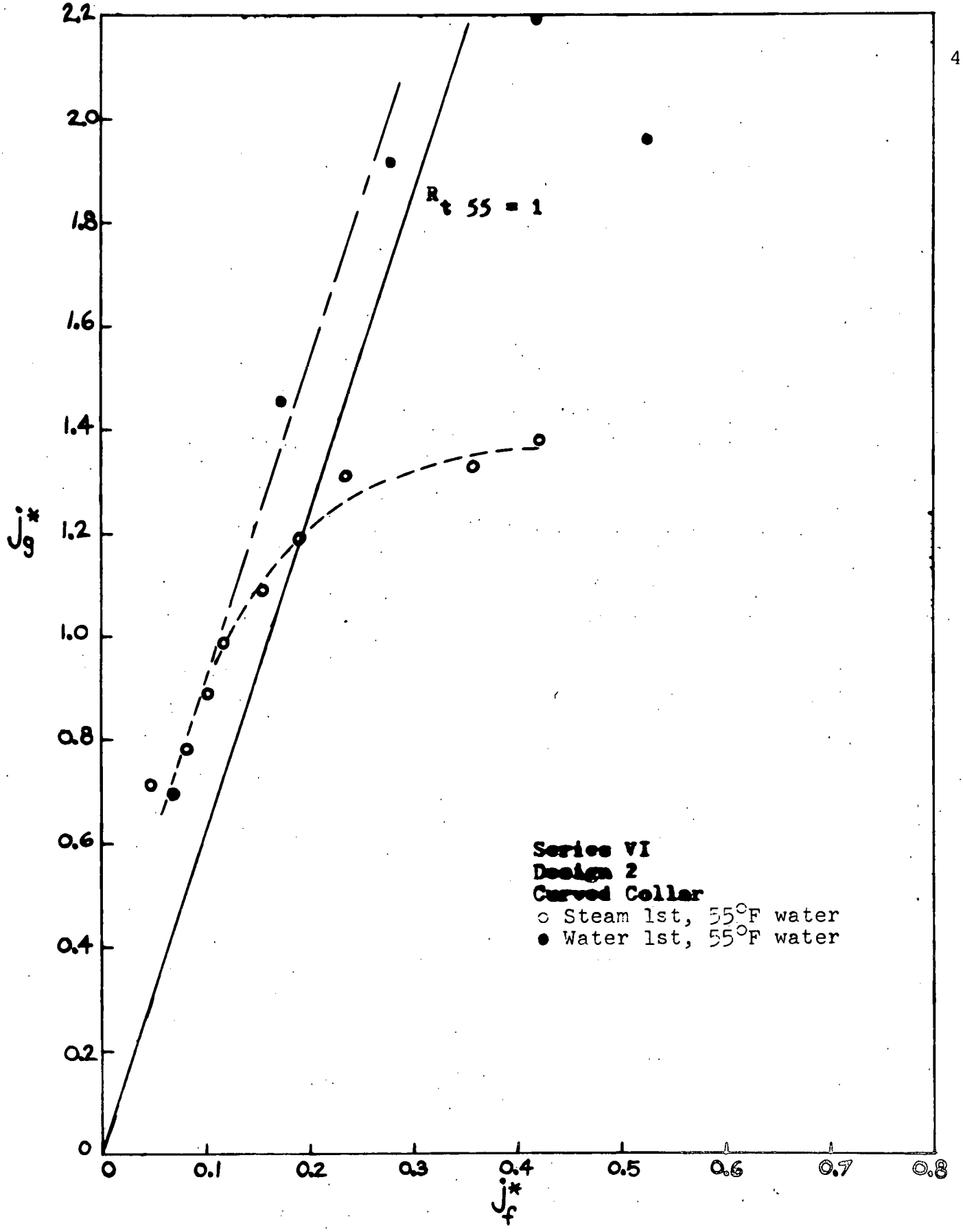

Figure 42. Series VI.
Results of Design 2 with semicircular collar baffle.

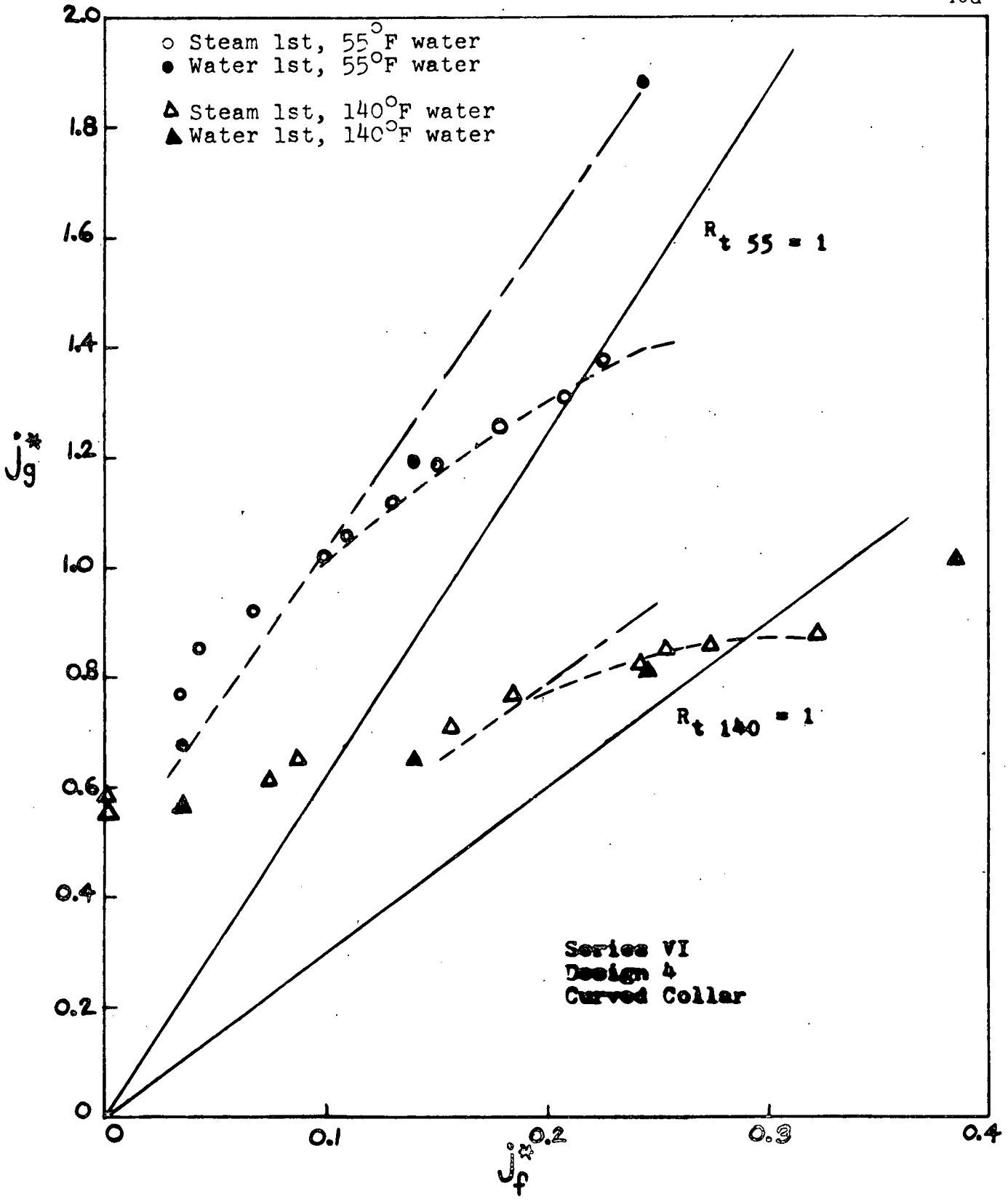

Figure 43. Series VI.
Results of Design 4 with semicircular collar baffle.

EXPERIMENTAL RESULTS - Addendum

Two supplementary tests were conducted to determine the effects of,

1) non-condensible gases dissolved in the steam and water supplies,

2) the size of the break.

These tests were run with Design 1 and without any baffling. (Figure 18). Neither test showed a significant difference from this result.

The lack of a difference in the first test indicated that non-condensible gases have little effect on the bypass-no bypass transition. One hundred times the mass of air dissolved in ground water was added directly to the steam flow in the experiment, yet no difference was observed.

In the other test, the area of the simulated cold leg break was doubled. The recorded plenum pressures showed a drop to one-fourth of the pressures recorded with the smaller size break. Since the gas velocity is proportional to the square root of the pressure, the velocity was reduced by one-half. Because the flow rate is the velocity times the area (ignoring compressibility) the effect of doubling the break area is cancelled by the reduction in pressure and there is no difference in the results.

INTERPRETATION OF RESULTS

The results of the steam-first type of test will be discussed and explanations for those results proposed. Recall that the steam-first tests more closely model the accumulator bypass situation than the water-first tests, because in the actual reactor accident, steam would be present in the core and downcomer before injection of emergency coolant began. The experimental results may be conveniently divided into three regions, as sketched in Figure 44.

1) Region 1, to the left of the intersection with the line of Thermodynamic Ratio equals unity.
2) Region 2, along the line of $R_t = 1.0$.
3) Region 3, to the right of $R_t = 1.0$, where the data level off.

Region 1

We see in Region 1 that a decreasing gas flow is required to end the bypass of water at increasing liquid flows. In this experiment, the water flow rates in this Region were too low for accurate measurement in the current steam-first tests. Therefore, interpretation of this Region lies mainly with the data from the Combustion Engineering and Aerojet steam/water interaction experiments. A more complete description of these tests and their results is contained in Appendix F.

In the Appendix it is suggested that the Region 1 behavior essentially follows the Wallis correlation. Since Region 1 lies to the left of the $R_t = 1.0$ line, it is not possible for the water to condense all of the steam at these flows. We would expect the system to behave somewhat like the case of countercurrent flow with a non-condensible gas, i.e., follow the Wallis correlation. However, because some water is able to penetrate the annulus (according to the Wallis model) it is possible that an amount of the steam can be condensed

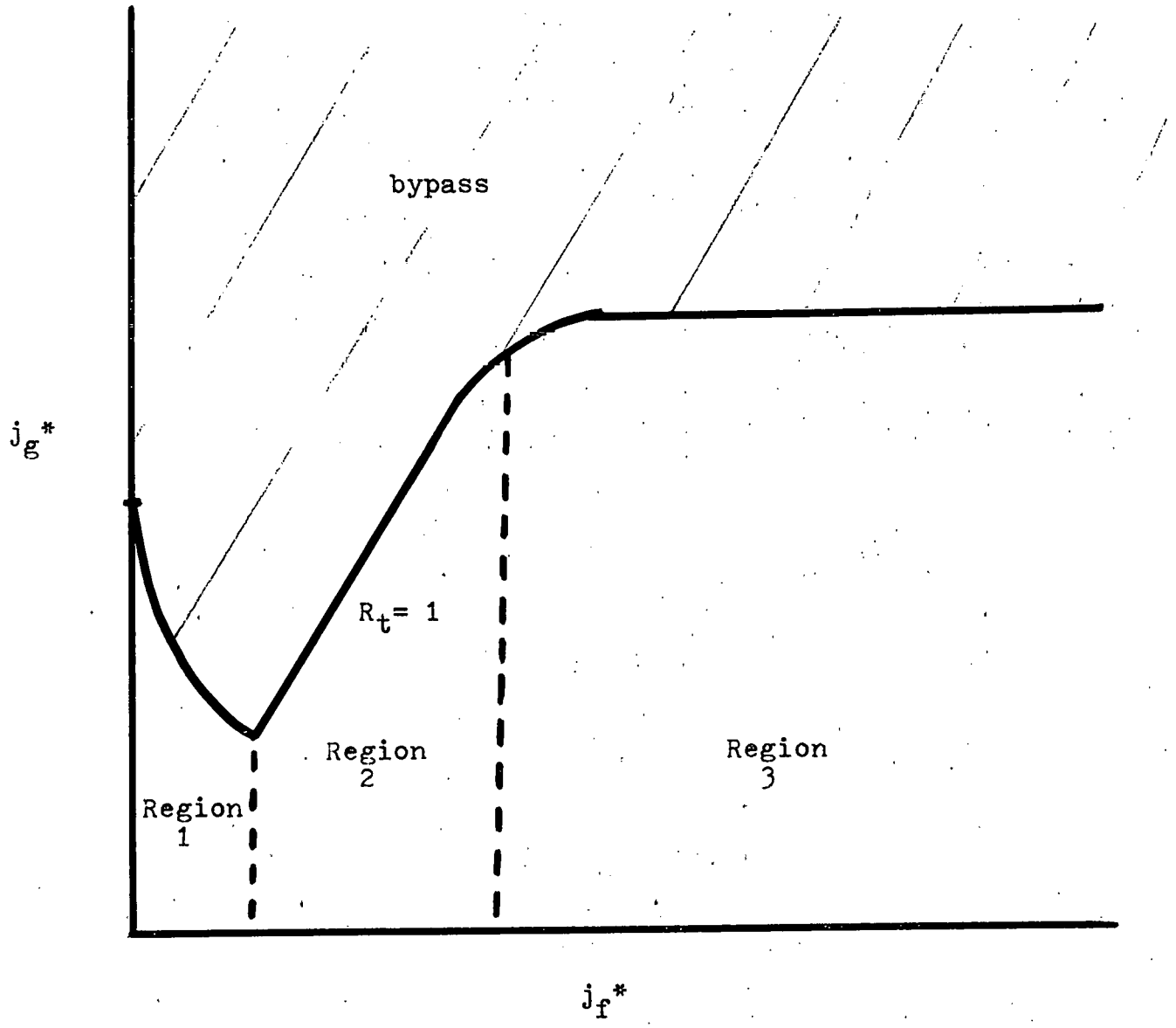

Figure 44. Sketch of the end of bypass locus in steam-first experiments.

in the lower plenum, reducing the actual steam flow into the annulus. The maximum amount of steam which can be condensed is given by the Thermodynamic Ratio equals unity line. Consequently, we assume that the data lie somewhere between the predictions of the Wallis correlation and the Wallis correlation plus that amount of steam which can be condensed in the lower plenum. The Aerojet data in particular (Appendix F) support this conclusion, and the Combustion Engineering data are in agreement (the appropriate data lie just above the line for the Wallis correlation), which leads us to hypothesize that this is the mechanism for Region 1 behavior.

Region 2

In this Region, the data in the graphs lies above the line $R_t = 1$, but it is difficult from the data to tell whether or not it is asymptotically approaching that line. It has been observed that some steam is escaping through the annulus (without being condensed) at all times. In water-first tests, the temperature of the water in the lower plenum does not reach saturation until just the point where the system bypasses all the liquid. Therefore, the difference between the data points and the line $R_t = 1$ is due to the steam which avoids being condensed in the lower plenum.

In order to understand the mechanism by which bypass ends in this Region, it is useful to think of the water-first test. We picture the water entering the annulus and falling into the lower plenum. When there is a very small steam flow, the water can condense all of the steam which enters. So, prior to bypass, steam which enters the lower plenum is completely condensed in the lower plenum by the water which has fallen through the annulus. This water-heater process continues until the water is no longer able to condense all of the

steam - which corresponds to arrival on the line of $R_t = 1$ in the graphs. At this time, some steam is forced into the annulus. When steam enters the annulus, it is able to be condensed by the incoming sub-cooled water; however, this warms up the water which is on its way to the lower plenum. If the water falling into the plenum is warmer, less steam can be condensed in the lower plenum, and thus, more steam is forced into the annulus. It can easily be seen how a self-feeding process would ensue, whereby all of the steam enters the annulus eventually, and the system, due to this large steam flow entering the annulus, expels all the water.

The events described, if correct, occur within a few seconds. The temperature of the water in the lower plenum is observed to be at saturation and the steam can be seen to begin to penetrate upward into the annulus just before bypass occurs. Waves appear there also. These spread quickly upward and, along with a sound like an accelerating jet plane, water is expelled out the "break". The amount of water reaching the lower plenum at that juncture is negligible.

We can now postulate that in the steam-first tests, the reverse of the process just described occurs, wherein a small amount of water is able to penetrate the annulus, condenses steam in the lower plenum, reducing the steam flow to the annulus, allowing more water to penetrate, which condenses more steam, etc. The location of steam condensation is now transferred to the lower plenum, which greatly reduces the steam flow into the annulus and allows all of the water to penetrate.

The line of Thermodynamic Ratio equals unity is therefore important in interpreting the results of the experiment. We find it is not possible for bypass to be ended at combinations of flows which lie above this line (except in Region 1).

Region 3

In discussing the behavior of the experimental data in this Region, let us first look at the flow pattern of the liquid in the apparatus during a bypass of water. Figure 45a illustrates how water is held in the upper portion of the annulus in tests run with cold water. Figure 45b shows that when the water is warmer, liquid is still supported in the annulus, but that it extends further down toward the lower plenum. Other information which may be useful is that the steam flow rate at which bypass is maintained with the colder water is higher than that at which bypass is maintained with warm water (see Figure 21, for example), that is $j_g^* \simeq 1.2$ for 55^oF water versus $j_g^* \approx 0.8$ for 140^oF water. These observations help in explaining the behavior observed in Region 3.

One might expect that the Region 2 type behavior would continue on to higher liquid flow rates. Instead, we see the tendency of the data to level off at higher liquid flows. The leveling off means that it suddenly requires much more liquid flow to end the bypass of water in the experiment with only small increases in the gas flow. This change occurs near some critical limit of the gas flow, and the level of this transition seems to depend upon the temperature of the inlet water.

In developing a theory to predict where the leveling off occurs, we can then consider the following two pieces of information: 1) the theory must show a dependence on the inlet water temperature, 2) the limiting steam flow at which the end-of-bypass locus shows the leveling off behavior must be decreasing with increasing water temperature. Figure 46 sketches these requirements. In this idealized view, we might expect, (as shown) that the set of lines of $R_t = 1$ represent the dependence upon water temperature. Further, we must have some other

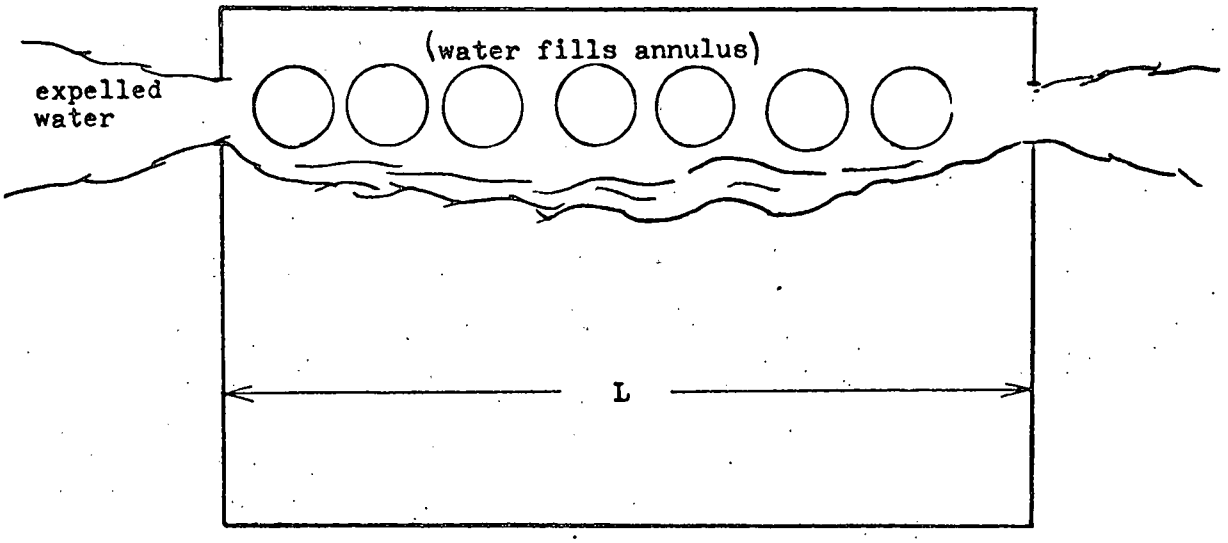

Figure 45a. Flow pattern of water in annulus during bypass (with cold injection water).

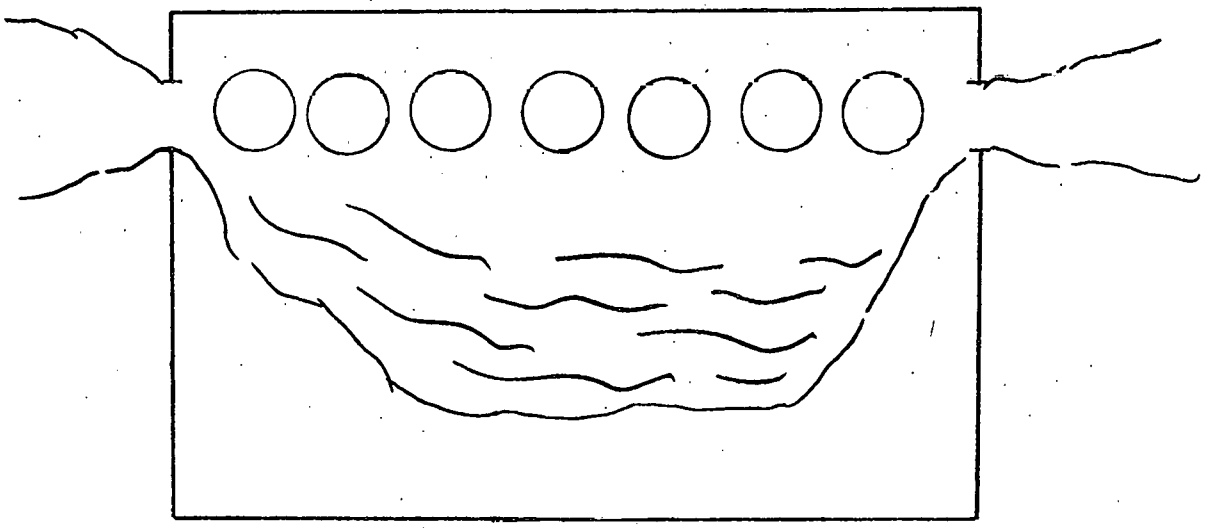

Figure 45b. Flow pattern of water in annulus during bypass (with warm injection water).

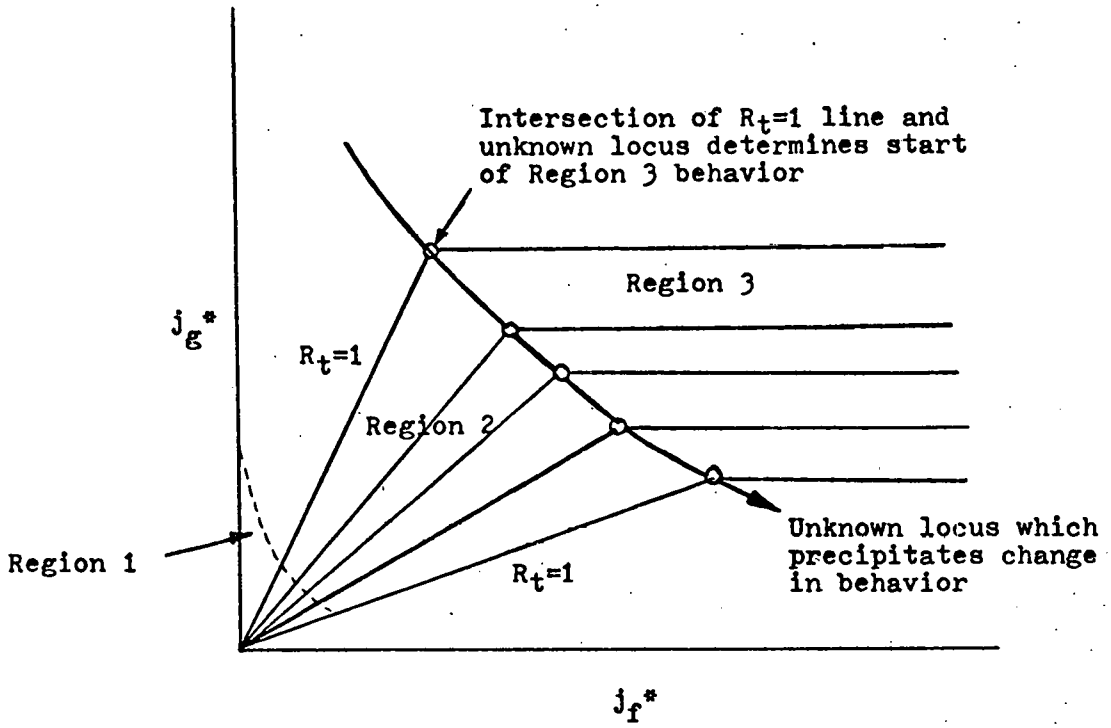

Figure 46. Sketch of requirements for theory predicting Region 3 behavior.

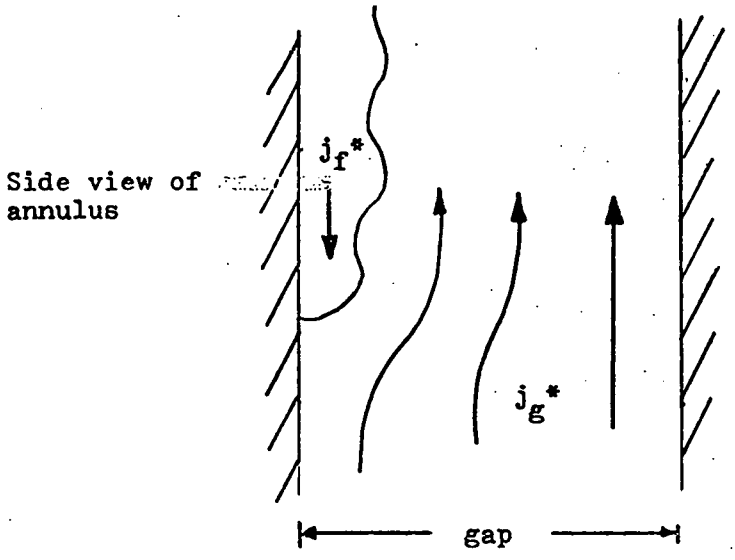

Figure 47. Thin film of liquid supported in annulus during bypass. Gas flow is upward past film.

determining criterion, which can be represented by another curve, such that the intersection of this curve with a given line of $R_t = 1$ determines the point at which conditions change to the leveling off behavior. This hypothesized locus remains to be investigated.

We may look back at the flow patterns of the water in the annulus under countercurrent flow bypass. Figure 47 shows a thin liquid film supported in an annulus. If the liquid film is thin, the gas is able to flow upward past the liquid and we think of the gap size (or the hydraulic diameter) as the important dimension to use in the dimensionless variables (Equations 1 and 2). The air/water experiments suggested that the hydraulic diameter, D_H, correlated the results well.

Now suppose that at higher liquid flows in the steam-first tests the water being supported in the annulus actually fills the annulus. (The observations show that this occurs.) We can postulate that the hydraulic diameter is no longer the characteristic dimension of the system, but rather that another dimension is more appropriate in considering how water is being held up in the annulus. Looking at Figure 45a we see that the dimension which is more appropriate to this flow pattern is the width, L, or perhaps half the width, of the annulus (half, because the flow is symmetrical). We can hypothesize that there is a bypass phenomenon which depends upon this width rather than the gap size when the water is held up - or "levitated" - in the annulus. The Wallis correlation for bypass shows the trend suggested by the unknown locus in Figure 46.

If we rewrite the dimensionless variable j* in terms of this new dimension we have,

$$j^*_{NEW} = \frac{j\rho^{1/2}}{[gL\Delta\rho]^{1/2}} \qquad (15)$$

and therefore, if the Wallis correlation (Equation 6), using the hydraulic diameter as the characteristic dimension describes bypass with thin films, we would expect the correlation using the width (or half the width) of the annulus to describe bypass when the flow is levitated and fills the annulus (as in Figure 45). The dimensionless variables in film-type bypass and in the levitated bypass are related by,

$$j^*_{NEW} = \left(L/D_H\right)^{1/2} j^* \tag{16}$$

and Equation 6 becomes,

$$j_g^{*\,1/2} + j_f^{*\,1/2} = \left(L/D_H\right)^{1/4} \tag{17}$$

D_H in this experiment was 0.74 inches, and L was 17.5 inches so that,

$$j^*_{NEW} = \left(\frac{17.5}{.375}\right)^{1/2} j^* = 4.8\, j^* \tag{18}$$

or if we take the characteristic dimension as half the annulus width, L = 8.75 inches, and,

$$j^*_{NEW} = 3.4\, j^* \tag{19}$$

This says that if we had plotted all the data based upon D_H as the characteristic dimension as we did in the experiment, then a bypass correlation based upon the annulus width as the characteristic dimension would have intercepts 4.8 or 3.4 times higher on such a plot, if our levitated bypass hypothesis is correct. We can take Figure 21 and plot the points where the data and the $R_t = 1$ lines intersect for the three inlet water temperatures (Figure 48). If the unknown locus has the form of the Wallis correlation with annulus width as the characteristic dimen-

sion, the three points should line up (on a square root plot) on a curve parallel to the line of Equation 6, but with $C = (L/D_H)^{1/4}$ instead. The Figure shows that these points could be thought of as lying on a curve where C is between 1.4 and 1.6 (the range owing to uncertainty as to exactly what the intersection points should be). The data are then showing that,

$$j_{NEW}^* = K\, j^* \tag{20}$$

where K is 2.0 to 2.5. This compares favorably with Equation 19, (based on L/2), and not quite so favorably with Eq. 18.

The hypothesis which is advanced then, is that at high liquid flows, the characteristic dimension in a Wallis-type correlation for bypass is the annulus width or half the width (or the circumference in a downcomer) rather than the hydraulic diameter; that this correlation and the intersection with the line $R_t = 1$ determine the levelling off in Region 3. More tests must be run with a greater range of water temperatures in order to determine experimentally where several more curves begin to level off so the result might be correlated better than was possible in this experiment. Scaling effects (e.g. surface tension) might also have influenced these results.

We can now put together a complete picture. The end of bypass phenomenon seems to be controlled by three things:

1) A thermodynamic consideration, representing the flows at which steam can just be condensed by the water (the line $R_t = 1$).

2) A Wallis-type bypass correlation based on film-type flow at low liquid flow rates. (The characteristic dimension being the hydraulic diameter.)

3) A Wallis-type correlation based on levitation of water in the annulus at high liquid flows where the water completely fills the upper portion of the annulus. (The characteristic dimension being the width of the annulus.)

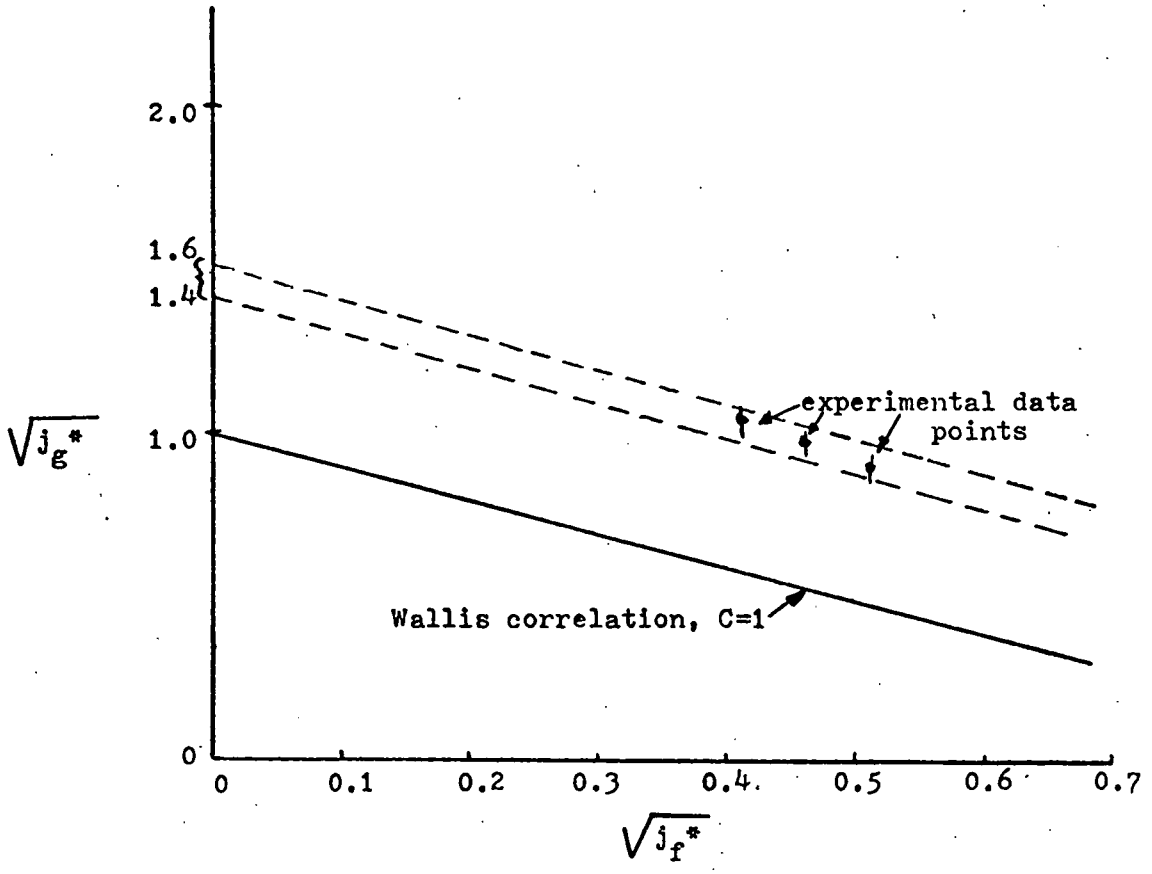

Figure 48. Plotting the data points from Figure 21 which lie on the intersection of lines of $R_t = 1$ and the end-of-bypass locus. The results are correlated by Equation 6 with a constant of 1.4-1.6, and suggest that a "levitated" type bypass (where the characteristic dimension is the annulus width) occurs.

These ideas are diagrammed in the Regime plot of Figure 49 for one typical inlet water temperature. In steam-first tests, at very low liquid flow rates, a film-type bypass plus some small factor to account for condensation is observed (Region 1, as discussed previously). If higher liquid flow rates are investigated, bypass ends when there is enough water to condense all of the steam (Region 2). This seems to be a transition to the levitated bypass curve. Once this second type of bypass curve is reached, the liquid is supported in the annulus and no water can penetrate the annulus. On the plot, if the levitated bypass curve is to the right of the $R_t = 1$ line, bypass ends at $R_t = 1$. But if the levitated bypass curve is to the left of $R_t = 1$ (above the intersection of the two), the water is all held up in the annulus and bypass cannot end. The intersection will occur at lower values of j_g^* with increasing water temperature, and therefore the critical gas flow to support the liquid will be less.

In the water-first tests (moving vertically upward from the abcissa on the plot), Regions 1 and 2 show the same behavior as in the steam-first tests. In Region 3, because the water is condensing all of the steam in the lower plenum, the levitated bypass curve is of no concern - bypass does not occur until the steam can no longer be condensed in the lower plenum. (A subsequenttest confirms that once this bypass has occurred, the steam flow must be reduced to approximately the critical Region 3 level before the bypass can be ended. So there is some hysteresis in Region 3.)

If the gas in the experiment was non-condensible, the slope of the line $R_t = 1$ would be zero. Therefore, we would have only the film-type bypass curve and no transition to the levitated-type bypass curve.

This flow regime map provides a consistent and predictable picture of the bypass phenomenon, and can be used as a basis for understanding future experiments.

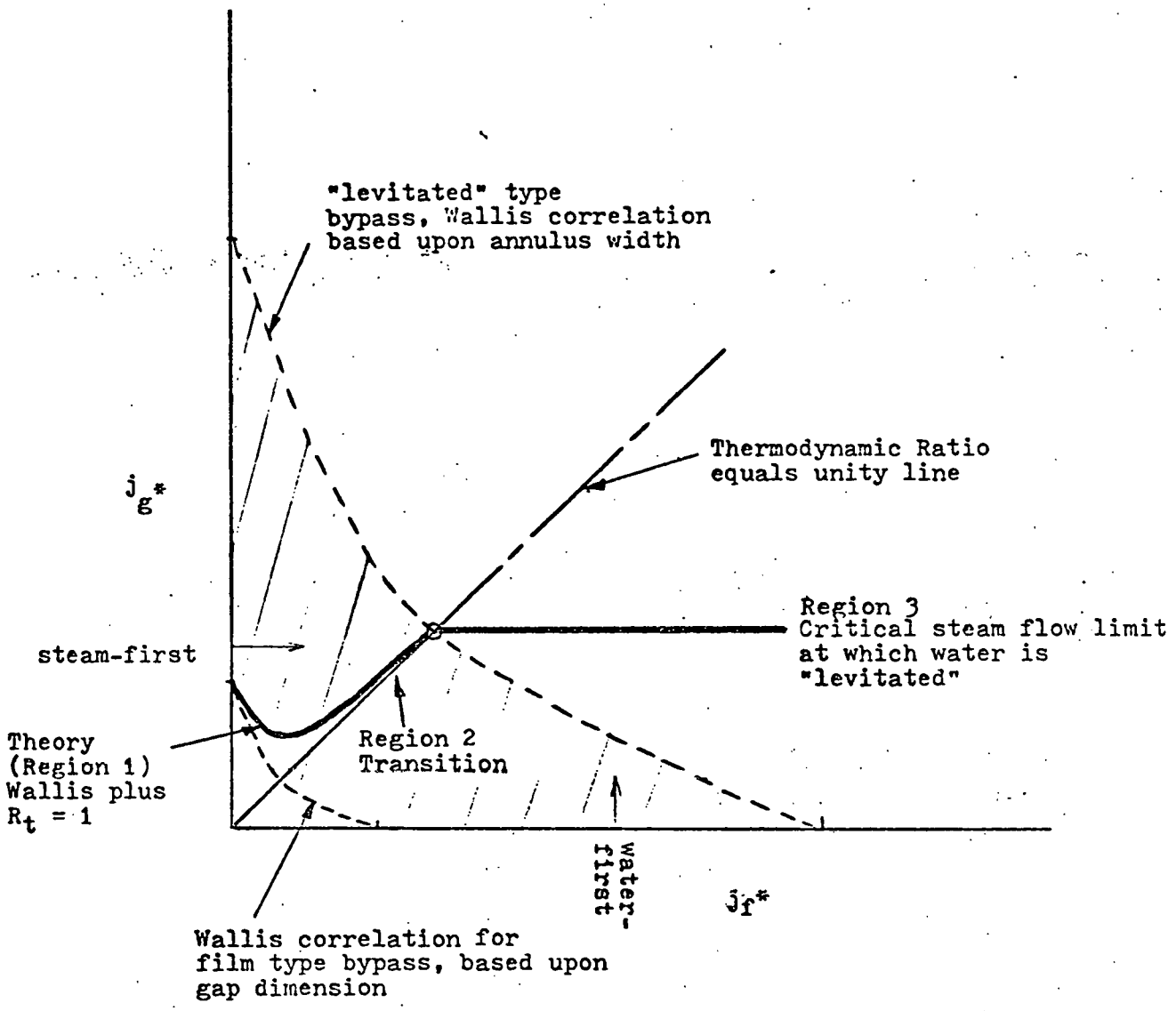

Figure 49. Completed bypass map. Region 1 is for film-type bypass plus a small amount for condensation. Region 2 (along $R_t = 1$) is the transition to levitated-type bypass. Region 3 is the critical steam flow limit for levitated bypass.

ENGINEERING APPLICATIONS

Figure 13 showed a plot of emergency coolant flow versus the annulus steam flow as calculated by some reactor vendors for typical reactor designs, predicting the conditions following one specific type of accident. It must be mentioned beforehand that these particular curves may not reflect current design since changes which are not public knowledge are continually being made by the reactor vendors. Nor are the curves representative of all types of accidents. This chart was the only available source of the kind of information needed here, and its purpose in this thesis is to illustrate how the results of this experimental work could be used with such a plot to predict the end of bypass of the water for this test annulus. The applicability of the experimental results observed in this investigation to the real nuclear reactor case must be demonstrated by further testing before predictions on that scale can be made with assurance. A number of factors not considered in this experiment could have an important bearing on events in the real situation.

The Figure 13 plot has been reworked in terms of the dimensionless variables used in this experiment - Figure 50. The curve for each design runs from the beginning of accumulator injection to the end, and several time intervals (and pressure readings) are marked along the route. By comparing plots of the experimental results with these curves, some idea of the point of "end-of-bypass", according to the bypass-no bypass locus determined in the experiment, is obtained. (Because of the good agreement of these results with the CE Annulus Penetration Data, we have some justification in assuming that this investigation produced information which may apply to the larger scaling.) The time at which end of bypass is predicted will depend upon several things: the steam and water flows, the water temperature, and the steam properties.

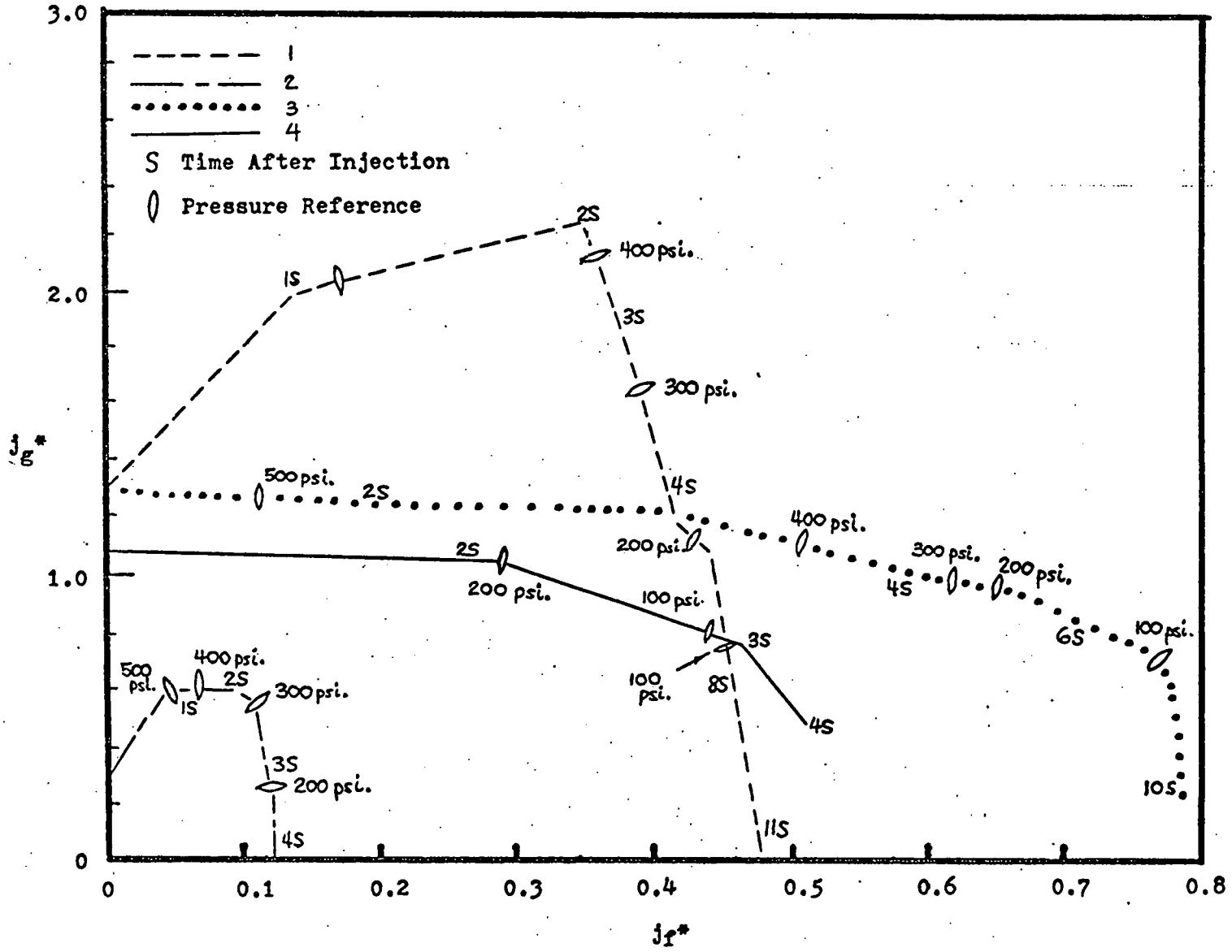

Figure 50. Figure 13, replotted in terms of dimensionless variables. Typical steam versus ECC water flows after a reactor accident. (Assumes a 10" downcomer gap for each design.)

Regions 1 and 2

It was noted in the Interpretation section that the end of bypass cannot occur before there is enough water being injected into the vessel to be able to condense all of the steam, and that the transition corresponds to the line of Thermodynamic Ratio equal to unity. Intuitively, because of the high pressures and temperatures calculated to occur in a real accident, one would expect that a lot of liquid would be necessary to condense the steam in the event of a LOCA, more so than under the conditions tested in the experiment.

Appendix D discusses the line $R_t = 1$, and gives the calculations for generating the slope of that line. In the same manner, we may calculate the slope of such a line for saturated steam from 100 to 500 psi, using,

$$j_g^* = j_f^* \left(\frac{\sqrt{\rho_g}}{\sqrt{\rho_f}}\right)^{1/2} \left[\frac{\Delta h_{water}}{\Delta h_{steam}}\right] \qquad (21)$$

(For these calculations, the saturated steam properties for the given pressure will be used. There may be some superheat of the steam, but even at 100° superheat this result is close to the saturated steam calculations because $\sqrt{\rho_g}$ and Δh_{steam} both increase. The actual steam temperature calculations were not available.)

The values are listed in Table VII. The number is the slope of the line for $j_g^* = m j_f^*$.

Table VII

Pressure (psi)	m, 120°F water	m, 55°F water
500	3.2	3.8
400	3.3	4.0
300	3.4	4.15
200	3.5	4.5
100	3.7	4.9

Figure 51 illustrates where these lines lie on the Figure 50 plot. The line of $R_t = 1$ at any particular instant during the accident would lie somewhere in the area for a given temperature.

We can also plot the Wallis correlation on the same chart (Figure 51) to see where Region 1 would lie, and we find it considerably below the curves toward the right.

Addressing ourselves only to the question of steam properties and ignoring for the moment the Region 3 behavior of the experimental results, we see that bypass could not possibly end 1) above the Wallis correlation on the left of the intersection with the $R_t = 1$ lines, or 2) above the appropriate $R_t = 1$ line to the right of the intersection.

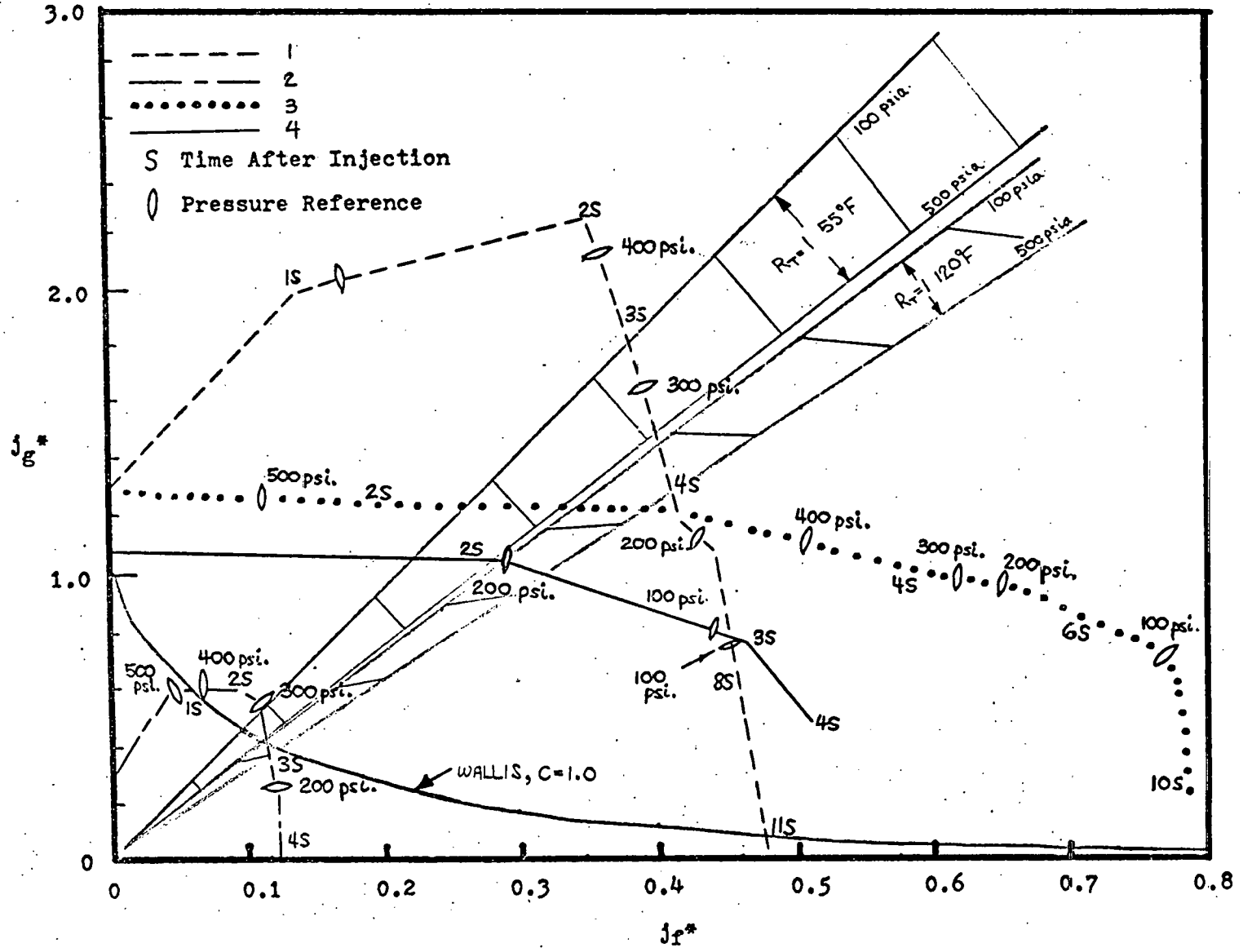

Figure 51. Including lines of Thermodynamic Ratio equals unity for different fluid conditions. Also, comparison with the Wallis correlation.

Region 3

Since the accumulator tanks are located in the reactor containment, and since that containment becomes very warm during reactor operation, it is quite possible that the emergency coolant temperature in the accumulators could be around 120°F. Figure 52 is a plot of the end of bypass locus we might expect for 120°F water, extrapolating from the experimental results. The Region 3 behavior predicts a levelling off of the end of bypass locus. If there are no obstructions in the annulus other than hot legs, the experimental results indicate that this levelling off would occur around $j_g^* = 0.9$ for the 120°F water. With the best types of baffling used in this experiment, we would expect a levelling off around $j_g^* = 1.6$. Thus we end up with the curves as sketched in Figure 52, basing the predictions on the results of the experiment.

We see that for some accidents and some designs the bypass-no bypass transition could lie directly across the reactor values, and that a slight change in the bypass locus could mean a significant difference in the time at which bypass ends, for those given conditions.

For the 120°F water, without baffling, it looks as if the water would not enter the lower plenum immediately upon injection, if the schedules of flow rates like the ones in the Figure were followed. Bypass would end partway through the accident in each case, at about the 200 psi level. With the baffling, numbers 2 and 4 would show little improvement in regard to an earlier end to bypass. Numbers 1 and 3, however, would show an end to bypass which is several seconds earlier compared to the case without baffles. This means that ECC injection and penetration to the lower plenum would begin about 3 seconds sooner with baffles for 1 and 2.

If we postulate that the inlet water is cool (55°F) at injection, then we can sketch a new curve (Figure 53) for the end of bypass locus.

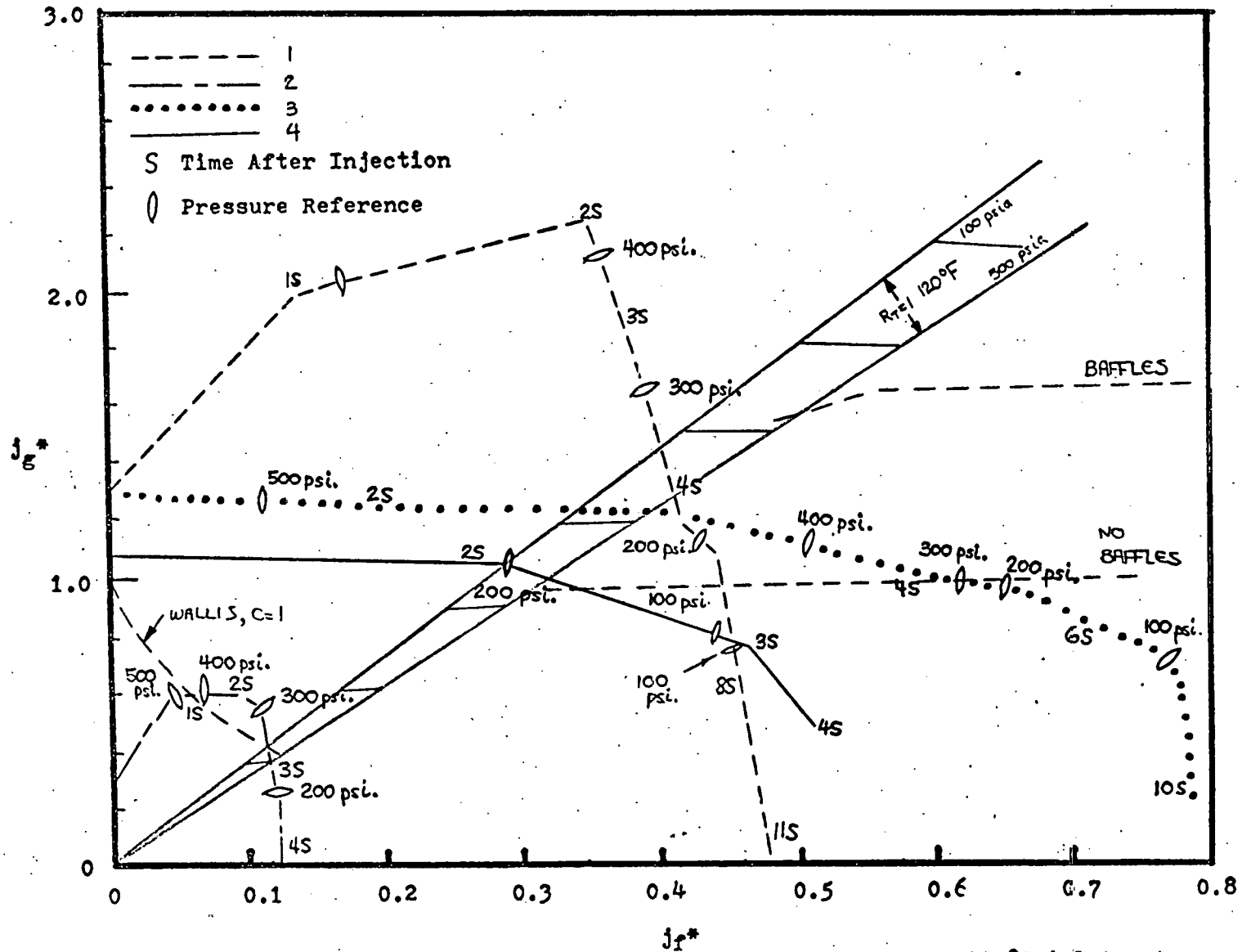

Figure 52. Extrapolating the end-of-bypass curve for 120°F inlet water, with and without baffles.

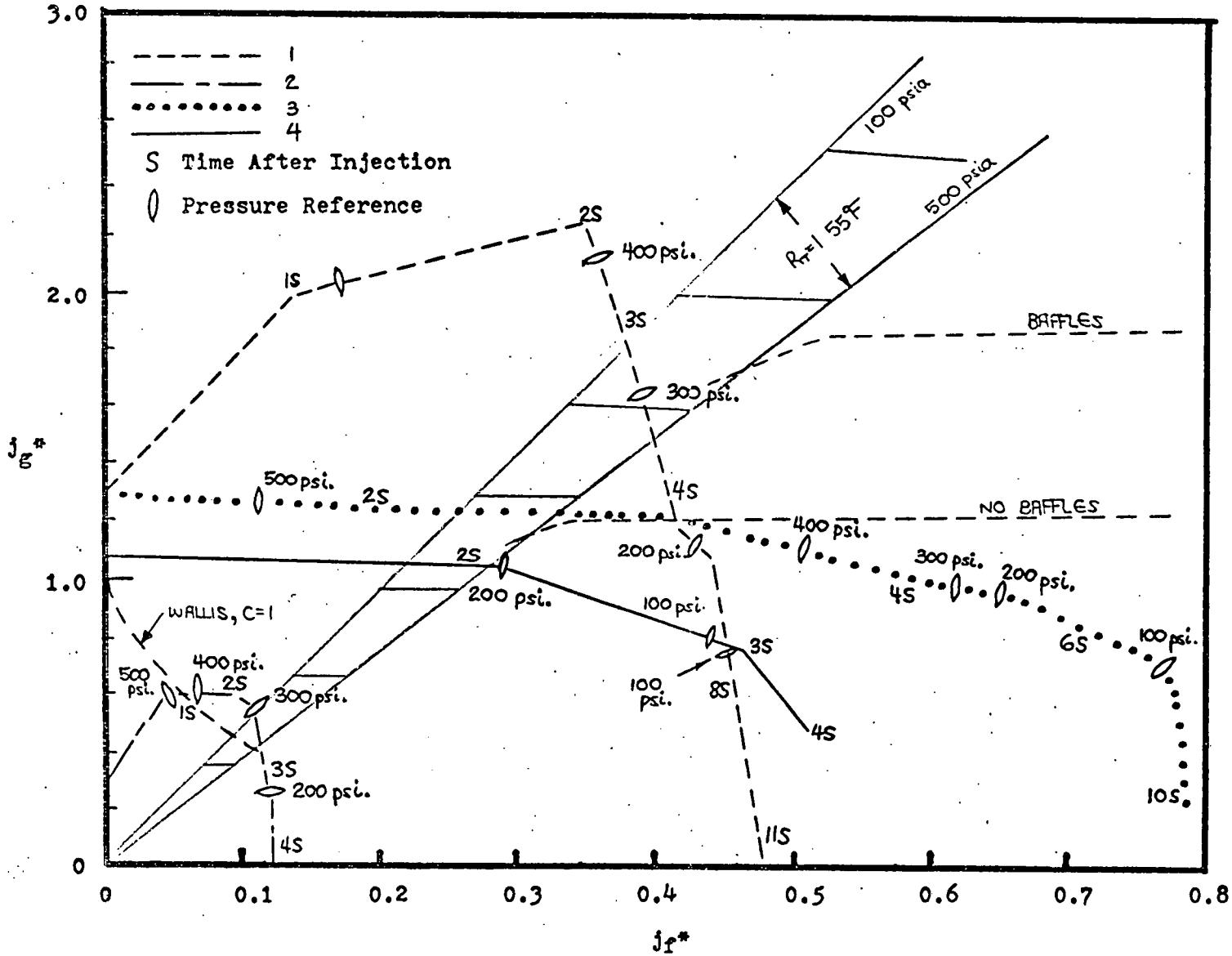

Figure 53. Extrapolating the end-of-bypass curve for 55°F inlet water, with and without baffles. Compare with Figure 52.

The levelling off in Region 3 would occur at $j_g^* = 1.2$ without baffling, and at $j_g^* = 1.8$ with baffling. Therefore, cooler inlet water could achieve about the same effect, according to this experiment, as the baffled 120°F water except that number 3, lying right along the critical limit might be improved significantly by the slight change. The baffled case turns out to make about the same prediction for 55°F water and 120°F water. The margin of safety in the prediction is improved though.

On the other hand, if the steam upstream of the cold leg in a real accident condenses and raises the temperature of the inlet water to saturation, then the system would be expected to behave like non-condensing countercurrent flow. We might then postulate that the Wallis correlation will hold (Figure 54). By choosing this conservative limit, and further a conservative constant in the equation, the criteria for end of bypass could be redefined to at least admit this. (Cooling the stored water to 55°F might result in coolant water of 120°F at injection if there is steam upstream of the cold leg - or indood, there could be injected water of just about any temperature between 32° and saturation temperature, which makes prediction difficult for the actual case.)

The experimental results show that under the stated assumptions, using some schedules of steam and water flows typical of accidents, reactor safety systems could lie on the borderline between bypass and no bypass in some cases. Also, that adding baffling or cooling the water as it is stored in the accumulators (or both) could mean an earlier end to accumulator bypass, depending upon other conditions at the time of the accident. We have seen that these changes gave improvements in this experiment.

We might briefly discuss the impact of installing baffles in reactors. The designs for baffling have not been exhausted. This experi-

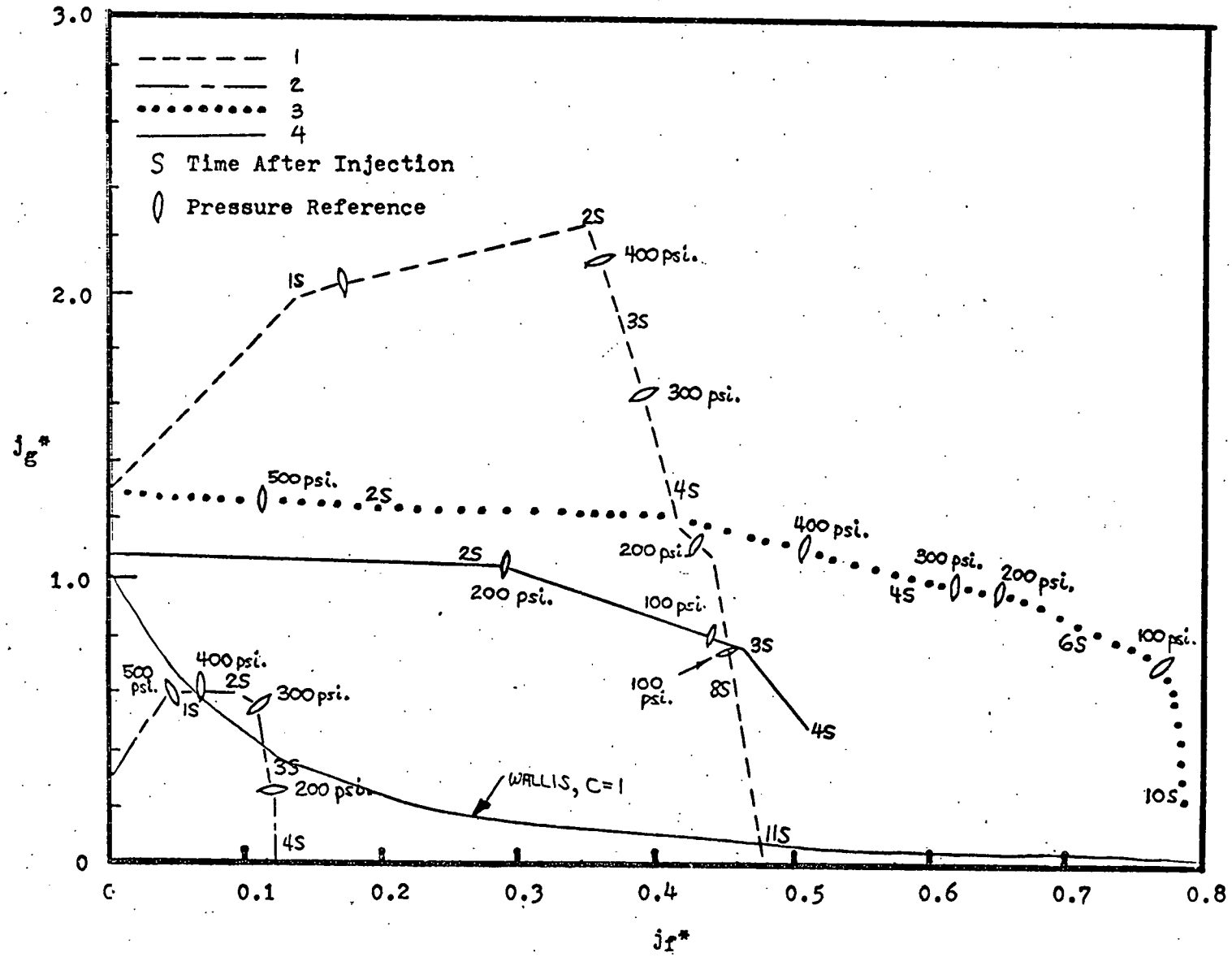

Figure 54. The Wallis correlation appears to be the lower limit in the case of injected liquid at saturation.

ment does not claim to have, nor was it intended to have, produced the optimum baffle. (Just offhand, we might suggest for instance a separate injection design with a nozzle which directs a steady stream of water directly downward in the annulus.) It has merely been demonstrated that baffling might bring about improvements in ending accumulator bypass. But, the installation of any kind of baffles in an actual reactor creates other problems.

The problems are a little different in two instances: it might be required that only every new reactor have baffling, or it could be required that all the older reactors also be back-fitted with baffling. The former case would not present as many difficulties as the latter. The long, straight type of baffles which were used in the experiment do not really interfere with the uniform flow of the water in the downcomer. Their main effect would be to create new thermal stresses in the pressure vessel if they are attached to it. (They could be attached to the core barrel and a small gap left between the baffle and the pressure vessel.) The altered stresses in either case would require new calculations in all design and operating conditions, but the cost of this, plus the cost of installation would be peanuts compared to the cost of a reactor plant (approximately $400 million per plant - and the redesign calculations would have to be done only once).

Backfitting existing reactors with baffles would generate quite a few problems. Mechanically, the pressure vessel cover would have to be removed, the core internals taken out, and the baffles welded in under radioactive conditions. Then there is also the problem of economics. Shutting down the nuclear power plant in order to install some type of baffling would be very costly. Presumably, alterations would be made at a

time when the reactor was about to be refueled. This would save on the shutdown time, but it would still take months, perhaps a year, to make the changes and have them approved. Although a specific number is hard to pin down, it costs several hundred thousand dollars per day when a PWR is shut down for repairs. The delay to install baffles would be costly.

Chilling the accumulator water is a step more easily accomplished both mechanically and practically. The work could probably be done during the normal time period for shutdown and refuelling, or not much longer. It would involve insulating and refrigerating the accumulator tanks. Since a typical accumulator (Table 2) holds around 7000 gallons, we can make a quick estimate of the costs to chill the water. Appendix G shows calculations for tanks with no insulation - about $40 per day in operating costs for four 7000 gallon tanks - and with about an inch of glass wool insulation - $6 per day for all four tanks. With insulation the costs are negligible. Amortizing the cost of the equipment over a forty year life of the plant would not change the daily operating cost significantly.

It must also be recalled that any changes in one part of the reactor system can have a cascade effect - because the PWR is such a complicated system, one change can cause interactions elsewhere which may not be desired. Chilling accumulator water, for instance, may have an effect on possible oscillatory behavior in the injection section. Such oscillations would depend on condensation (of the steam upstream in the cold leg by the water) and hence upon the sub-cooling of the injected water. We also saw in this experiment that there is a critical steam flow limit above which bypass does not end (Region 3). In the reactor accident, the steam mass flow in the annulus depends upon the pressure drop to the break. If the pressure increases by a factor of ten during bypass, the steam flow may be reduced below the

critical limit by the increased pressure drop and bypass could end. But then steam flow could increase again as the pressure drop in the annulus became smaller, causing bypass to begin again - and there could be oscillatory behavior between these two conditions, bypass, and then no bypass. For this reason, changes recommended on the basis of one experiment require further study.

A bypass locus like that found in the experiment could, however, serve as a map in determining whether or not, under certain given conditions, bypass is occurring. The better the safety system operates, the less the damage to the reactor in the event of a major accident. If we relate damage done to a reactor during an accident to the shutdown time needed to make repairs, the costs of several hundred thousand dollars per day provide an economic incentive to understand and improve the Emergency Core Coolant injection system so that damage will be minimized. In that respect, this experiment represents a significant contribution toward understanding the steam/water interaction of the "accumulator bypass" problem.

CONCLUSIONS

1) Bypass is an on/off process in the presence of condensation. When the steam flow is set at a constant level in the experiment and the liquid flow is increased, all of the water is bypassed until a critical value of the liquid flow is reached. At that point, the condensation location is transferred to the lower plenum, and all of the liquid penetrates into the plenum.

2) The Wallis correlation, which applies to non-condensing countercurrent flow situations, appears to be the lower limit of the bypass locus in this experiment. That is, if the water would be at saturation temperature, the system would be non-condensing in the presence of steam, and experimental results point to the Wallis correlation as a good model for that situation in this scaled reactor geometry.

3) The experiment was concerned mainly with the results of tests in which steam flow was held constant, liquid flow was increased, and the point at which bypass ended determined. The experimental results of these tests may be divided into three regions:

A) Region 1 concerns high steam and low liquid flows. In this Region, little condensation of the steam is possible, and the system follows the Wallis correlation plus a small difference to account for that little bit of steam which can be condensed.

B) The Region 2 results follow along the line of Thermodynamic Ratio equals unity, that is, the locus where the steam can just be condensed 100% by the liquid. Bypass cannot end until this combination of flows is reached because the end of bypass occurs when the steam condensation location is no longer in the annulus but in the lower plenum instead. If the steam cannot all be condensed in the lower

plenum, then steam is forced into the annulus and initiates a process whereby more, and then all, of the steam enters the annulus, expelling the water.

C) The Region 3 results show a levelling off in the graphs. Looked at one way, this means that it suddenly requires much larger liquid flows to put an end to bypass. Looked at another way, it means that small increases in steam flow will suddenly support a great deal of liquid in the annulus and expel it.

4) The temperature of the water affects the experimental results. Region 1 follows the same pattern whether cold or warm water is injected. But with warmer water, it takes more liquid to condense all of the steam so that the line of Thermodynamic Ratio equals unity is lower than with chilled water. The same is true of Region 3. The critical steam flow at which suddenly much larger amounts of liquid are required to end bypass is also lower with warmer water. (See experimental results). The system thus ends bypass at lower steam flows with warmer water.

5) There is a difference in the results if steam-first or water-first tests are conducted. Subsequent tests showed a hysteresis effect in Region 3.

6) The amount of water entering the lower plenum during bypass in this experiment was negligible. If $j_g^* > 1$ and bypass is occurring, the tiny amount of water that is penetrating is due to chance interactions and is not a dependable supply of "emergency coolant".

7) Pressures in the lower plenum increased by a factor of ten when bypass occurred, over the pressure just before bypass took place. The measured pressures were lower in tests with warmer water.

8) The results of the CE Annulus Penetration and the Aerojet semiscale tests are predicted very well by the results of this experiment.

This fact is doubly interesting (and surprising) when one considers that the scale and the geometries used were very different in each of these tests.

9) Concerning the injection geometries tested (which included three simulated cold legs - adjacent in some tests - sometimes two inlet legs, and sometimes even a single inlet) there was no experimental evidence of a significant difference in any of the tests using any of these injection arrangements.

10) Some baffling arrangements, particularly the straight bars, made significant improvements according to the experimental results. The Region 3 critical steam flow was increased by 50% with the best baffling, which meant that the end of bypass took place at a 50% higher steam flow with baffling as opposed to without it.

11) The collar-type baffling showed some improvement in the experiment, but only about one-fourth of the improvement shown with the straight baffles.

12) The simulated thermal shield did not yield any changes at all.

13) Doubling the size of the break area in one test did not alter the results.

14) Some water was observed to be stored in the annulus during bypass, which later fell into the lower plenum when bypass ended. The quantity was not determined in this experiment.

15) One must be careful about extrapolating the experimental results to reactor scale, but the agreement with the CE and Aerojet experimental results gives some indication that the scaling effect may not be very great.

RECOMMENDATIONS

1) Since the end of bypass locus in these experiments depended upon the inlet water temperature as well as the steam and water flows, further tests are recommended to determine how such things as having steam upstream in the cold leg or having hot annulus walls affects the temperature of the incoming emergency coolant. This suggests countercurrent steam-water tests with hot walls.

2) The experimental results show that bypass ends at higher steam flows when colder water is used. From the narrow viewpoint of ending bypass, chilling the accumulator water in the reactor containment might aid in ending bypass, should it occur in a reactor. This approach has advantages, both mechanical and practical, over baffling.

3) Baffling also helped to promote water penetration in our experiments. Further investigation of baffles in larger-scale tests is recommended.

4) Further experiments in larger-scale rigs should be conducted to determine scaling effects. The CE apparatus provides an existing facility for such tests. An effort showing that results similar to the 1/30 scale results were obtained would show that scaling effects were small up to 1/5 scale.

5) Studies quantifying the amount of water being stored in the annulus during bypass should be conducted, to see whether this volume of water penetrates at the end of bypass.

6) Besides baffling as a means of directing the incoming emergency coolant, other injection schemes, such as direct injection with a vertical nozzle in the annulus, might be tested in models.

REFERENCES

1. Acceptance Criteria for Emergency Core Cooling Systems for Light-Water Cooled Nuclear Power Reactors, Atomic Energy Commission, 1973, p. 74.
2. Emergency Core Cooling Systems for Light-water Cooled Power Reactors, Lawson, C.G., October 1968, p. 49.
3. Ibid., Page 49.
4. Acceptance Criteria, op. cit., p. 191.
5. Acceptance Criteria, op. cit., p. 188.
6. Acceptance Criteria, op. cit., p. 191.
7. Acceptance Criteria, op. cit., p. 190.
8. Wallis, G.B., Block, J.A., Crowley, C.J., Flow Patterns in a Simulated Reactor Downcomer Annulus, AEC Report #COO-2294-1, March 1974.
9. Crowley, C.J., Report prepared for G.B. Wallis, The Air/Water Interaction in a Scaled PWR Downcomer Annulus, January 1974. (See supplement to this report.)
10. Wallis, G.B., One-Dimensional Two-Phase Flow, McGraw-Hill, 1969, p. 339.
11. Pushkina and Sorokin, Breakdown of Liquid Film Motion in Vertical Tubes, Heat Transfer - Soviet Research, Vol. 1, No. 5, p.p. 56-64, September 1969.
12. Experimental work performed by Suresh Makkenchery at Dartmouth College, 1972.
13. Wallis, G.B., Two-Phase Flow, op. cit., p. 336f.
14. Wallis, G.B., Two-Phase Flow, op. cit., p. 356.
15. Flow Patterns in a Simulated Downcomer Annulus, op. cit.
16. Brown Instrument Company, Flow Meter Engineering Handbook, Minneapolis-Honeywell Regulator Co., 1946.
17. Letter Report for Steam-Water Interaction Tests, Annulus Penetration Tests, Broderick, J.R., Loiselle, V., Nuclear Power Systems, Combustion Engineering, 1974.

APPENDICES

APPENDIX A. Scaling Water and Steam Flows

The calculations contained in this section were part of the preliminary work determining the magnitude of the water and steam flows required to model accumulator bypass.

Water Flow

The study at Dartmouth which investigated the flow patterns of water in an annulus[8] indicated that the results could be scaled with the dimensionless Froude number,

$$F_o = V_o (g\,d)^{-1/2} \qquad (1)A$$

which depends upon the velocity of the fluid in the inlet pipe. (Another parameter for the flow patterns was a dimensionless size given by the gap dimension over the pipe diameter.) The Froude number can also be written,

$$F_o = 4Q/\pi g^{1/2} d^{5/2} \qquad (2)A$$

by making use of continuity ($Q = V_o A$).

Knowing that V_o is on the order of 8-10 ft/sec in a 2.5 ft. diameter cold leg pipe during ECC injection, F_o is calculated to be on the order of 1.0. Then,

$$Q = (1.0)\ \frac{\pi}{4} g^{1/2} d^{5/2} \qquad (3)A$$

At 1/30 scaling, the cold leg diameter becomes 1 inch. Calculating the required flow rate to model ECC injection gives a value,

$$Q = 12 \text{ gpm}. \qquad (4)A$$

At full scale, Q = 60,000 gpm. or 8400 lb/sec, a number which compares favorably with the peak in Figure 5.

Steam Flow

Obtaining the necessary water flow rate was no problem, but the available steam supply was not known to be adequate. As an order of magnitude estimate for the steam flow required to model the accumulator bypass phenomenon, Figure 50 indicated that the magnitude of the steam flow calculated for actual blowdown conditions could reach a $j_g^* = 2.2$.

In order to model the blowdown with this apparatus then, we would also like to be able to reach a j_g^* of about this magnitude, so that,

$$j_g^*\,\text{model} = j_g^*\,\text{actual} \qquad (5)A$$

This $j_g^* = 2.2$ corresponds to a mass flow rate of steam of about 13 lb/min (see Appendix E). The maximum mass flow of the steam supply was found to be near 14 lb/min. Therefore, the steam supply appeared to be satisfactory.

Ignoring compressibility effects, the steam velocity in the annulus can be calculated,

$$V = \frac{W}{A} \qquad (6)A$$

$$= \frac{(10\ \text{lb/min})\ (1\ \text{min}/\ 60\ \text{sec})}{(.04\ \text{lb/ft}^3)\ (\frac{.375 \times 17.5}{144})\text{ft}^2}$$

$$= .90\ \text{ft/sec}$$

This result was used to estimate the pressure drop that might be expected to exist in the annulus as a result of having a break area 8.3 times

smaller than the annulus area. Again, neglecting compressibility effects, assuming continuity says the exit velocity is roughly 750 ft/sec.

Bernoulli and the same assumptions give,

$$p + \frac{\rho V_1^2}{64} = \frac{\rho V_2^2}{64} \qquad (7)A$$

$$p = 2.4 \text{ psi} = 68" H_2O$$

which suggested that the annulus ought to be made fairly strong and thick-walled. Indeed, actual pressures observed in this range of steam flows - no water flow - were on the order of 50 inches of water, the discrepancy undoubtedly due to compressibility. Upstream steam pressure was 20 psia, so the system was expected to be able to handle the pressure drop in the annulus.

Finally, a check was performed to indicate if choking would occur in the apparatus. The sonic (or choking) velocity of steam in the near atmospheric conditions range can be estimated,

$$C = \sqrt{\frac{\Delta p}{\Delta \rho}} = 1380 \text{ ft/sec} \qquad (8)A$$

using the range 10 to 20 psi as the interval.

At flow rates of 10 lb/min = 1/6 lb/sec = 4.2 ft^3/sec, the maximum area to cause choking is about

$$A = \frac{4.2 \text{ ft}^3/\text{sec}}{1380 \text{ ft/sec}}$$

$$= 3 \times 10^{-3} \text{ ft}^2 = .433 \text{ in}^2$$

and there are no flow areas that small in the apparatus. (This estimate is only for a single phase fluid, and does not take into account the possibility of homogeneous two-phase flow in which sonic velocities may be drastically reduced.)

APPENDIX B. Heat Losses

The heat losses have been divided into two portions, losses from the piping and losses from the barrel on which the annulus was mounted. The annulus, the baseplate, and the plastic windows are assumed to be essentially adiabatic.

The expression for the heat loss from the apparatus is,

$$q = \frac{\Delta T}{R_{c1}+R_k+R_{c2}} \qquad (1)$$

where R_{c1} and R_{c2} are the convective resistance to heat transfer on the steam and air sides of the apparatus walls, respectively. R_k is the conductive resistance of the steel in the apparatus. R_{c1} and R_k are very small in comparison to R_{c2}, since heat transfer with condensing steam and in steel is very rapid. The heat transfer is mainly limited by the convective properties of the air on the outside. Therefore, the expression can be simplified to,

$$q = \frac{\Delta T}{R_{c2}} = \bar{h}\, A_T\, \Delta T \qquad (2)$$

The convective heat transfer coefficient, $\bar{h}$, for air is about 2 Btu/hr-ft^2-$^\circ$F. With 19 ft. of uninsulated piping leading into the apparatus, the surface area is,

$$A_p = DL = 10 \text{ ft}^2$$

The surface area of the barrel is,

$$A_b = (\text{side area-window area}) + \text{bottom area}$$
$$= 23 \text{ ft}^2$$

therefore the total heat loss for a ΔT of 145°F is,

$$q = \bar{h}\,(A_p + A_b)\,\Delta T = 107 \text{ Btu/min.}$$

The steam flow ranged from 2 to 14 lb/min in the experiment. Since the enthalpy provided by the steam was 1150 Btu/lb, the heat content of the incoming steam ranged from 2300 Btu/min to 16,000 Btu/min. The heat losses range from 4.5% to 0.7% of the total heat influx. In the usual operating range then, the losses are only a few percent.

Because of the high conductivity of the steel and the high rate of heat transfer with condensing steam, the apparatus warms up very quickly, so that the time to prepare the apparatus for testing was short.

APPENDIX C. Orifice Plate Calculations

The device used to measure the steam flow rate was an orifice plate designed according to the specifications in Reference 16, Chapter X, Orifice Calculation for Steam Flow. The recommended equation is:

$$W = 1271.9\ ECD^2\ F_{HM}\ F_1\ F_2 \qquad (1)$$

where:

W = rate of flow of steam in lb/hr

E = area correction factor

C = coefficient of discharge

D = internal pipe diameter (inches)

F_{HM} = The square root of the manometer reading (inches of mercury)

F_1 = square root of the dry saturated steam density at operating pressure, lb/ft^3

F_2 = correction factor for superheated or wet steam.

In designing the orifice plate it is first necessary to calculate C, so this value may be used to determine the orifice diameter. If the design is begun on the basis that a .2 inch height of water corresponds to 1 lb/min (60 lb/hr) steam flow rate, the resulting operating range of the manometer for the steam supply is from 0.2 inches to about 35 inches of water.

The coefficient E, determined from Figure 9 of the reference is equal to 1.002. Following the appropriate figures and tables for the other coefficients,

$D^2 = 4.2725 \quad inches^2$

$F_1 = 0.22 \quad (lb/ft^3)^{\frac{1}{2}}$

$F_2 = 1.0000$

with the upstream steam property of about 20 psi saturated vapor.

To determine F_{HM},

$$F_{HM} = \left[0.2" H_2O \times \frac{1 \text{ ft.}}{12 \text{ in.}} \times \frac{30" Hg}{34 \text{ ft } H_2O}\right]^{1/2} = 0.12 \qquad (2)c$$

Solving Equation 1 for C ,

$$C = \frac{60}{(1271.9)\,(1.002)\,(4.2725)\,(0.22)\,(0.12)} = 0.43 \qquad (3)c$$

From Table 49 of the reference it is found that d/D = .67 for C = 0.43 in a 2 inch pipe, and therefore the orifice should be,

$$d = (2)\,(.67) = 1.34 \qquad (4)c$$

inches in diameter.

The plate was constructed with an orifice of this size. It was made out of thin aluminum, and as suggested by the reference, had square edges.

Using Equation 1c then, a table was prepared showing the steam mass flow rate for every 0.1 inch increment of the height of water in the manometer, and this table used as the source of the flow rates in plotting experimental results.

Pipe taps were recommended as the type pressure tap to use in a 2 inch pipe with an orifice ratio (d/D) less than 0.70. The size of the taps was 1/8 inches diameter, both were located on the top of the pipe, and connected to a 52 inch manometer by copper tubing. The downstream tap was located 8 nominal diameters (16 inches) from the plate. The upstream tap was 2.5 diameters (5 inches) from the plate.

Finally, for upstream configurations of one elbow (or tee) before the orifice plate, and a d/D of 0.67, the minimum upstream recommended straight run of pipe is 13 diameters plus 2 pipe diameters for using pipe taps, giving 30 inches total. The actual length in the apparatus was

48 inches. For the downstream section, the minimum is 4 pipe diameters (8 inches) and the actual length was 24 inches.

APPENDIX D. Calculating R_t, Thermodynamic Ratio

The reference lines of $R_t = 1$ on the plots of experimental data represent the combinations of steam and water flows at which the enthalpy of the steam is just enough to raise the temperature of the liquid to saturation, or in other words, the steam can just be 100% condensed by the water. This turns out to be a straight line on a graph of j_f^* versus j_g^*. Above such a line there is more steam than is able to be condensed; below the line there is more than enough water to condense all of the steam.

In terms of an energy balance,

$$R_T = \frac{W_w (c_p) (\Delta T)}{W_s h_{fg}} = 1.0 \qquad (1)D$$

where W_w, W_s = the water and steam mass flows,

c_p = heat capacity of water, 1 Btu/lb-^oF,

ΔT = amount of sub-cooling of water,

h_{fg} = the enthalpy difference between saturated vapor and saturated liquid.

In general,

$$W/\rho^{1/2} \alpha j \rho^{1/2} \alpha j^* \qquad (2)D$$

rearranging,

$$W \alpha j^* \rho^{1/2} \qquad (3)D$$

and substituting this relationship into Equation 1D,

$$R_T = \frac{j_f^* \rho_f^{1/2} (c_p) (\Delta T)}{j_g^* \rho_g^{1/2} h_{fg}} = 1.0 \qquad (4)D$$

So, when the energy balance is solved for $R_t = 1$,

$$j_g^* = j_f^* \left(\frac{\rho_f}{\rho_g}\right)^{1/2} \left[\frac{c_p \Delta T}{h_{fg}}\right] \quad (5)$$

Now $\rho_f = 62.4$ lb/ft^3, $\rho_g = .04$ lb/ft^3, $h_{fg} = 970$ Btu/lb, and $\Delta T = (212 - T)$ (T is inlet water temperature).

Substituting,

$$j_g^* = j_f^* \left(\frac{62.4}{.04}\right)^{1/2} \left[\frac{(1)\ (212-T)}{970}\right]$$

$$= 4.0 \times 10^{-2}\ (212-T)\ j_f^*$$

For an inlet water temperature of 55°F,

$$j_g^* = 6.3\ j_f^* \quad (6)$$

which is a straight line of slope 6.3 on the experimental plots. The subscripted numbers for each line therefore refer to the inlet water temperature.

If T = 100°F, $j_g^* = 4.5\ j_f^*$

If T = 140°F, $j_g^* = 2.9\ j_f^*$

- -

The same calculations can be made for the steam properties used in the Combustion Engineering Annulus Penetration Tests and the Aerojet semiscale (preliminary) tests, so that this information is available for use in Appendix F.

The steam properties in the CE test were 30 psi saturated steam at 250°F, for which $\rho_g = 0.073$ lb/ft^3 and $h_{fg} = 945$ Btu/lb. The water properties do not vary significantly. Using Equation 5,

$$j_g^* = j_f^* \left(\frac{62.4}{0.073}\right)^{1/2} \left(\frac{212-T}{945}\right)$$

$$= 3.0 \times 10^{-2}\ (212-T)\ j_f^*$$

If $T = 60^{\circ}F$, $j_g^* = 4.6\ j_f^*$

If $T = 120^{\circ}F$, $j_g^* = 2.7\ j_f^*$

If $T = 155^{\circ}F$, $j_g^* = 1.7\ j_f^*$.

In the Aerojet semiscale tests, without hot walls, the inlet water temperature was $190^{\circ}F$. The steam was at 50 psi (saturated), so that $\rho_g = 0.118$ lb/ft^3 and $h_{fg} = 924$ Btu/lb. Water at $190^{\circ}F$ has a density of 58 lb/ft^3. From this,

$$j_g^* = j_f^* \left(\frac{58}{0.118}\right)^{1/2} \left(\frac{22}{924}\right)$$

$$= 0.53\ j_f^*$$

This is the determination of the lines of $R_t = 1$ for the figures in Appendix F, later on.

APPENDIX E. Calculating j_g^* and j_f^*

It is useful to be able to directly calculate the j_g^* and j_f^* values from the measured steam flow (in lb/min) and the measured water flow (in gallons per minute).

From the general definition,

$$j_x^* = \frac{j_x \rho_x^{1/2}}{[g D_H \Delta\rho]^{1/2}} \qquad (1)E$$

$$= \frac{[W_x \text{ lb/sec.}]}{A \rho_x^{1/2} [g D_H \Delta\rho]^{1/2}} \qquad (2)E$$

D_H is 0.061 ft.

The factor,

$$[g D \Delta\rho]^{1/2} = [32 \times 0.061 \times 62.4]^{1/2} = 11 \text{ lb}^{\frac{1}{2}}\text{ft}^{-\frac{1}{2}}\text{sec}^{-1}$$

and,

$$A = \frac{(0.375)(17.5)}{144} = 0.045 \text{ ft}^2$$

Gas Flux.

$$j_g^* = \frac{(W_s \text{ lb/sec})}{(11)(.04)^{1/2}(.045)} \qquad (3)E$$

$$= \frac{(W_s \text{ lb/sec})}{.102} = \frac{(W_s \text{ lb/min})}{6.15}$$

Liquid Flux.

$$j_f^* = \frac{(W_s \text{ lb/sec})}{4.03} = \frac{(W_s \text{ lb/min})}{240} \qquad (4)E$$

The conversion to gpm is 1 lb/min = .120 gpm so that,

$$j_f^* = \frac{(W_s \text{ gpm})}{29} \qquad (5)$$

And these conversions (3) and (5) can be used in plotting the experimental results.

APPENDIX F. Comparison of Experimental Findings with Combustion Engineering and Aerojet Data

Accepting the hypothesis that the steam/water interaction end of bypass process occurs in three stages, this section looks at how the experimental result compares with the Combustion Engineering Annulus Penetration Data and the Aerojet semiscale preliminary tests (the ones which used steam, but no hot walls). The test results are found to corroborate this experiment.

From the experiment, the end of bypass occurs in three different Regions:

Region 1. At low liquid flows - results follow the Wallis correlation plus an amount based on the small bit of condensation of the steam by the small water flow (in the lower plenum).

Region 2. Data follow along the line of Thermodynamic Ratio equals unity. (See Appendix D for the calculations of this line in the CE and Aerojet tests.)

Region 3. The data level off at some critical gas flow. The gas flow where this occurs depends upon the inlet water temperature. (See Experimental Results.)

Combustion Engineering Data

The Combustion Engineering experiment was conducted in a cylindrical annulus which was 1/5 reactor scale. The experiment had a single 6 inch diameter inlet pipe and a single (enlarged) outlet hole 180° removed from the inlet.

Steam conditions were 250°F and 30 psi (saturated), and various inlet water temperatures were tried. In this experiment, the steam flow would first be established at the value to be tested, and then the water flow would be turned on, also to the value to be tested. The amount

FIGURE F1. CE ANNULUS PENETRATION TESTS (Reference 17).

CE Test Point	Annulus Steam Flow, lb/sec	Cold Leg Water Flow, lb/sec	Cold Leg Water Temperature, F	Thermodynamic Ratio	Cold Leg Water Mom. Flux, lb_m/hr^2-ft	Ann. Steam Mom. Flux, lb_m/hr^2-ft	Percent Water Collected
1 62	20.6	193	155	0.9	2.11×10^{11}	2.3×10^{10}	6.0
2 60	10.1	208	155	0.55	2.11×10^{11}	0.57×10^{10}	8.3
3 59	20.1	100	155	1.64	5.27×10^{10}	2.3×10^{10}	5
4 57	10.2	103	155	1.1	5.27×10^{10}	0.57×10^{10}	55
5 41	20	102	60	1.05	5.16×10^{10}	2.3×10^{10}	11.5
6 53	20.2	102	125	1.35	5.23×10^{10}	2.3×10^{10}	15.5
7 56	20.4	209	125	0.75	2.09×10^{11}	2.3×10^{10}	8
8 39	10	118	60	0.57	5.16×10^{10}	0.57×10^{10}	80
9 47	20.4	202	60	0.6	2.07×10^{11}	2.3×10^{10}	5
10 45	10.1	215	60	0.32	2.07×10^{11}	0.57×10^{10}	78
11 33	10.8	51.6	60	1.23	1.29×10^{10}	0.57×10^{10}	50.5
12 R1	5.7	161	60	0.24	1.16×10^{11}	0.14×10^{10}	84
NS2	0.0	206	60	--			90

p = 30 psia

$T_{steam} = T_{sat} = 250.34$ F

Annulus Width	2.5 in.
Annulus Flow Area	1.77 ft^2
Cold Leg Pipe Diameter	6.065 in.
Cold Leg Flow Area	0.2006 ft^2

$$R_T = \frac{W_s(h_s - h_f)}{W_w(h_f - h_w)} = \frac{\text{Energy given up in steam condensation}}{\text{Energy required to de-subcool the water}}$$

of water reaching the lower plenum would be measured and divided by the time interval of collection to determine the flow rate of penetration. Twelve data points were taken in all in the experiments, as shown in Figure F-1. Each run was made at least twice, and number 60 was run four times (because it did not make sense according to the CE interpretation). Unfortunately, they did not run enough tests to draw conclusions like those in this thesis work.

Suppose we look at the CE data in the light of this experiment. We can roughly sketch curves (Figure F-2) corresponding to the locus of end of bypass for different water temperatures (60^{o}, 120^{o}, and 155^{o}F) by extrapolating the results of the thesis experimental results. We sketch: 1) The Wallis correlation ($C = 1.0$); 2) The $R_t = 1$ lines for each water temperature (Appendix D); 3) The extrapolated levelling off from Region 3 of the experimental results.

Now suppose we take the inlet flow rates of steam and water, using the hydraulic diameter of the annulus in the Wallis method of dimensionless variables ($D_H = 5.0$ inches), plot the annulus inlet j_g^* and j_f^* for each CE data point, and put this together with the sketches of the curves in Figure F-2. Data in this experiment were also plotted using inlet values of the water flow. We would expect that test points lying above the locus corresponding to a given water temperature would bypass the water, while points lying below the appropriate locus would not. In terms of the chart, we see that 33, 41, 47, 53, 56, 57, 59, 60, and 62 would be expected to bypass while 39, 45, and R1 would not. Furthermore, predictions can be made as far as the amount of water penetrating the annulus to the plenum. The points 41, 47, 53, 56, 59, and 62 should allow virtually none of the water to penetrate, while 33, 57, and 60 would allow a small amount, corresponding to Wallis' correlation (plus an amount for condensation) to penetrate, and finally 39, 45, and R1 should allow almost all of the water to penetrate.

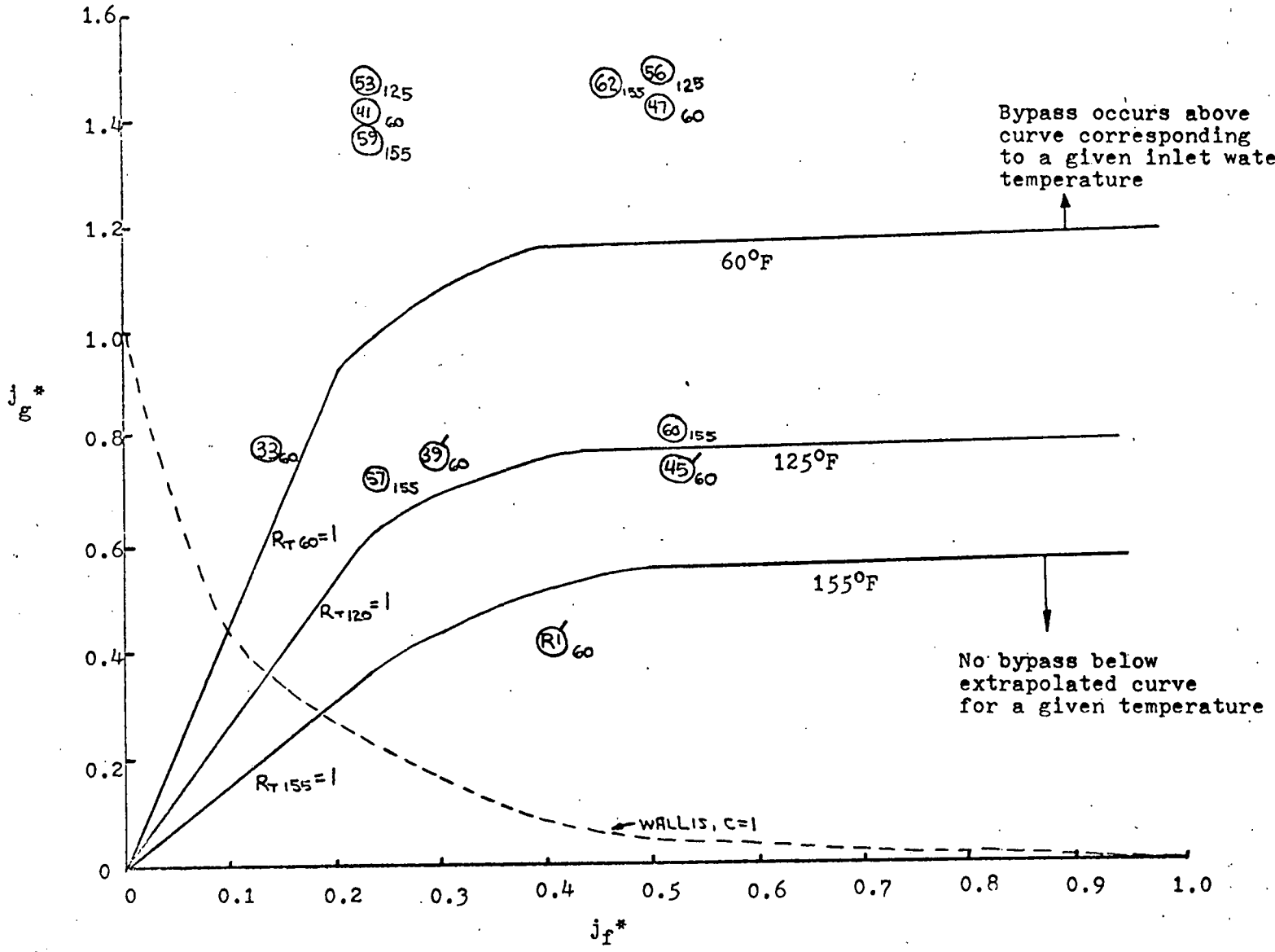

Figure F2. Plot of CE data on experimental bypass graph. Circled numbers are data point numbers. Subscript numbers indicate inlet water temperature. Flags on data point indicate the ones which should not bypass water. (Data point numbers from Figure F1.)

Figure F-2 is the "before" picture. Let us look at the "after" picture and see how the results compare with the predictions. Figure F-3 is based on the momentum flux of the fluid (as measured) which penetrated the annulus. It can be seen that very little water penetrated for the points that bypassed water, verifying that they did expel most of the water as predicted. For points with $j_g^* \simeq 1.4$, this amount is due to chance; for the remaining three which bypassed a lot of liquid, we see that they do lie near the prediction of the Wallis correlation, and a little above it, as we expected. Data points 39, 45 and R1 allowed most of the water to penetrate. (The slight decrease from 100% in the amount penetrating can be accounted for. Geometry accounts for 10% because a test, NS2, indicated only 90% penetration even with no steam flow at all.)

On the whole the results of the CE tests can be explained amazingly well by the results of this experiment, including even the anomalous point 60. This is also a very useful indication in that similar results were obtained in differently scaled tests and with different geometries.

Aerojet Semiscale Data

The solid line in Figure F-4 is a compilation of the Aerojet semiscale preliminary test results as plotted using $j_g^{*1/2}$ and $j_f^{*1/2}$ (which was the method Aerojet used in plotting data).

The dotted line represents the $R_t = 1$ line for the inlet water temperature of 190°F and the steam conditions of the experiment (as calculated in Appendix D). The levelling off of the curve on the right is the extrapolation of Region 3 behavior observed in this experiment to 190°F water.

The dashed line is the Wallis correlation, which is a straight line when plotted on a square root graph.

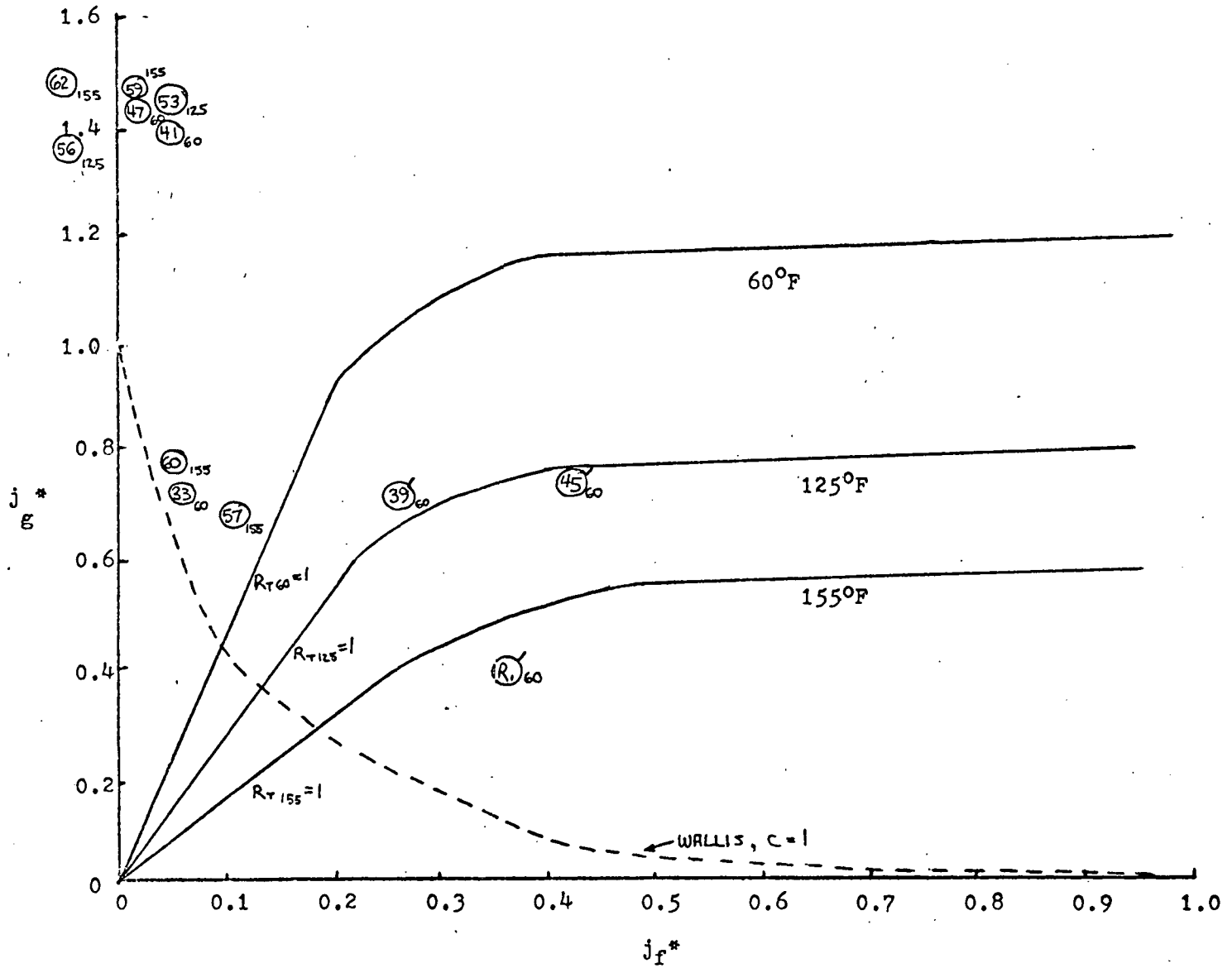

Figure F3. Plot of CE data based on water penetrating the annulus. Symbolism is the same as in Figure F2 (which is based on amount of water injected). The results corroborate the experimental findings.

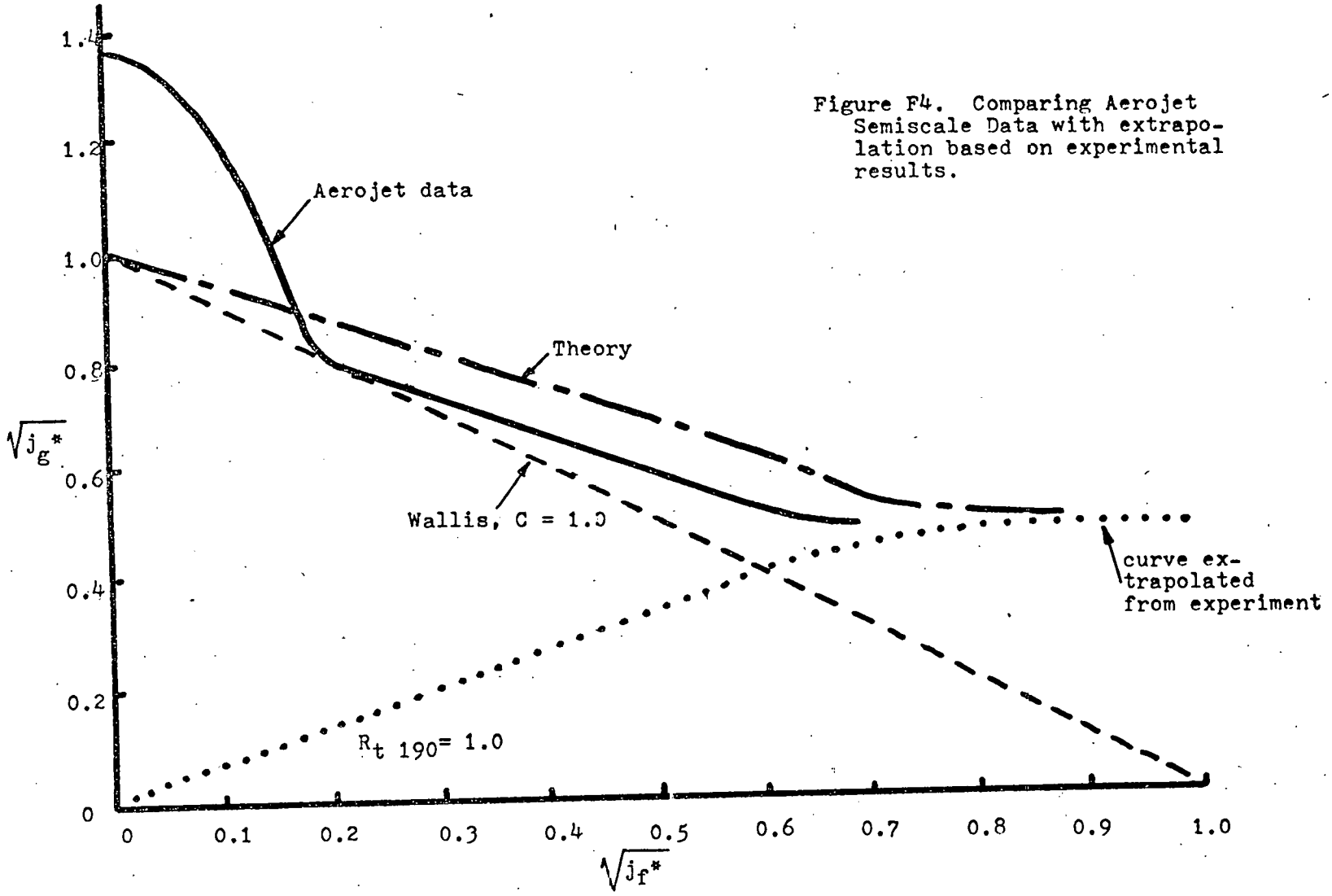

Figure F4. Comparing Aerojet Semiscale Data with extrapolation based on experimental results.

The other broken line indicates the theory, which is the Wallis correlation line plus the $R_t = 1$ line, out to the point where we would expect the data to level off (Region 3).

The behavior to the left on the data curve is about the same as was seen in the CE data, since a $j_f^{*1/2} \approx 0.2$ is a $j_f^* \simeq 0.04$, so that the amount of water represented there is negligible. (Using the square root plot tends to distort the data somewhat at low liquid flows.) Ignoring the "bump", the data approximate a line of

$$j_g^{*1/2} + 0.8\, j_f^{*1/2} = 0.9 \qquad (1)F$$

out to about $j_f^{*1/2} = 0.5$ where the data level off at a value of $j_g^{*1/2} = 0.5$. We see that the intersection with the $R_t = 1$ line is very far over on the right. (The slope of the line is small for 190°F water.) The actual data are bracketed by the theory and by the Wallis correlation above the line of $R_t = 1$. This leads us to believe that the Wallis correlation plus the $R_t = 1$ line is the appropriate theory for the Region 1 behavior of the experimental results. If the constant in the Wallis correlation is 0.9, the theory and the data are nearly identical.

The result here also indicates that the Wallis correlation may be the conservative limit for the end of bypass determination. If the inlet water is at saturation, the slope of the $R_t = 1$ line would be zero, and the theory (Wallis + $R_t = 1$)* reduces to the Wallis correlation alone.

* The theory, Wallis + $R_t = 1$, refers to the Wallis correlation plus some amount to account for condensation. At a given liquid flow, Wallis' correlation predicts a certain critical gas flow required to initiate bypass. But some liquid is allowed to enter the lower plenum also and can condense an amount of steam corresponding to the j_g^* for the given j_f^* on the $R_t = 1$ line. Therefore, more steam than predicted by the correlation is actually required to cause bypass because of condensation. The j_g^* values required for bypass (at a given liquid flow) would be that j_g^* predicted by the correlation <u>plus</u> that j_g^* defined by the line $R_t = 1$, the latter accounting for condensation.

APPENDIX G. Cost to Chill Accumulator Water

Each accumulator tank holds about 7000 gallons (900 cubic feet of liquid). Assuming a spherical tank shape, this corresponds to a diameter of 12 ft. and a surface area of around 230 square feet. The heat transfer expression is,

$$q = \frac{A \Delta T}{L_{1/k_1} + L_{2/k_2} + 1/\bar{h}} \qquad (1)$$

The term L_1/k_1 is the conductive heat transfer resistance for insulation. L_2/k_2 is the resistance of the steel of the tank, which will be small compared to other terms. The term $1/\bar{h}$ is the convective resistance on the outside of the tank, and its value is about $\left[2 \text{ Btu/hr-ft}^2\text{-}^\circ\text{F}\right]^{-1}$.

Without insulation, chilling water to 60°F,

$$q \approx \frac{(230)\,(120-60)}{(.5)}$$

$$\approx 28{,}000 \frac{\text{Btu}}{\text{hr.}} = 8.4 \text{ kw}$$

for a cost, with four tanks, of,

$$8.4 \text{ kw} \times 4 \times \frac{24 \text{ hr}}{\text{day}} \times \frac{5¢}{\text{kw-hr}} = \$42/\text{day}$$

If about an inch of glass wool insulation is added (k = 0.03 Btu/hr-ft-$^\circ$F),

$$q = \frac{13{,}800}{3 + .5} = 4{,}000 \frac{\text{Btu}}{\text{hr}} = 1.2 \text{ kw}$$

and the cost is reduced to about 1/7 of the cost without insulation ($6/day).

APPENDIX H. Uncertainty Analysis

Water Flow

The rotameters used in the experiment for water flow measurement could be read to an accuracy of 1%. Therefore, when one rotameter was used (Designs 3 and 4) the uncertainty was 1%, and when two rotameters were used (Designs 1 and 2) the uncertainty was 2%.

In the cases of the Designs 2 and 3, because one injection leg was very near the break opening, some water tended to escape at large liquid flows even without steam flow. The amount was measured, and the most loss observed was 1/2 gallon at 15 gallons per minute, which made the flow rates a little over 3% above the actual flow rate down into the annulus. This error was small enough that the flow rates were not corrected to account for this loss in graphing the experimental results.

Steam Flow

Main steam line pressure, while constant over the course of a test run, tended to vary slightly as the day progressed, so that pressures ranged from about 17-20 psia in the line. Since 20 psia steam properties were used in designing the orifice plate used to measure the steam flows, the drop in line pressure could cause an error in measurement which made the steam flow 8% higher than it should have been.

Coupled with this are the apparatus heat losses (Appendix B) which make the uncertainty 4.5% to 0.7% over the range covered by the orifice plate.

The manometer used to measure the pressure difference could be read to an accuracy of 0.05 inches of water. At 2 lb/min steam flow, the accuracy is 2%. At higher steam flows, the error was negligible.

Therefore, steam flow measurements at very low flow rates would have produced a possible error of 15%, while the measurement of steam flow rates which were higher would have resulted in a possible error of less than 9%. Practically, the experiment did not involve tests in which the steam flows were less than about 4 lb/min - for which the un-

certainty is 12%. Uncertainty was therefore close to 10% for the steam flow in the experimental range.

Pressures

In plenum pressure measurements during bypass, the pressures tended to oscillate by several inches of water. Pressure measurements are average readings, plus or minus several inches of water (more than 2 inches but less than 10 inches, generally).

AIR/WATER INTERACTION IN A SIMULATED PRESSURIZED WATER REACTOR DOWNCOMER ANNULUS

by

Christopher J. Crowley

March 1974

SUPPLEMENT: REFERENCE 9

ABSTRACT

In this report air and water countercurrent flow in a simulated PWR annulus is investigated. The annulus is represented by a flat plate or "unwrapped" version of the gap between the pressure vessel and core barrel in a Pressurized Water Reactor. The water flow scales the flow of Emergency Core Coolant water in that reactor's safety system, and the air flow models steam flow that would be present in the event of a Loss of Coolant Accident. Several possible configurations of cold leg inlets, and simulated hot legs are considered. Also modelled is a "broken" cold leg.

The data is represented in terms of dimensionless parameters balancing the momentum flux of each component with buoyant forces in the annulus.

TABLE OF CONTENTS

LIST OF FIGURES

NOMENCLATURE

TERMS

annulus	the region between the core barrel and pressure vessel in a nuclear reactor
annulus length	the vertical dimension of the annulus, from top to core support depth
annulus width	the "unwrapped" dimension corresponding to circumference in a reactor
cfm	measure of air flow, cubic feet per minute
cold leg	the pipe which carries incoming reactor coolant
ECC	Emergency Core Coolant
gpm	measure of water flow, gallons per minute
gap spacing	the dimension which is the space between the core barrel and the pressure vessel
LOCA	Loss of Coolant Accident

SYMBOLS

A	area
C	A constant in the Wallis correlation reflecting the effect of inlet and outlet geometry on flooding
D, d	diameter
F_o	Froude number
g	acceleration of gravity
j	volume flux of a component
j*	dimensionless fluid flux representing a balance between momentum flux and buoyant forces, as in Equations (1) and (2)
Ku	Kutateladze number; a dimensionless number relating momentum flux to buoyant and surface tension forces
m	variable in Wallis correlation reflecting amount of turbulence in countercurrent flow
N_f	dimensionless viscosity (see Equation (4))
Q	volumetric flow rate
V	velocity

ρ fluid density

σ liquid surface tension

ν liquid kinematic viscosity

SUBSCRIPTS

f liquid component

g gas component

o inlet pipe

Remarks:

To alleviate some confusion concerning the use of the term "flooding"--

The point at which the surface waves first appear and water begins to blow out of the annulus is called the "flooding point". Since experimental results followed the Wallis correlation, and since each point on the Wallis correlation is a "flooding point", the partial bypass of water is synonymous with what has been called "flooding" in the text.

INTRODUCTION

Previous reports [1] have considered a reduction in the flow of Emergency Core Cooling System (ECCS) water to the lower plenum of a nuclear reactor and thence to the core, as a result of rapid heat transfer effects that convert a portion of the cooling water to steam. An additional phenomenon known as "flooding" may also serve to hamper the flow of ECC water to the lower plenum.

Flooding occurs when certain conditions obtain in two-phase, countercurrent flow in a vertical annulus. In general, flooding can occur when there is a downward flow of fluid and some upward flow of gas in the annulus. A situation such as this may exist in a water reactor during the postulated Loss of Coolant Accident (LOCA), where, during the blowdown of the pressure vessel and the injection of ECC water, steam becomes the upward flowing gas component and ECC water is the downward flowing liquid component in an annulus formed by the core barrel and the wall of the pressure vessel.

When a film of liquid flows downward in a countercurrent two-phase flow situation, as long as the liquid flow remains fairly smooth and stable the upward gas flow establishes only a very small shear stress on the surface of the film, and the liquid flow continues relatively unaffected by the gas flow. Experimental results indicate that for some liquid flow, a certain gas flow will cause large waves to develop on the surface of the vertically flowing (unstable [2]) film. There occurs simultaneously a large increase in the gas pressure drop, and a portion of the liquid reverses its direction, to be carried upward by the gas flow and discharged from the top of the annulus.

During a reactor loss of coolant accident, it is hypothesized that this same flooding phenomenon may take place: steam escaping from the core upward through the annulus could create flow instabilities in the ECCwater being injected, causing the water to be blown out of the annulus through the ruptured cold leg pipe.

The experiments discussed in this report were performed to adapt previous flooding correlations to the reactor geometry, using air and water as the two components of the countercurrent flow, in order to investigate the applicability of flooding conditions to the case of emergency core cooling.

The first series of experiments was conducted with an apparatus like that shown in Figure 1. One cold leg pipe at the centerline of an annulus "unwrapped" into a plane gap was modeled. The blowholes to either side of the annulus represent the "broken" cold leg.

A second test series used the same apparatus, but included two simulated hot legs - Plexiglas disks which filled the gap between the walls. Because these hot leg pipes penetrate the annulus, they are able to interfere with the flow of water in the annulus.

Finally, a series of experiments was conducted in which the scaling of the apparatus, particularly the length of the annulus, more accurately scaled (1/30) reactor geometry. Further, this series of tests included additional modifications which made it possible to model a 4-loop reactor. Three cold legs, 4 hot legs, and the "broken" leg were simulated. Two geometries, in which there are either alternating hot and cold legs or adjacent hot and cold legs, were considered. Also tested was the situation of a two-loop reactor (as in the second series) to discover if the decrease in length of the annulus had any effect.

THEORY AND CORRELATIONS

The gas flux upward and the liquid flux downward may be represented by j_g and j_f respectively. The correlation for flooding in annular flow in vertical tubes has been developed in terms of the momentum fluxes of each of these components. Dimensionlessly, these momentum fluxes can be represented by [2]

$$j_g^* = j_g \rho_g^{1/2} [g D(\rho_f - \rho_g)]^{-1/2} \quad \text{and} \tag{1}$$

$$j_f^* = j_f \rho_f^{1/2} [g D(\rho_f - \rho_g)]^{-1/2} \tag{2}$$

where j_g^* and j_f^* represent balances between the momentum fluxes and the hydrostatic forces - the dynamic processes at odds in the vertical countercurrent flow annulus. D is the diameter of the tube, which in this case will become D_h, the hydraulic diameter for the apparatus.

The correlation that fits previous data, sometimes called the Wallis correlation, is [2]

$$j_g^{*1/2} + m j_f^{*1/2} = C. \tag{3}$$

The value of m in turbulent flow is one. If surface tension effects are small, m is found to be one when the dimensionless number $N_f > 300$ [3], where

$$N_f = \frac{g^{1/2} D}{\nu_f} \left[\frac{\rho_f - \rho_g}{\rho_f}\right]^{1/2} \tag{4}$$

If the fluid is water, the kinematic viscosity, ν_f, is 1.4×10^{-5} ft^2/sec at $50^{\circ}F$ and the corresponding value of N_f is approximately 4500. It would be expected in this experiment then, that $m = 1$.

The constant C is determined by the configuration of the apparatus. For flooding occurring in annular flow in vertical pipes, C has been found

to lie between 0.725 and 1.0. The precise value of the constant depends on the manner in which liquid and gas enter and exit the annulus.

The form of the correlation for these experiments would thus be predicted to be,

$$j_g^{*1/2} + j_f^{*1/2} = C \quad (0.725 \leq C \leq 1). \tag{5}$$

This equation yields a straight line when plotted on coordinates of $j_g^{*1/2}$ versus $j_f^{*1/2}$. This line represents an upper limit beyond which operation is impossible (i.e., liquid flow is restricted by the gas flow), although any combination of flows is permissible below the line.

The liquid flow in the inlet pipe is scaled by the dimensionless Froude number,

$$F_o = V_o \left[g\, d\right]^{-1/2} \tag{6}$$

Using the continuity equation

$$Q = V_o A = V_o \left[\frac{\pi}{4} d^2\right]$$

the Froude number in (6) is expressed in terms of the volumetric flow rate,

$$F_o = Q \left[\frac{\pi}{4} g^{1/2} d^{5/2}\right]^{-1} \tag{7}$$

The Froude number has been shown [3] to be a useful parameter in describing flow patterns in an annulus.

The air flow range to be used in the experiment was scaled according to the dimensionless Kutateladze number,

$$Ku = j_g \rho_g^{1/2} \left[g\sigma(\rho_f - \rho_g)\right]^{-1/4}$$

which balances the momentum flux of the air with buoyant and surface tension forces. This balance is similar to that of Equation (1) but it also takes into account the effect of surface tension in pipes of small diameter. The Kutateladze number may also be appropriate for describing the flooding behavior of thin liquid films in large tubes.

APPARATUS

The physical apparatus simulates the geometry of a reactor vessel scaled 1/30 (except that the annulus length was not scaled in proportion in some experiments). The annulus formed by the core barrel and the wall of the pressure vessel was cut axially and "unwrapped" into a planar gap. Typical dimensions for a real reactor, by way of comparison are: core height--28 feet, core diameter--17 feet, inlet nozzle diameter --30 inches, lower plenum height--6 feet, and annulus gap--10 inches. The apparatus shown in Figure 1 has been scaled for the water flow (using the Froude number) and air flow (using the Kutateladze number). Its dimensions are labelled.

The lower plenum (the lower chamber in the Figure) is made of galvanized sheet metal. The upper plates forming the annulus are made of 3/8 inch Plexiglas. The gap between these two Plexiglas sheets is maintained by the use of spacers and held together by many C-clamps.

Water enters the pipe on the front face, falls through the annulus and is collected in the lower plenum. The plenum is drained between test runs. Air enters the top of the lower plenum (via the stovepipe) and exits through two blowholes located in the spacers at the same level as the water entrance-- simulating the broken cold leg pipe in a LOCA. The air is supplied by a Cadillac blower. Fluctuations in air supply are smoothed by taking the air from a fifty-five gallon chamber into which the air is first blown. The supply to the apparatus is controlled by a valve, and measured by means of a Pitot tube place approximately twenty pipe diameters downstream of the

nearest bend. This is connected to a Magnehelic pressure gauge.

Some physical limitations of the apparatus must be mentioned. At high air flow rates the Plexiglas bows out despite reinforcing. This means that the gap is no longer uniform and the data are therefore inaccurate. At high water flows the flow pattern of the incoming water is such that it is possible for water to flow directly out the blowholes even without any air flow. Because of the uneven thicknesses in sheets of Plexiglas and the spacers, some water does leak out the sides of the annulus. This was observed during the course of experiments, and buckets strategically placed to catch the flow leakage captured about five gallons of leakage in a thirty minute period. Since not all of this can be attributed to leakage alone (some water had exited from the blowholes and run down the side of the apparatus), the amount of this leakage may be estimated at .1 gpm, and is relatively insignificant throughout the trials.

Figure 2 shows the remainder of the experimental setup.

EXPERIMENTAL PROCEDURE

1) Set water flow at the desired flow rate by means of valve regulating flow through the rotameter. The drain valve on the apparatus remains open so that water drains rather than fills the lower plenum.

2) Divert air flow (by means of another valve) from blower drum through apparatus. Increase air flow by roughly equal steps through each trial.

3) Close drain valve and allow water to fill plenum.

4) Using stopwatches, measure the time it takes to fill plenum between 1/2- and 1-inch markings on the sight-glass. Double the 1/2" timing and average the two results.

5) Take a reading from Magnehelic gauge for air flow rate in terms of inches of water (on a 2.0" scale, graduated by .05") as measured by Pitot tube.

6) Check rotameter reading.

7) Open drain valve again to allow collected water to exit.

8) Repeat procedure for next air flow, increasing until the amount of water reaching the lower plenum is a small fraction of the initial flow rate.

The computer programs * in Appendix A convert the timing measurements and manometer readings to water and air flow rates in gallons per minute and cubic feet per minute, respectively, based upon the apparatus dimensions for the former, and the pitot tube equation for the latter. The programs then calculate j_g^*, j_f^*, $j_g^{*1/2}$, and $j_f^{*1/2}$ according to Equations 1, 2, and 5 of this report. A second set of programs equips the computer to plot the results from the data.

EXPERIMENTAL LIMITATIONS

Data could not be taken at values of j_g^* which are any higher than achieved because of bowing of the Plexiglas sheets used to form the annulus. Data also could not be taken at values of j_g^* which are any lower because of the limits of the Magnehelic gauge used to measure the air flow. All data thus cover the limits set by the equipment used, and cannot be extended without modifying the apparatus.

WATER FLOW PATTERNS

The water flow patterns in the annulus with no steam flow corresponded very well to the patterns as categorized by Wallis in his study of flow patterns in an annulus [3].

The ratio of gap spacing to water pipe diameter in this experiment is .375.

Dimensionlessly, the water flow in the inlet tubes is given in terms of the Froude number. For a 1-in. diameter tube, when the flow

---

* Developed by Douglas Knutson of Thayer School and rechecked to verify accuracy.

is 4 gpm, the Froude number is 1.0. Since volumetric flow is directly proportional to the Froude number, F_o can be estimated simply for other flow rates, e.g., a flow of 2 gpm corresponds to $F_o = .5$.

SERIES I

EXPERIMENTAL RESULTS

The apparatus was first used as pictured in Figure 1, with a single inlet pipe representing a cold leg. The gap spacing was set at 3/8 in. and the annulus width at 18.0 in. Qualitatively, the following observations were made during the course of this experiment. At low liquid flow rates (below approximately 8 gpm) the flow of liquid through the annulus remained unaffected by the air flow until a certain value of the air flow was reached. Visually, one could see that no water was being carried toward the "broken" cold leg until, as the air flow increased, large turbulent waves began at the bottom of the annulus. Within a matter of seconds they spread upward, causing the fluid in the entire length of the annulus to be turbulent and resulting in discharge of water through the blowholes. This was assumed to be the point at which flooding occurred. Under these conditions the flow pattern of the water at the top of the annulus did not maintain its original parabolic shape, but oscillated with a wave motion of low frequency at the boundary of the pattern as water spewed out of the simulated break. This is sketched in Figure 3.

Above about 8 gpm, water was able to exit through the blowholes with a very tiny air flow, or none at all. Therefore, larger water flow rates than this were not considered in this experiment.

Figure 4 plots the data taken in this experiment.

It is seen that for all the flow rates measured, the fluid flow remained relatively unaffected by the air flow until the point where

flooding occurred. A constant of C = .94 in Equation (5) correlates the data well, and lies in the predicted range.

SERIES II

MODIFICATIONS

The only difference between the Series II tests and the previous tests was the insertion of two Plexiglas disks in the annulus to simulate the penetration of hot leg pipes into the annulus. The same procedure used in previous runs was followed.

The two Plexiglas disks were 1.6 inches in diameter and .375 in. thick. The thickness corresponded to the spacing of the gap. The diameter of the hot leg disks corresponded to a 46 in. diameter pipe scaled by 1/30 - that of the cold leg was 1 inch, representing a 30-inch diameter inlet pipe (inner diameter) at the same scaling.

Horizontally, the disks were centered between the center of the inlet pipe and the blowhole in the spacers. The resultant edge-to-edge spacing of a disk and the inlet was about three inches, corresponding to 80 in. in a full-sized reactor.

EXPERIMENTAL RESULTS

The results of the Series II tests are shown graphically in Figure 5. As in Series I, the liquid flow is unaltered by increasing air flow until the air flow reaches a certain value. At this point, which corresponds to Equation (5) with a constant C = 0.94, flooding does not occur, but the water flow is reduced by the increasing air flow, causing the data points to "bend to the left". The actual onset of flooding is well correlated by Equation (5) with C = 1.0.

This behavior was initially thought to be attributable to leaks created when unsealing the test section to make the required modifica-

tions, but care was taken to reseal the apparatus. Furthermore, similar results were observed in the Series III tests. The reasons for the hot legs altering the flooding line are not clear, although the value of the constant C was expected to vary with the precise flow geometry.

The flow patterns in the Series II tests were essentially the same as in Series I, except that the simulated hot legs disrupted the oscillating flow in the upper annulus and made it irregular.

SERIES III

MODIFICATIONS

The basic apparatus remained essentially the same as in the previous trials, however, for the Series III experiments, the length of the annulus was shortened in order to scale this dimension more accurately. The size of the annulus from the top to the core support depth (the approximate bottom of the annulus) was reduced to twelve inches. Figure 6 compares all of the dimensions with corresponding full-scale dimensions.

In this series of experiments, modifications were also made to include three 1-inch diameter cold legs, and four 1.7-inch diameter hot legs, in order to permit modeling of the correct number and arrangement of pipes existing in a 4-loop reactor. Further, hot and cold legs were made interchangeable to permit different loop arrangements to be tested.

The broken cold leg was still modeled by a blowhole, of approximately half the area of a cold leg pipe, in each side of the gap at the level of the penetrations.

The water flow rates were maintained as constants in the various test runs. The values used in the experiments were 1, 2, 3, and 4 gpm through each of three cold legs (for totals of 3, 6, 9, and 12 gpm).

These water flow rates correspond to Froude numbers of .25, .5, .75, and 1.0 in each cold leg.

H-C-H

The first set of runs used as a model the reactor design in which hot and cold legs alternate, in an even spacing, around the pressure vessel. In shorthand, this configuration is designated as H-C-H. Figure 7 is a plot of data points obtained for the various water flow rates. The line is a plot of Equation (5) with C = 1.0. It will be seen that the data points approach the flooding limit asymptotically.

At low water flow rates, the data seem to approach a limit given by Equation (5) with C = 0.94. This is in agreement with the Series I data. At higher flow rates, the flooding limit is approximately given by Equation (5) with C = 1.0.

In the Series I tests, the water flow was not affected by the air flow until a flooding condition was nearly reached. Here, obviously, the water flow decreases long before flooding. This may be due to entrainment or diverting of the water by the air flow, unrelated to flooding. Placing the inlet water flow closer to the "broken" leg enables water to be diverted directly out the break at low air flows, before flooding occurs.

Figure 8a shows the water flow pattern at 3 gpm (total), which is a Regime 0 river flow *. As air is introduced, the outer rivers bend toward the outside (Figure 8b). With much higher air flows, the rivers break up, and the pattern is like that in Figure 9b. Otherwise, the flow patterns for the remainder of runs appeared as in Figure 9.

* The flow regimes and their boundaries are described in Reference 3.

C-C-H

The geometry was changed in the next set of test runs to model the case in which two cold legs are adjacent, followed by two adjacent hot legs, and so on. The notation for this configuration is C-C-H. Figure 10 illustrates the data.

The data is seen to exhibit the same asymptotic behavior as in the H-C-H geometry, approaching the limit given by Equation (5). At low flow rates, the C = 0.94 correlation does not seem to apply.

Comparing the results with Figure 7, the values of j_f^* are seen to be significantly less at corresponding j_g^* (for a given starting water flow rate). This seems to bear out the suggestion that spreading out the water flow, or placing a cold leg closer to the "broken" leg will reduce the water flow when little air flow is present. In this case, one cold leg is immediately adjacent to the break. Visually, it can be verified that water is diverted through the break long before flooding occurs.

The sketches in Figure 11 show how water can escape even at low flow rates. Another unusual feature in this instance is that the turbulence of flooding, when it occurs, is confined to the side of the annulus which contains the two intact cold legs.

Figure 12 illustrates flow patterns observed at higher water flow rates. Unlike the previous (H-C-H) case, this geometry displays some asymmetry in the annulus at all flow rates. The data reflect this asymmetry.

C-H

Finally, tests were run with a configuration the same as that of the Series II tests to isolate the effect of decreasing the length of the annulus. These results are shown in Figure 13.

Comparison with the Series II results (Figure 5) reveals some interesting features. The two results are quite similar. As before, the water flow is relatively unaffected by the air flow up to a certain point (at the lower flow rates - 3 and 6 gpm). This point is given by Equation (5) with the value of the constant somewhat less than 0.94, (Figure 16), but again, the data seem to alter slope at one line and then proceed to asymptotically approach the flooding limit where C = 1.0.

The increasing effect of even small air flows on water flow is seen in Figure 15 as the water flow rate increases from 3 to 9 gpm. This supports the contention that as the flow becomes more spread out (toward the break) there will be a greater effect on the water flow at low air flows.

On the whole, the data is similar enough for the two tests to indicate that the decrease in length of the annulus does not significantly affect the results.

CONCLUSIONS

Flooding appears to be an important factor in the behavior of the countercurrent fluid flow in a scaled downcomer annulus. Test results using the various reactor configurations indicate that the Wallis correlation (Equation (5)) predicting flooding, is a useful model in interpreting the results for air-water flow.

1) The manner in which water is introduced into the annulus is seen to affect the results to some extent. In Series I when a single inlet was used at the centerline of the annulus, the results showed a flooding behavior at a point corresponding to C = 0.94 in Equation (5), and the water flow was unaffected by the air flow below this flooding point.

2) In the Series II and III tests it was discovered that by altering the injection pattern, specifically spreading it out by having

three inlets instead of one (or by including simulated hot legs), water flow was affected by air flow before a flooding condition was reached. In these cases, the results tended to asymptotically approach the limit of

$$j_g^{*1/2} + j_f^{*1/2} = 1.0 \ .$$

The closer an injection pipe to the broken cold leg, the greater was this effect.

3) The decrease in the length of the annulus was not seen to significantly affect the results, so far as flooding is concerned.

4) The flow patterns in the C-C-H configuration tended to be very unsymmetrical in appearance. This asymmetry is supported by the data. In other tests, flow patterns agreed with the results of Wallis [3] and the description of the behavior during flooding.

5) Some abnormalities in the flow patterns observed may be attributed to the geometry used. The "unwrapping" of the annulus to a plane gap results in two "edge effects" that are not present in the actual cylindrical case. Also, the side blowholes do not precisely model the "guillotine" ruptured cold leg pipe.

In general, the data taken in this series of tests seems to asymptotically approach, at high air flow rates, an upper limit as described by the Wallis correlation with C = 1.0. At low air flow rates, the data seem to "bend to the left" - away from the condition where fluid flow is unaffected ($j_f^{*1/2}$ = constant) below the flooding point. The amount of water and method of injection seem to influence this "bending away", becoming more pronounced as the pattern of flow is spread out across the annulus.

RECOMMENDATIONS

1) Similar tests should be conducted with a cylindrical annular geometry.

2) If further flat plate tests are conducted, the effect of various different ways of modeling the cold leg break should be investigated.

3) Both types of tests might be conducted on scale models with steam rather than air as the countercurrent flow component. Steam, which is the actual gas of interest in the LOCA, would tend to condense rapidly in the presence of the ECC water, and might significantly affect the flooding limit.

UNCERTAINTY ANALYSIS

In most cases the Magnehelic gauge could be read to $\pm$ .02 inches of water. In terms of the flow rate, this is about $\pm$ 8 cfm, or in terms of j_g^*, $\pm$ .5.

For the water flow, error occurring in timing was about $\pm$ 1.5 sec (because of using two stopwatches). This influences larger flow rates (shorter timing periods) to a larger extent than lower flow rates. For instance, it takes 50 sec to fill the plenum 1 inch at 2 gpm and 14 sec at 7 gpm. That is, the timing error varies from $\pm$ 4% to 10%. In addition, error in using the sightglass to measure the water level is estimated at about .05 in, corresponding to $\pm$ 5% error. From the data printouts in Appendix A, it can be seen that the actual data lie well within these limits. The flows of water at low air flow rates are very nearly the original constant values.

Another uncertainty is the dimension of the annulus gap as it begins to bow at higher air flows. This changes j_g and j_f. Because of the irregularity of the bowing, the effect on uncertainty has not been estimated.

REFERENCES

1. Block, James A., The Effect of Hot Walls, memos to the AEC.

2. Wallis, Graham B., One-Dimensional Two-Phase Flow, McGraw-Hill Co., New York, 1969, p. 336.

3. Wallis, G. B., Block, J. A., and Crowley, C. J., AEC Report COO-2294-1, 1974.

FIGURE 1
APPARATUS

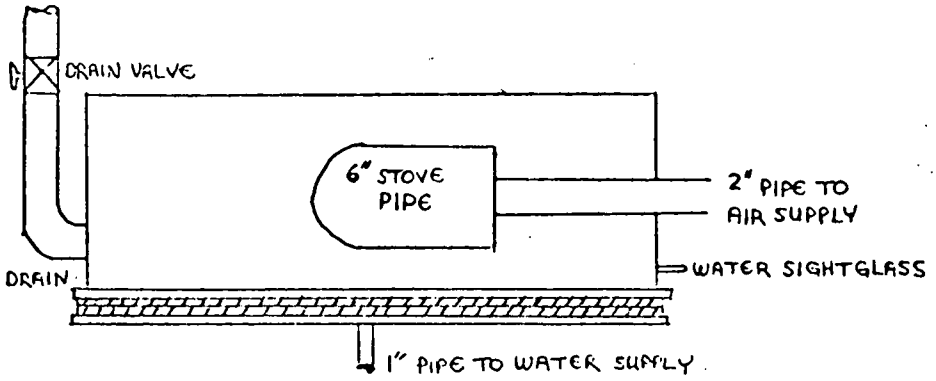

TOP VIEW

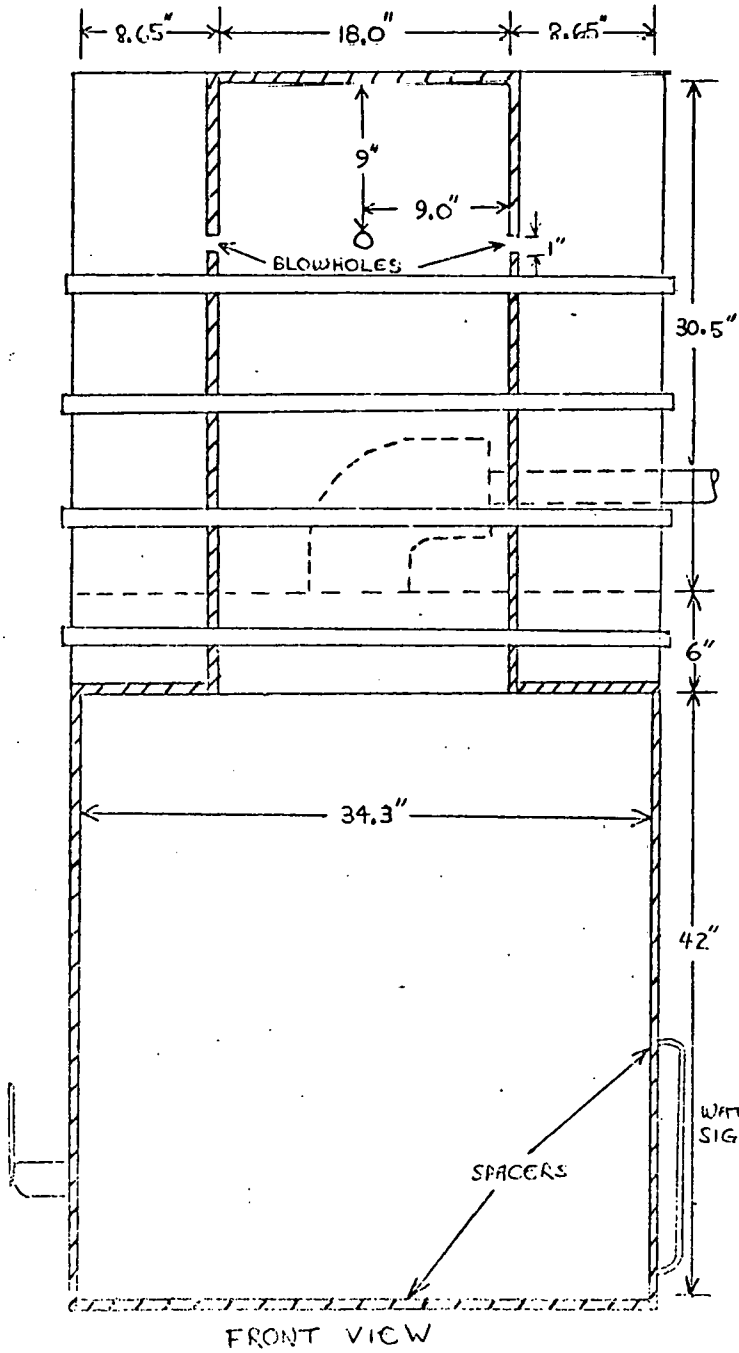

FRONT VIEW

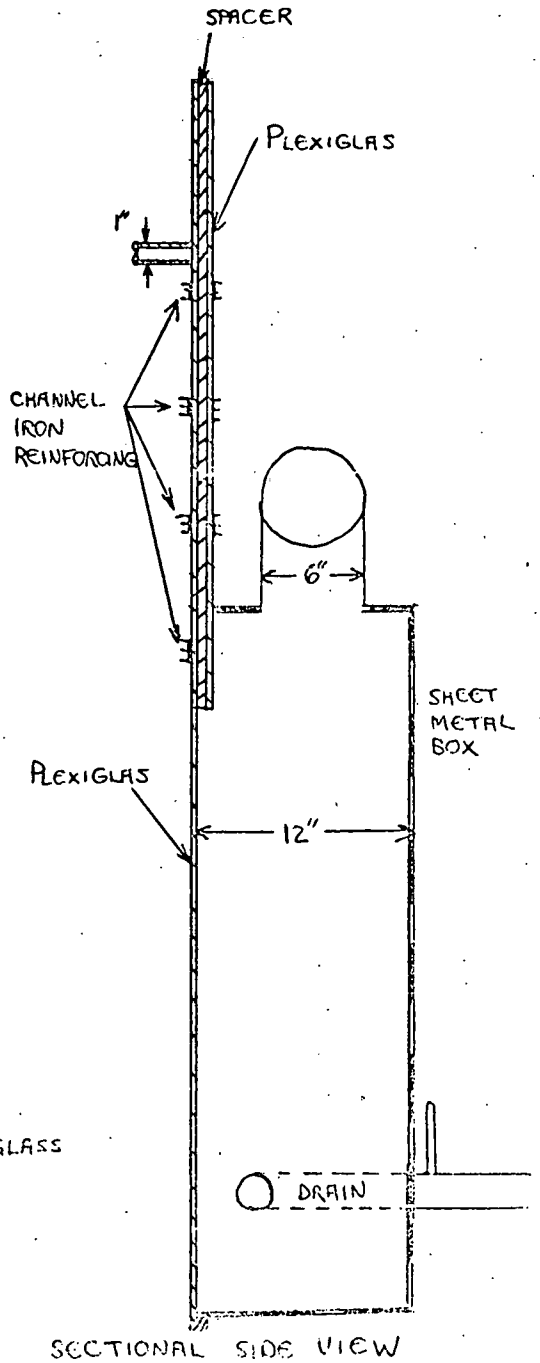

SECTIONAL SIDE VIEW

FIGURE 2
EXPERIMENTAL COMPONENTS
(NOT TO SCALE)

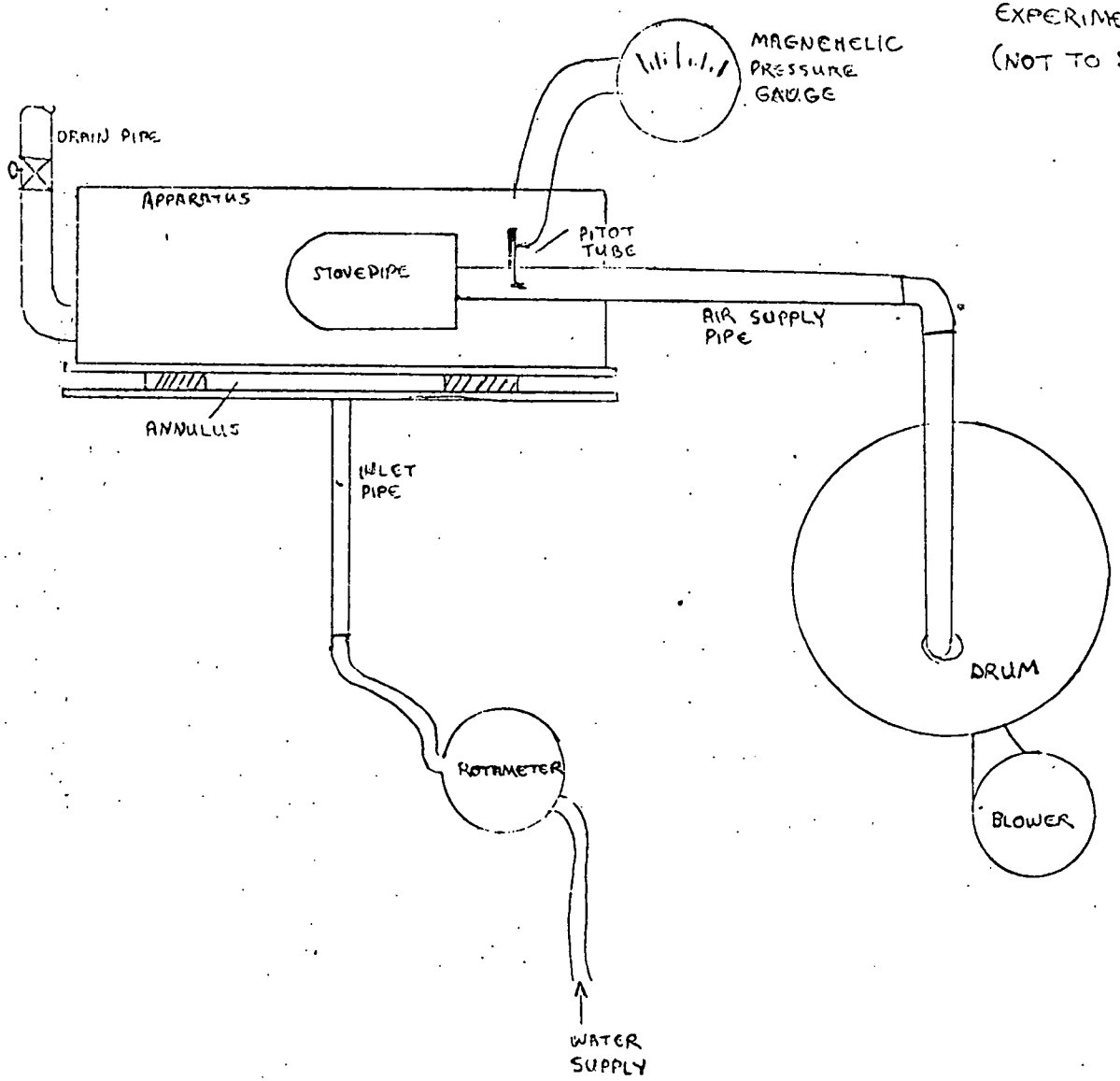

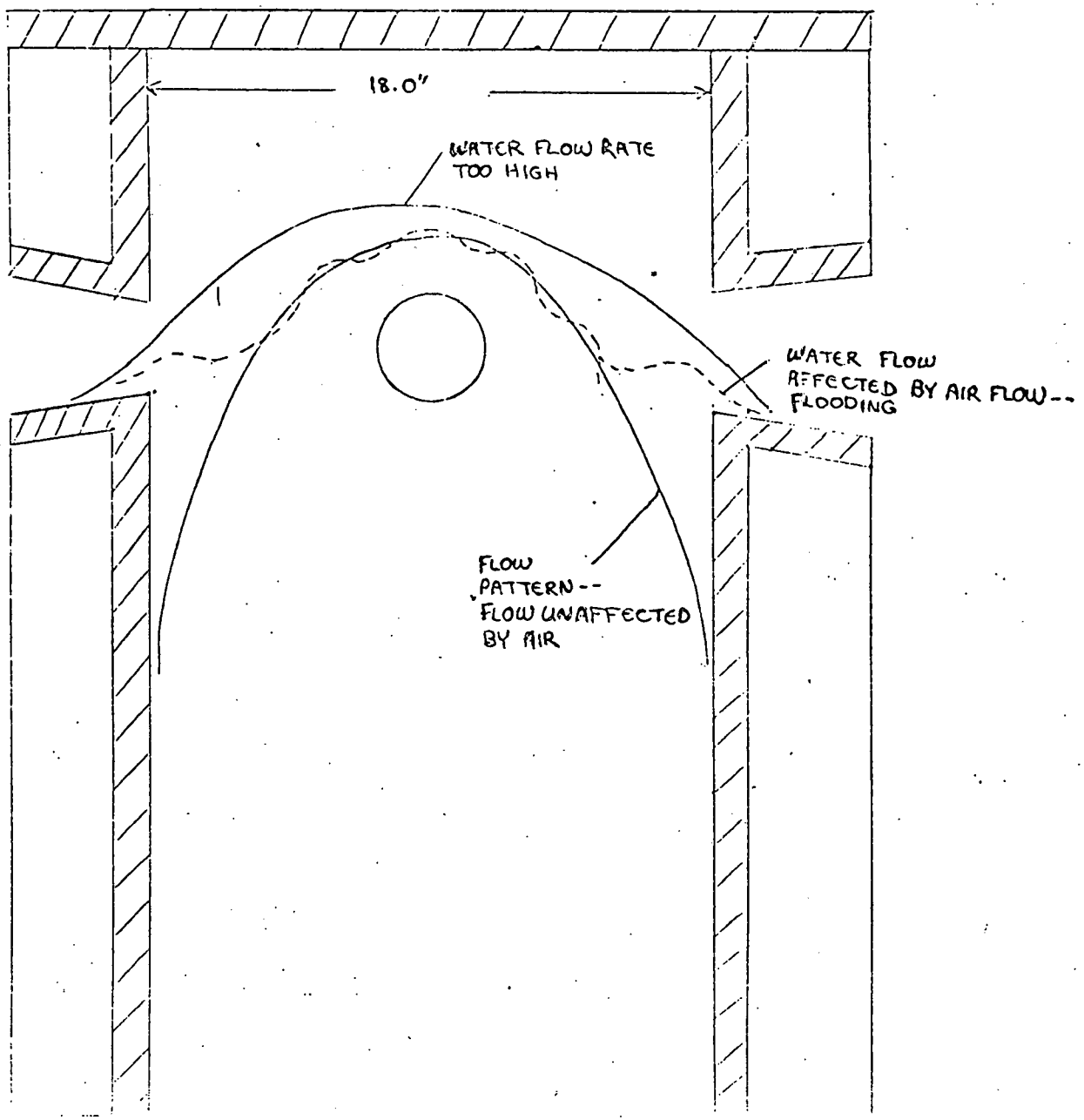

FIGURE 3.
FLOW PATTERNS IN ANNULUS
(NOT TO SCALE)

Single Cold Leg Data

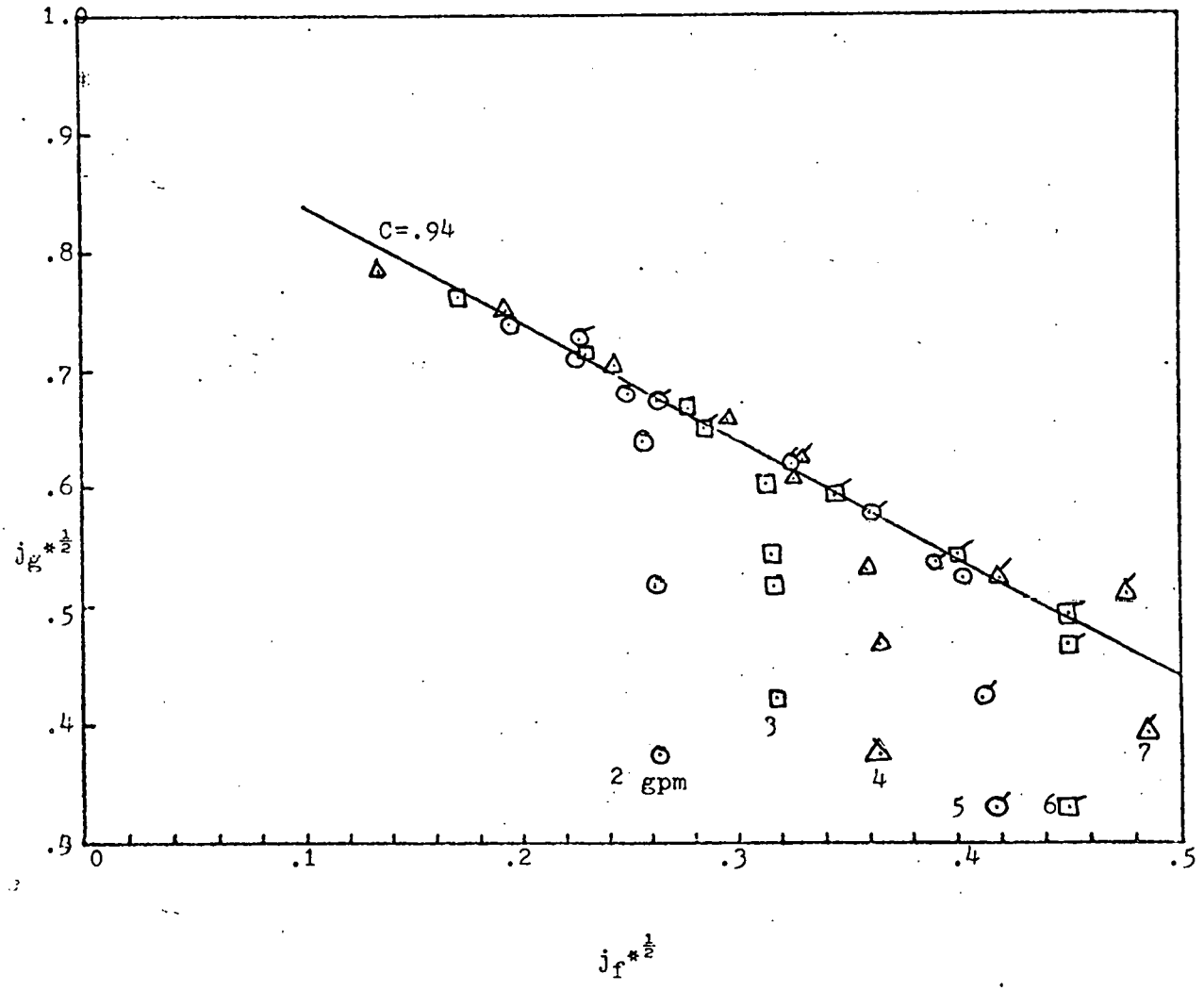

Figure 4

Simulated Hot Leg Data

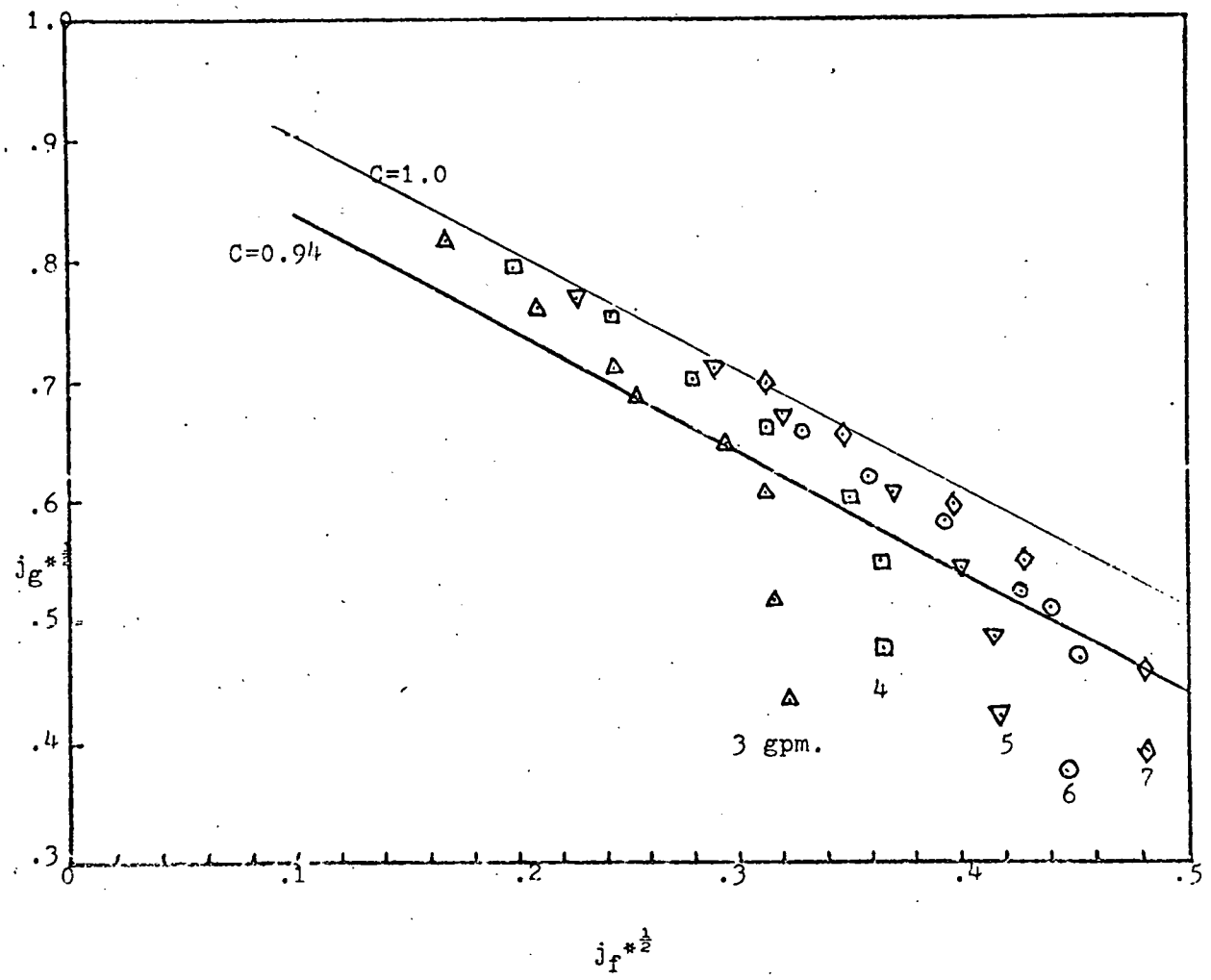

Figure 5

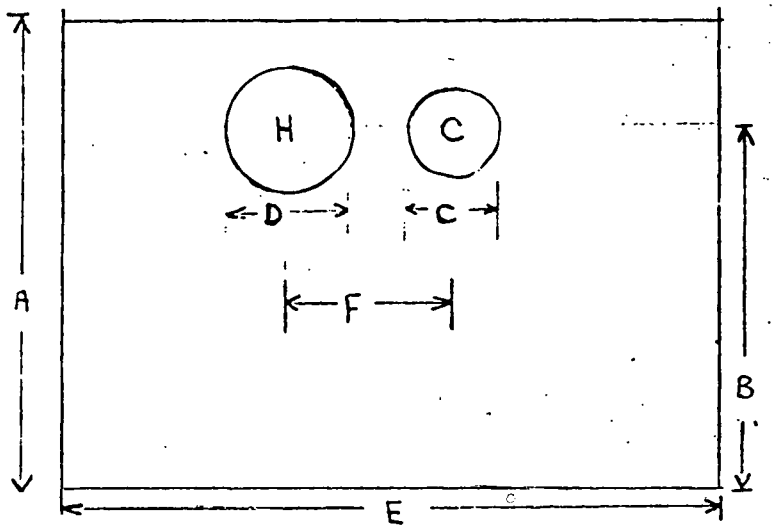

Dimension	Scaled (inches)	Actual (inches)
A	12	360
B	9	270
C	1	30
D	1.7	51
E	18	540
F	2.3	69
GAP	0.375	10

Figure 6.

H-C-H

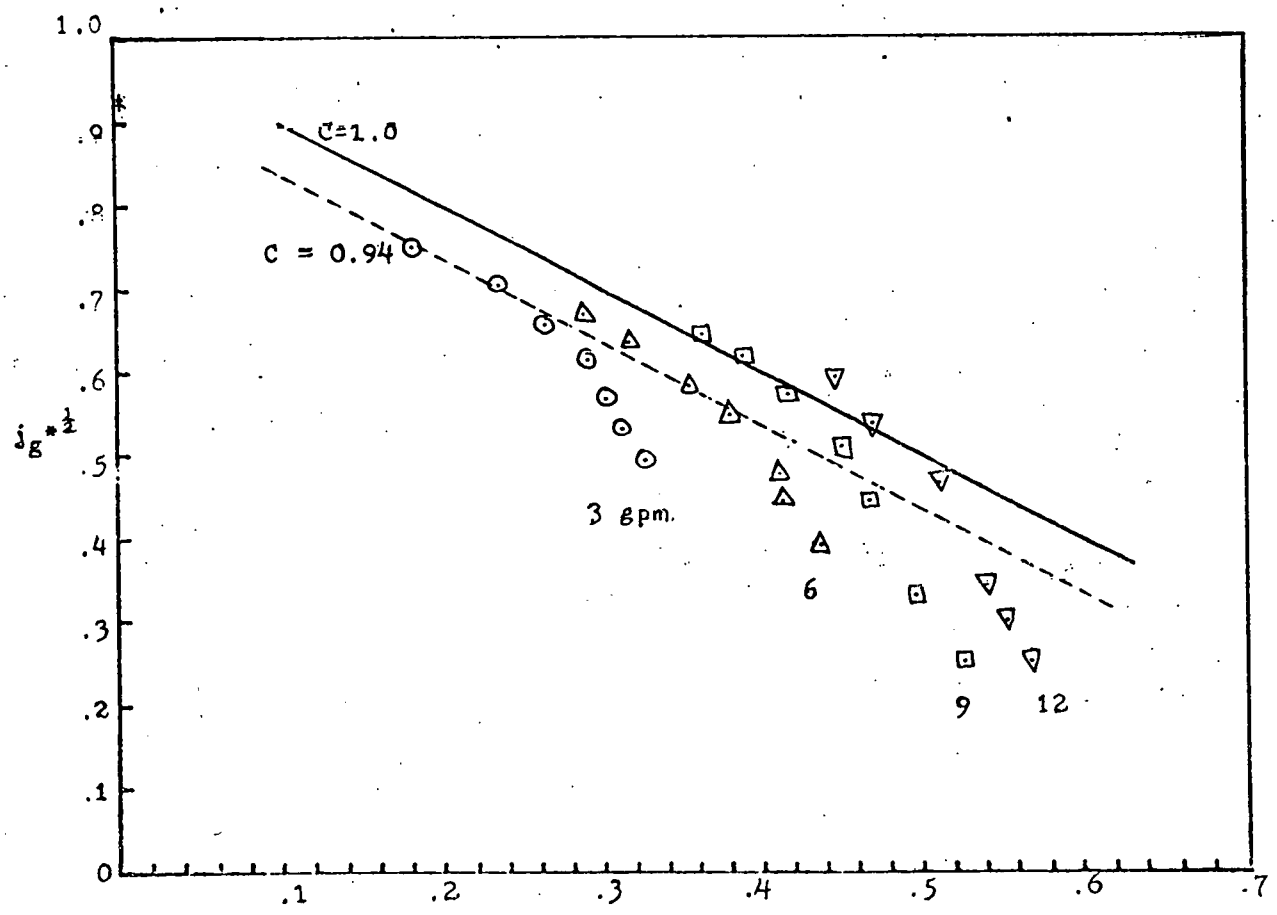

Figure 7

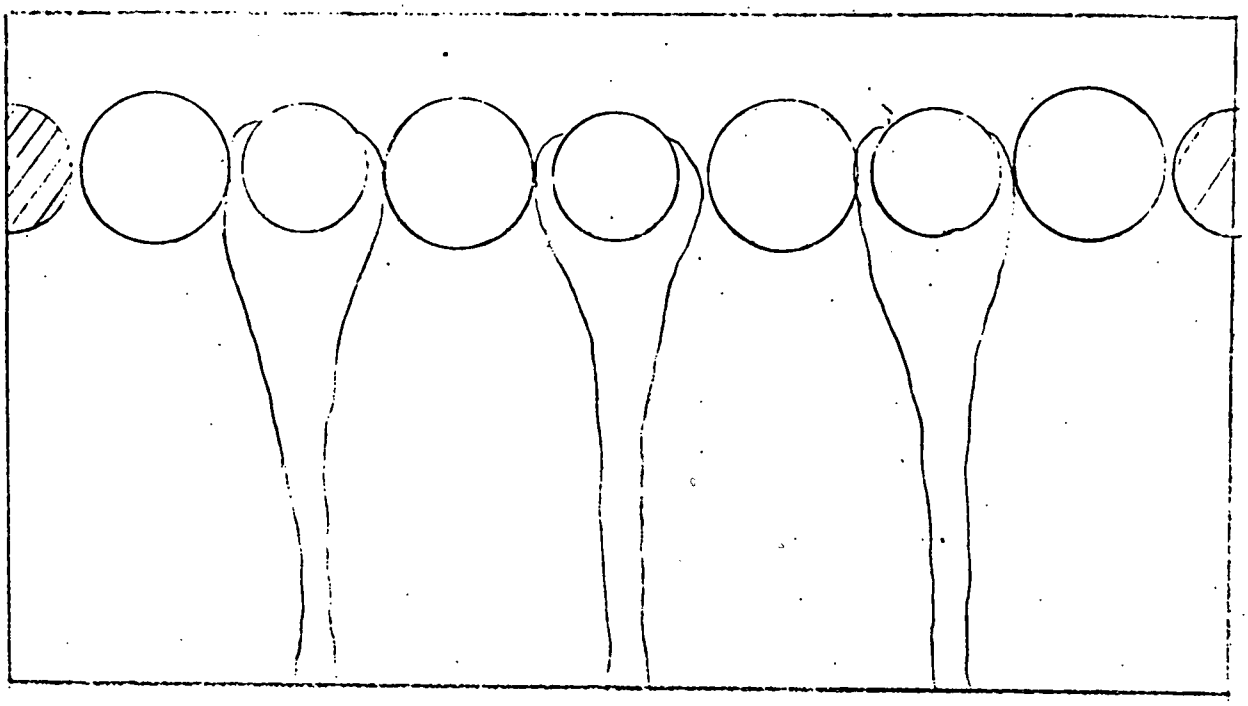

a.

H-C-H . Low Froude number (.25).
No air flow.

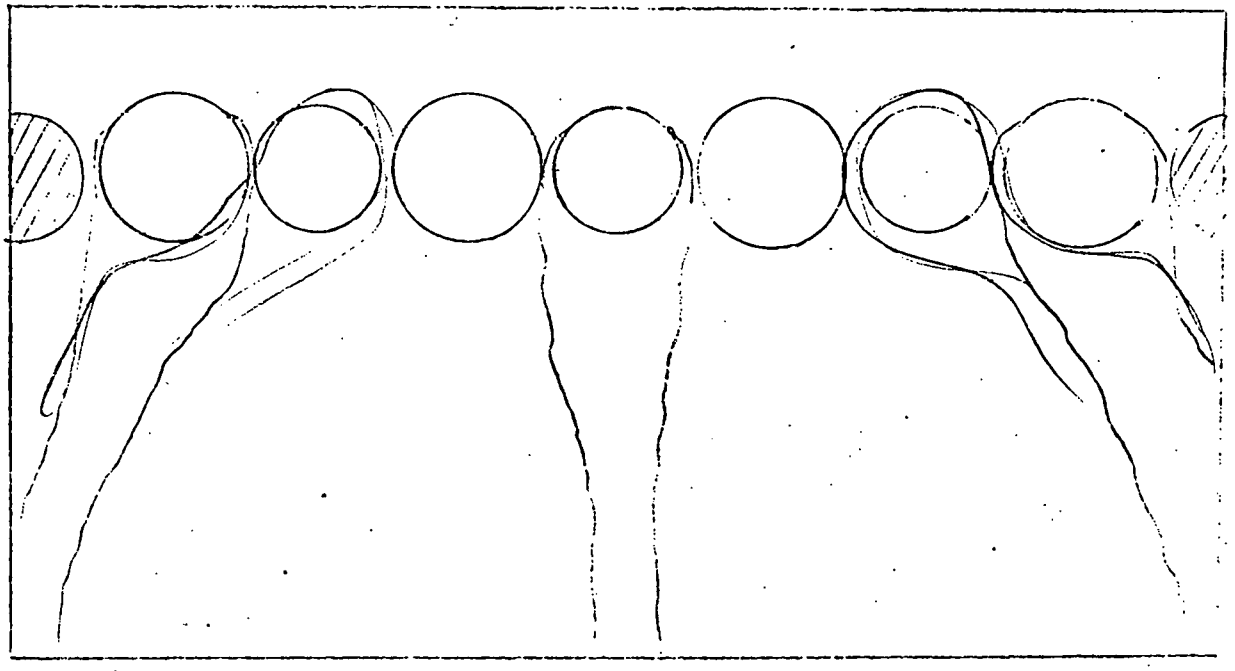

b.

H-C-H. Low Froude number (.25).
With air flow. (SMALL).

Figure 8.

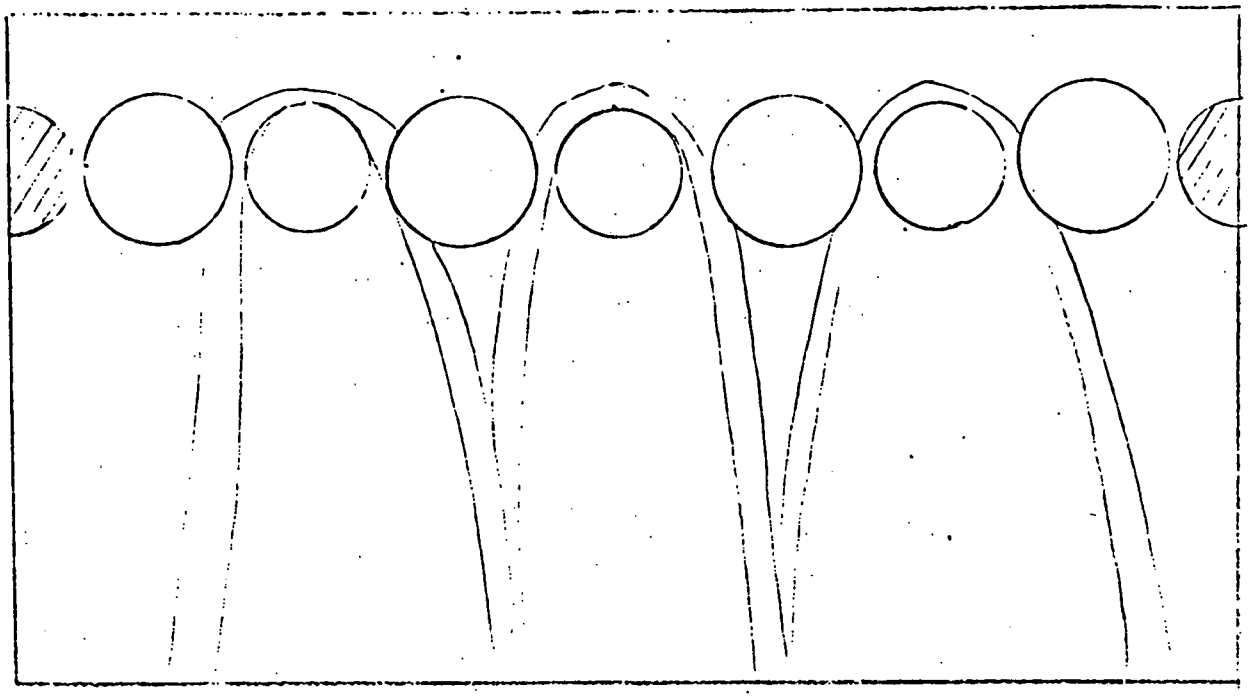

a.

H-C-H. Higher Froude numbers (.5 to 1.0).
No air flow.

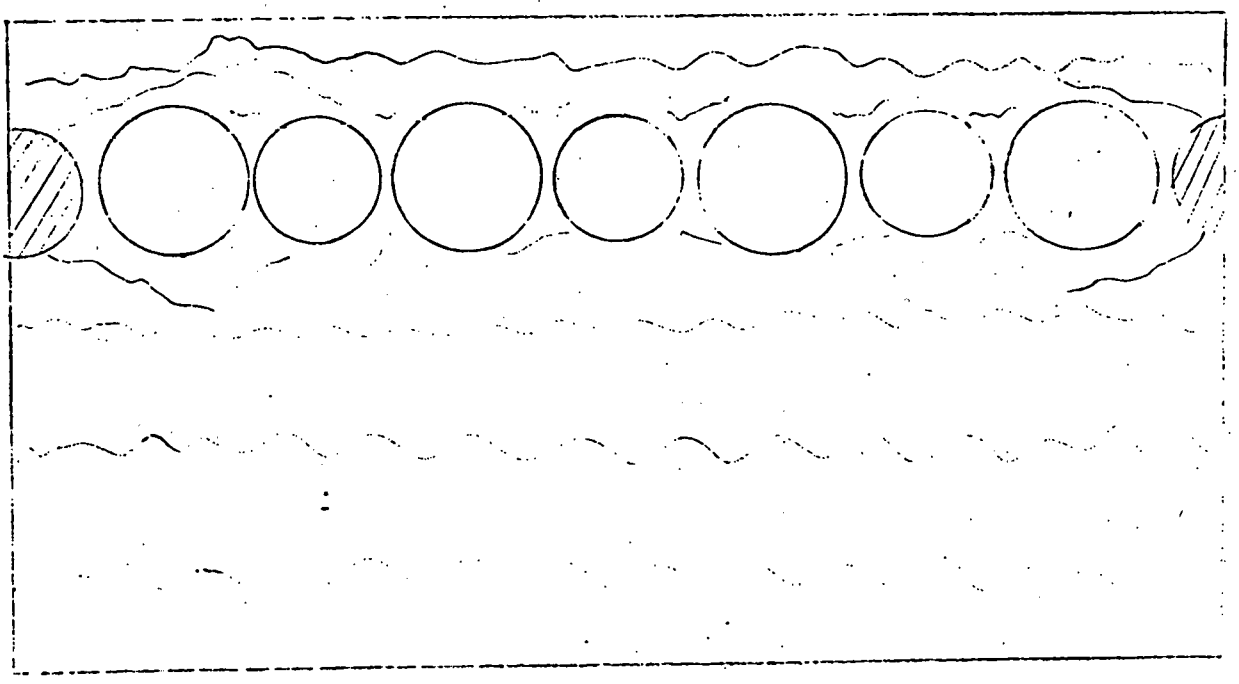

b.

H-C-H. Higher Froude numbers (.5 to 1.0)
Air Flow.
(Also Figure 4 at high air flows.)

Figure 9.

C-C-H

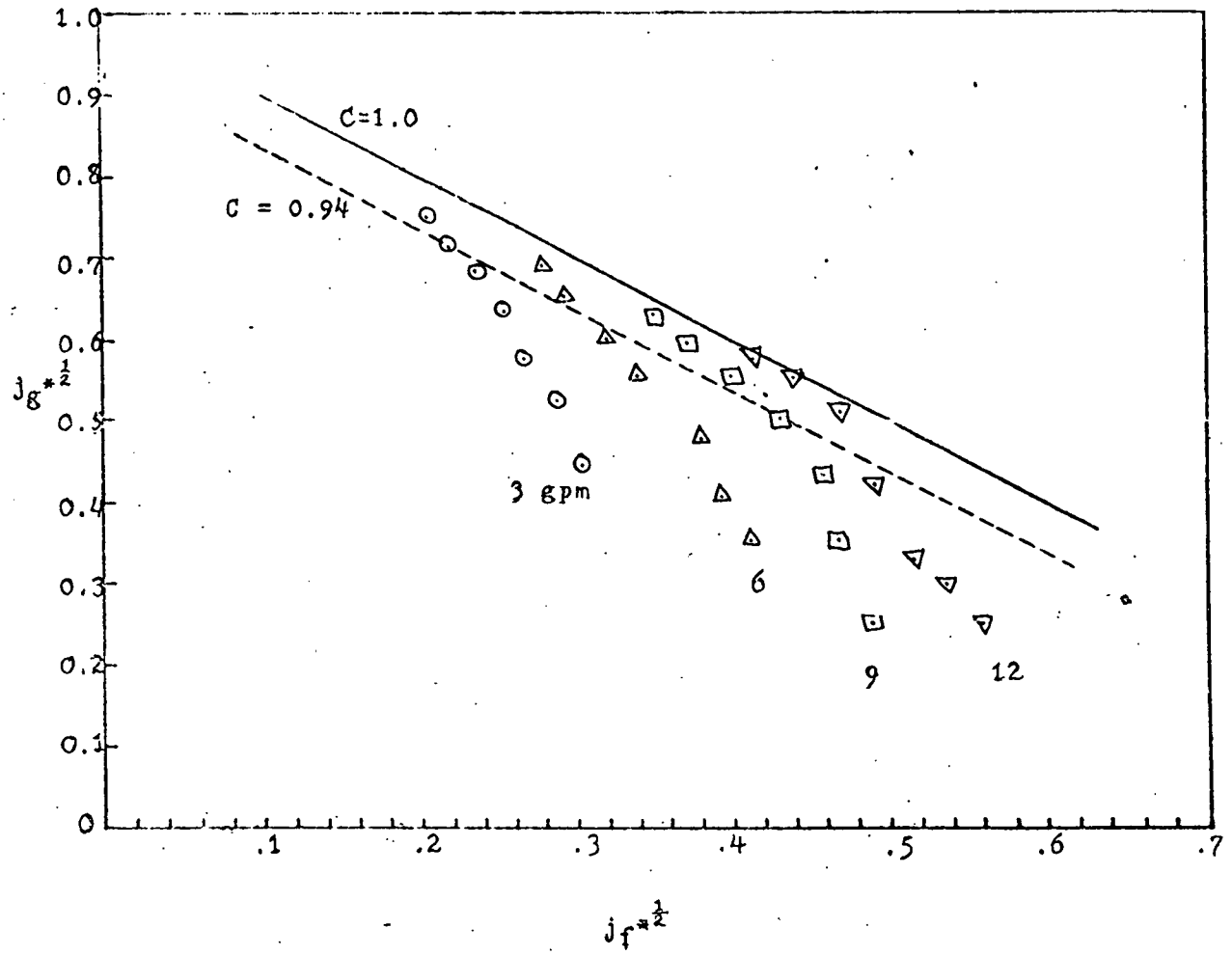

Figure 10.

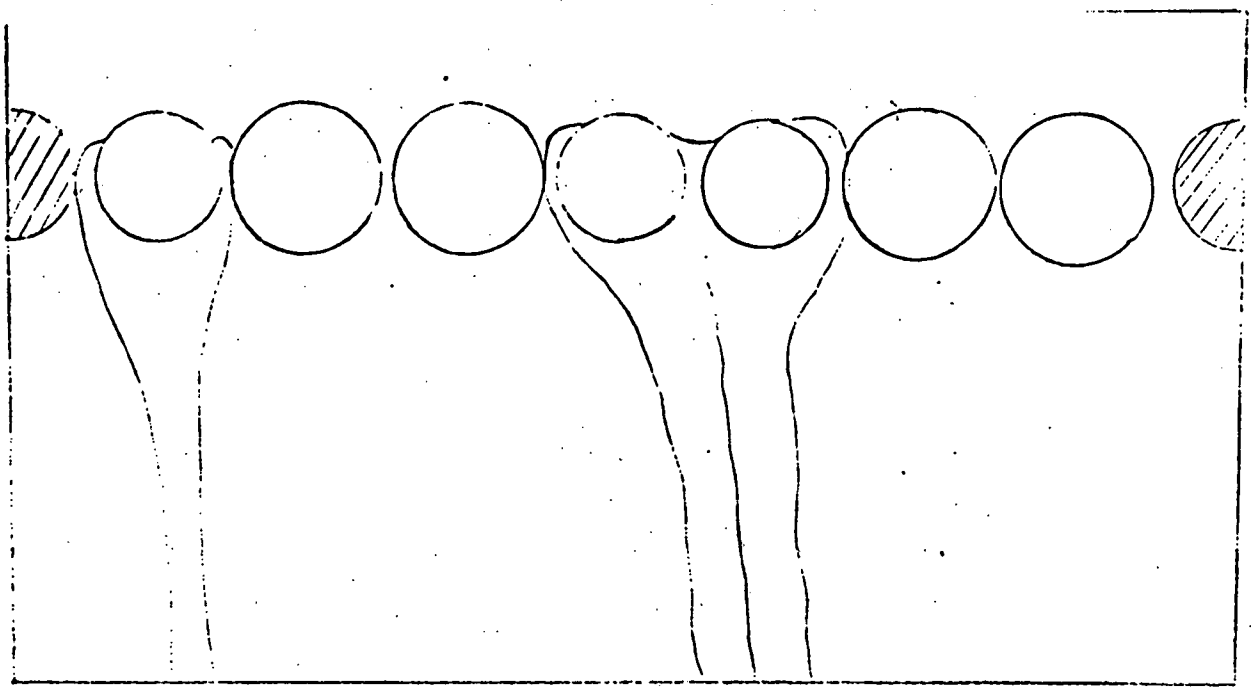

C-C-H. Low Froude number (.25).
No air flow.

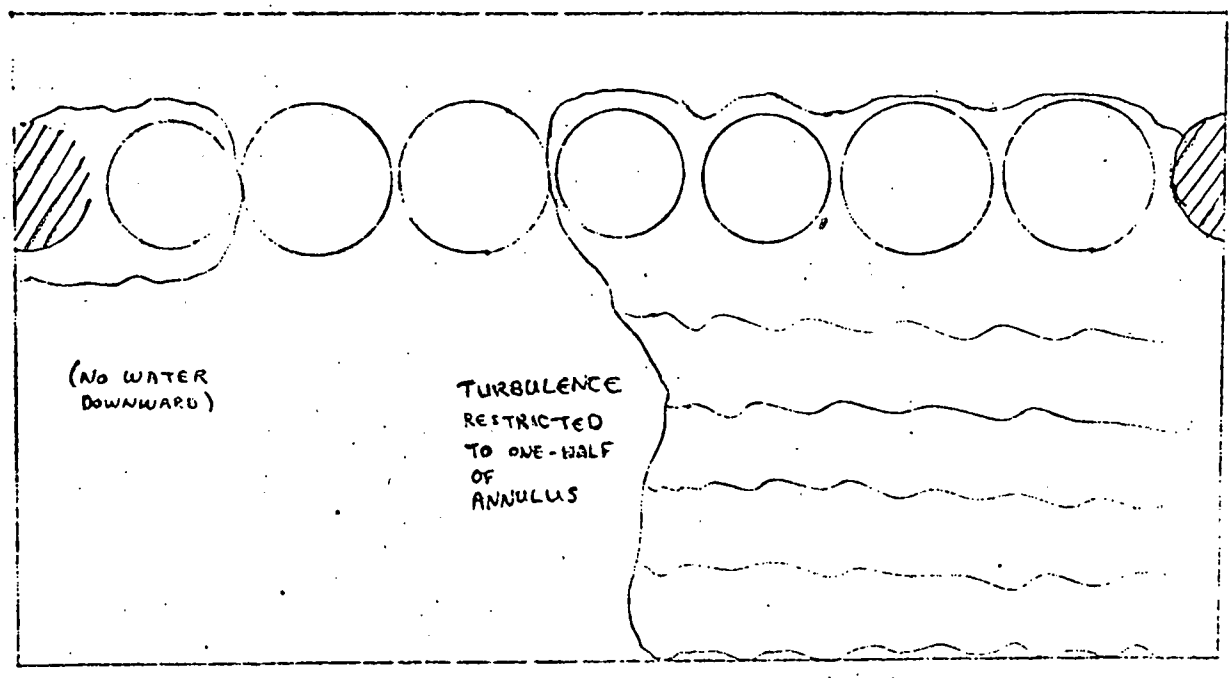

C-C-H. Low Froude number (.25).
With Air Flow (low and high).

Figure 11.

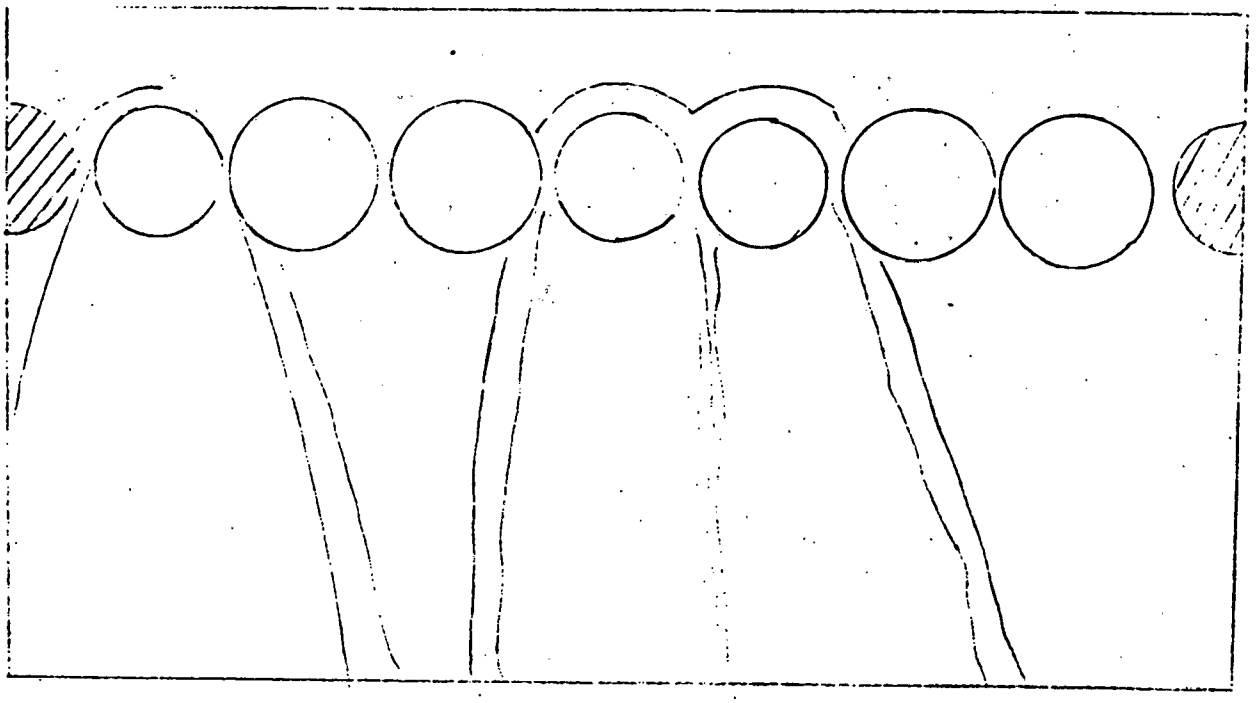

C-C-H. Higher Froude numbers (.5 to 1.0).
No air flow.

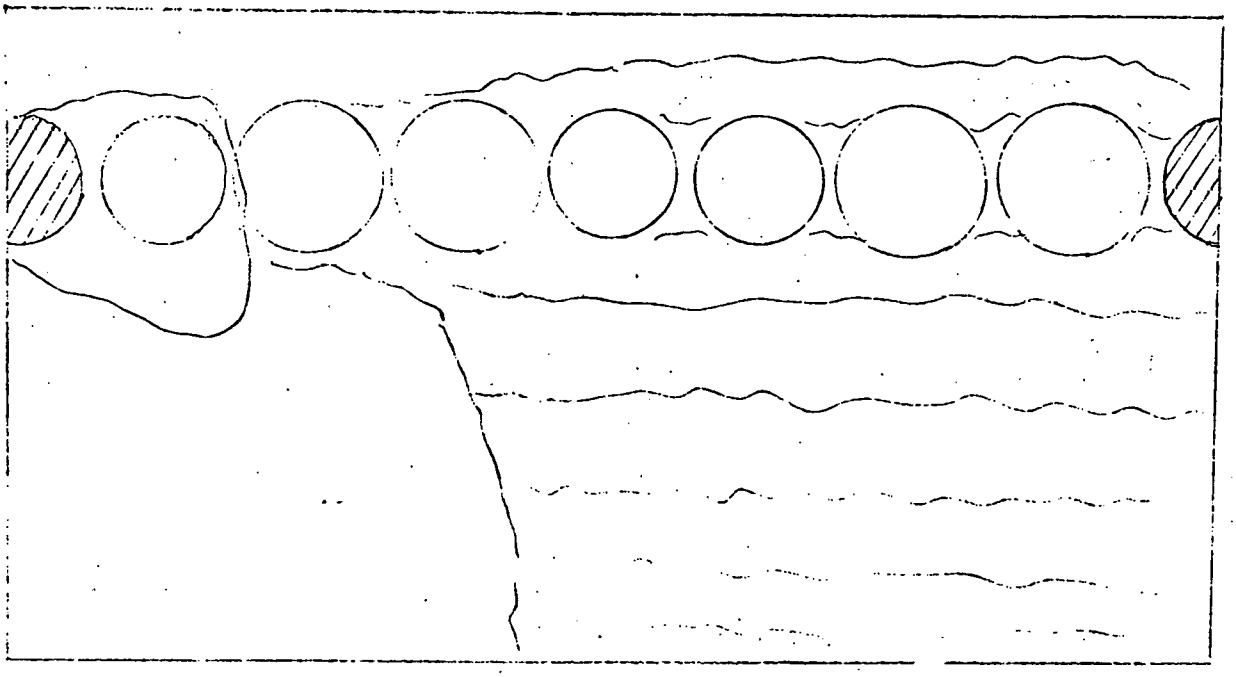

C-C-H. Higher Froude numbers (.5 to 1.0).
With air flow.

Figure 12.

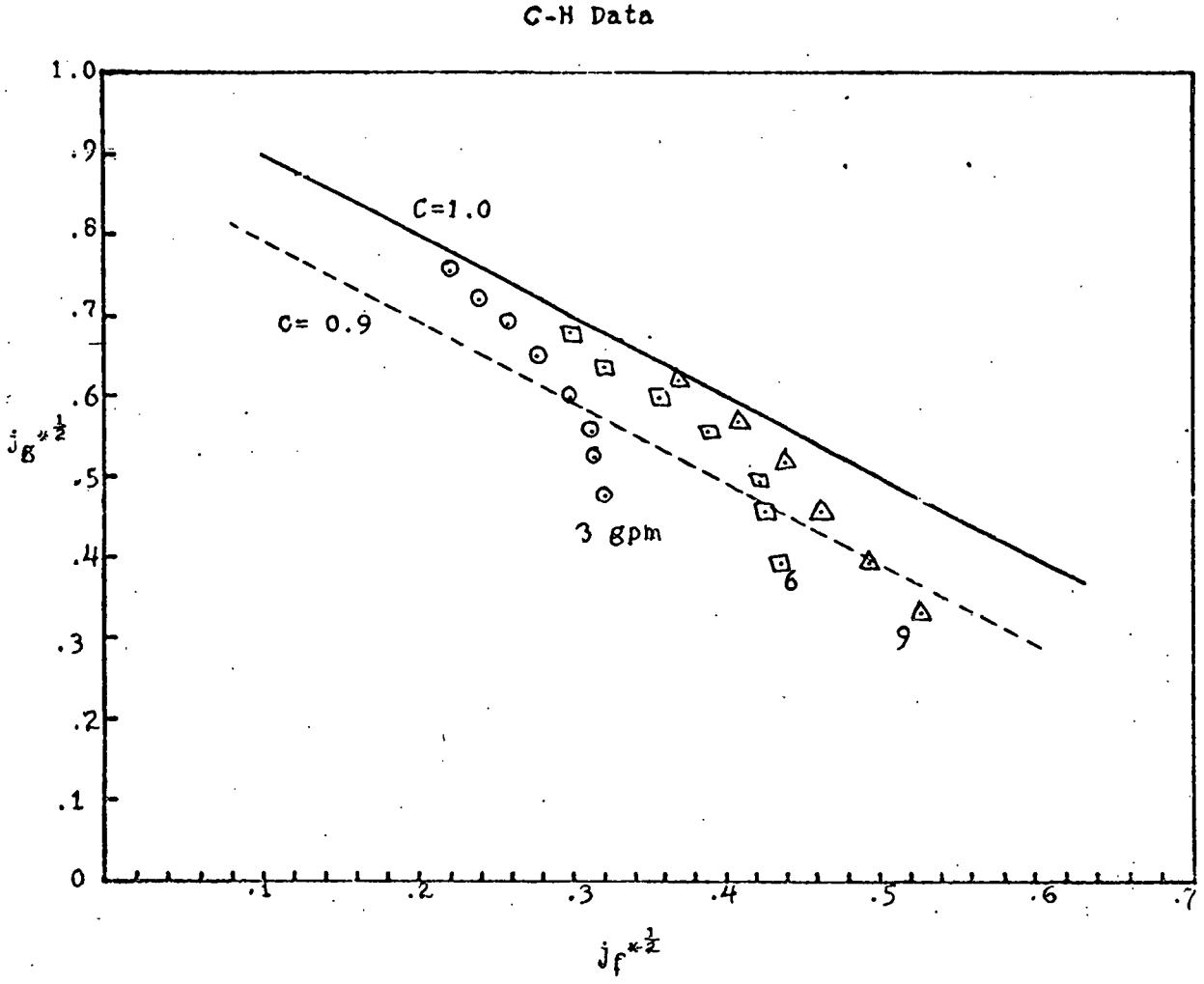
C-H Data
1.0
.9
.8
.7
.6
.5
.4
.3
.2
.1
0
C=1.0
C= 0.9
3 gpm
6
9
.1
.2
.3
.4
.5
.6
.7
$j_g^{*\frac{1}{2}}$
$j_f^{*\frac{1}{2}}$

FIGURE 13